Dissertation

Submitted to the

Combined Faculties for the Natural Sciences and for Mathematics

of the Ruperto-Carola University of Heidelberg, Germany

for the degree of

Doctor of Natural Sciences

Presented by

Master of Science (M.Sc. Biotechnology) Kirti Shukla

Born in: New Delhi, India

Oral examination: 5.11.2014

Regulation of NF-κB signaling and cell cycle progression by microRNA-30c-2-3p in breast cancer

Referees: Prof. Dr. Stefan Wiemann

Prof. Dr. Petra Kioschis

Thesis Declaration

I hereby declare that I have written the submitted dissertation myself and in this process, I have used no other sources or help other than those listed in the references or otherwise mentioned.

Place and date:

……

Kirti Shukla

To my grandparents

Smt. Rajeshwari Devi and Shri. Suresh Chand Sharma

Acknowledgements

I would like to sincerely thank Prof. Dr. Stefan Wiemann for giving me the wonderful opportunity to work in his lab and for supporting me during the challenging phases of my research. His supervision allowed me to grow as an independent researcher and a critical thinker.

I would also like to extend my gratitude towards my Thesis Advisory Committee members Prof. Dr. Peter Angel, Prof. Dr. Petra Kioschis and Prof. Dr. Michael Boutros for making constructive suggestions regarding this project throughout. Also, I thank Prof. Dr. Peter Angel, Prof. Dr. Petra Kioschis and Prof. Dr. Rüdiger Hell for agreeing to be my PhD examiners. My graduate school, HBIGS (Hartmut Hoffmann-Berling International Graduate School of Molecular and Cellular Biology) supported me during the last three years of my PhD study and helped in widening the horizon of my scientific knowledge.

A lot of people were involved in shaping the research I performed during my PhD. I learned a lot from Dr. Aoife Ward, a colleague and dear friend. I thank her for patience and kindness towards me. I am truly grateful that Dr. Rainer Will, Angelika Wörner, Heike Wilhelm and Ewald Münstermann shared their knowledge with me. It was an enriching experience scientifically, working with them. I am also thankful to Aleksandra Balwierz and Dr. Johanna Sonntag for being such great friends. Especially I thank, Dr. Johanna Sonntag for translating the summary of my thesis to German. I cannot thank enough my colleagues Ashwini Kumar Sharma and Thomas Hielscher, who performed bioinformatic analysis on my data. My other colleagues and previous members of the division Dr. Cindy Körner and Dr. Ioanna Keklikoglou also played an important role by providing valuable scientific inputs. I would like to thank my other colleagues Dr. Christian Breunig, Chiara Giacomelli and Alexander Bott, for a friendly atmosphere at work including. Daniela Fischer deserves a special mention for her help in official matters.

Finally, I would like to express my sincere gratitude for my parents Devendra Mohan Sharma and Renu Sharma, who taught me the importance of attaining education. This included not only scientific side but also moral and spiritual development to become a better human being. I am grateful to my sister Latika and brother Shivam, who were true friends throughout my educational journey. I am also thankful to my husband Dipan Shukla and his parents, who supported and encouraged me to realize my dream.

Table of contents

Abbreviations

7AAD	7-Aminoactinomycin D
A.M.D	Average migratory distance
Amp	Ampicillin
APS	Ammonium persulfate
ATCC	American Type Culture Collection
ATP	Adenosine triphosphate
BAFF	B-cell-activating factor
BCA	Bicinchoninic acid
BCL-2	B-cell lymphoma 2
BD	Becton Dickinson
BSA	Bovine serum albumin
CCNE1	Cyclin E1
CDK	Cyclin dependent kinase
CDKN1A	Cyclin-dependent kinase inhibitor 1A (p21, Cip1)
CDKN1B	Cyclin-dependent kinase inhibitor 1B (p27, Kip1)
cDNA	Complementary DNA
CMV	Cytomegalovirus
CMFDA	5-Chloromethylfluorescein Diacetate
CSF2	Colony stimulating factor 2
CST	Cell Signaling Technology
Ct	Cycle threshold
CYLD	cylindromatosis (turban tumor syndrome)
DMEM	Dulbecco’s modified eagle medium
DMSO	Dimethylsulfoxide
DNA	Deoxyribonucleic acid
DTT	Dithiothreitol
EDTA	Ethylenediaminetetraacetic acid
EGF	Epidermal growth factor
EGFR	EGF receptor
ERBB2	v-erb-b2 erythroblastic leukemia viral oncogene homolog 2
ER	Estrogen receptor
FADD	Fas (TNFRSF6)-associated via death domain
FBS	Fetal bovine serum
GO	Gene Ontology
IKK	inhibitor of NF-kappaB kinase
IL	Interleukin

kDa	kilo Dalton
L	Liter
LB	Lysogeny broth
LPS	Lipopolysaccharide
M	Molar
m	milli
MAPK	Mitogen-activated protein kinases
METABRIC	Molecular Taxonomy of Breast Cancer International Consortium
miRNA	microRNA
M-PER	Mammalian Protein Extraction Reagent
mRNA	messenger RNA
mut	Mutant
MYC	v-myc avian myelocytomatosis viral oncogene homolog
n	nano
NEAA	Non-essential amino acids
NF-κB	Nuclear factor kappa B
NIK	NF-κB-inducing kinase
NLS	Nuclear localization signal
ORF	Open reading frame
PAGE	Polyacrylamide gel electrophoresis
PBS	Phosphate buffered saline
PCR	Polymerase chain reaction
PR	Progesterone receptor
qPCR	quantitative PCR
qRT-PCR	quantitative real-time PCR
RANKL	Receptor activator of nuclear factor-κB ligand
RB1	Retinoblastoma protein
RHR	Rel homology region
RIP1	Receptor (TNFRSF)-interacting serine-threonine kinase 1
RISC	RNA induced silencing complex
RNA	Ribonucleic acid
RNAi	RNA interference
RT	Room temperature
SDS	Sodium dodecyl sulfate
siRNA	small interfering RNA
STAT3	Signal transducer and activator of transcription 3
TAK1	Transforming growth factor β activated kinase-1

TCGA	The Cancer Genome Atlas
TBS	Tris buffered saline
TBST	Tris buffered saline with 0.1% Tween®20
TEMED	N,N,N',N'-tetramethyl-ethane-1,2-diamine
TNBC	Triple negative breast cancer
TNF-α	Tumor necrosis factor alpha
TNFR1	Tumor necrosis factor receptor superfamily, member 1A
TNFR2	Tumor necrosis factor receptor superfamily, member 1B
TRADD	TNFRSF1A-associated via death domain
TRAFF	TNF receptor–associated factor 2
UTR	Untranslated region
wt	Wild-type

Summary

NF-κB signaling is frequently deregulated in a variety of cancers and is constitutively active in estrogen receptor negative breast cancer subtypes. These molecular subtypes of breast cancer are associated with poor overall survival. During my PhD work, I focused on mechanisms of NF-κB regulation in breast cancer by miRNAs, key regulators of eukaryotic gene expression, which bind their target mRNAs via seed sequences and inhibit gene expression at the post transcriptional level. In a previous study, miR-30c-2-3p was found to be one of the strongest negative regulators of NF-κB signaling in a genome-wide miRNA screen. I uncovered the underlying molecular mechanisms by which miR-30c-2-3p regulates NF-κB signaling and cell cycle progression in breast cancer by combining *in vitro* data with publically available breast cancer patient datasets.

I could show that miR-30c-2-3p directly targets TRADD, an adaptor protein of the TNFR/NF-κB signaling pathway as well as the cell cycle protein, CCNE1. Ectopic expression of miR-30c-2-3p downregulated essential cytokines IL8, IL6 and CXCL1, reduced cell proliferation, and invasion in MDA-MB-231 breast cancer cells. RNAi-induced silencing of TRADD phenocopied the effects on invasion and cytokine expression also observed with miR-30c-2-3p, while inhibition of CCNE1 phenocopied the effects of the miRNA on cell proliferation. The tumor suppressive role of miR-30c-2-3p was confirmed in a cohort of 781 breast tumors with matched mRNA and miRNA expression data where higher expression of miR-30c-2-3p was associated with better survival. Furthermore an anticorrelation with expression of target genes and miR-30c-2-3p was seen in these breast cancer patients. These findings are important in the context of breast cancer where NF-κB signaling has been implicated to play a role in tumor initiation, progression, metastasis and resistance to chemotherapy.

During my thesis work I could establish that miR-30c-2-3p negatively regulates both NF-κB signaling and cell cycle progression, that are two important signaling pathways frequently deregulated in breast cancer. As a result, miR-30c-2-3p directly effects several hallmarks of cancer cells, i.e., proliferation, expression of inflammatory cytokines as well as invasion, and can be potentially used for therapeutic intervention in miRNA based cancer therapy.

Zusammenfassung

Der NF-κB Signalweg ist bei einer Vielzahl von Krebsentitäten dereguliert und konstitutiv bei Brustkrebs Subtypen aktiviert, die durch einen negativen Estrogen-Rezeptor Status gekennzeichnet sind. Diese molekularen Subtypen des Brustkrebs sind mit einer schlechten Überlebenswahrscheinlichkeit assoziiert. Der Fokus meiner Doktorarbeit lag auf den Regulationsmechanismen, die miRNAs auf den NF-κB Signalweg im Zusammenhang mit Brustkrebs ausüben. miRNAs sind maßgeblich für die Regualtion der eukaryotischen Genexpression auf postranskriptionaler Ebene verantwortlich, durch das Binden ihrer Ziel mRNAs über *Seed* Sequenzen und der daraus folgenden Inhibition der Genexpression. In einem genomweiten miRNA Screening konnte in einem vorhergehenden Projekt die miR-30c-2-3p als einer der stärksten Negativregulatoren des NF-κB Sigalwegs identifiziert werden. Im Rahmen meiner Doktorarbeit habe ich, durch die Kombination von *in vitro* Daten und öffentlich zugänglichen Datensätzen, Mechanismen aufdecken, mit denen die miR-30c-2-3p den NF-κB Sigalwegs und den Zellzyklus bei Brustkrebs beeinflusst.

Ich konnte zeigen, dass miR-30c-2-3p sowohl die Expression von TRADD, einem Adaptorprotein des TNFR/NF-κB Siganlwegs, als auch die Expression des Zellzyklus Proteins CCNE1 direkt beeinflusst. Die ektopische Expression von miR-30c-2-3p regulierte die Expression essentieller Cytokine wie IL8, IL6 und CXCL1 herunter, reduzierte die Zellproliferationsrate und verminderte die Invasionfähigkeit von MDA-MB-231 Brustkrebszellen. RNAi-induziertes *silencing* von TRADD hatte Auswirkungen auf die Invasionsfähigkeit und die Cytokin Expression, wie auch schon unter Einfluss von miR-30c-2-3p. Im Gegensatz dazu hatte die Inhibition von CCNE1 ähnliche Effekte wie miR-30c-2-3p auf die Zellproliferation. Die tumorsupressive Rolle der miR-30c-2-3p wurde in einem 781 Brustkrebsproben umfassenden Datensatz, bestehend aus mRNA und miRNA Expressionsdaten bestätigt. Eine erhöhte Expression von miR-30c-2-3p konnte mit einer positiven Prognose assoziiert werden. Desweiteren konnte eine gegenläufige Korrelation der Zielgene von miR-30c-2-3p und miR-30c-2-3p bei diesen Brustkrebspatientinnen beobachtet werden. Diese Erkenntnisse sind im Kontext von Brustkrebs wichtig, da der NF-κB Signalweg mit Tumorentwicklung, Tumorprogression, Metastasenbildung und Chemotherapie-Resistenz in Verbindung gebracht wird. Die miR-30c-2-3p könnte daher ein vielversprechender Kandidat für die miRNA basierte Therapie von Brustkrebs sein.

1. Introduction

1.1. Breast cancer

Breast cancer is a heterogeneous disease which can be defined by molecular subtypes that are associated with distinct molecular signatures and clinical outcomes including response to drugs. The main molecular subtypes of breast cancer are: luminal A, luminal B, human epidermal growth factor receptor 2 (HER2) or ERBB2+ enriched, and basal-like tumors [1]. These subtypes are based on gene expression profiling and cluster analysis of breast tumors [2-4]. Each of these subtypes is associated with different overall survival and unique intrinsic gene expression patterns (Table 1) [3, 5, 6]. The mutation status of the tumor suppressive gene, *TP53* is also significantly different in these molecular subtypes with the basal-like tumors having 80% mutations compared to 12% and 29% in luminal A and luminal B, respectively [6]. This data showed that the TP53 pathway is largely functional in luminal A tumors but inactivated in more aggressive subtypes of breast cancer [6].

Table 1: Characteristic intrinsic gene expression pattern associated with each molecular subtype of breast cancer. Data from [3, 5, 6].

Molecular subtype	Intrinsic gene expression pattern
Luminal A	High expression of *ESR1*, *GATA3*, *FOXA1*, *XBP1* and *MYB*
Luminal B	Low to moderate expression of ER cluster (above), high expression of *GGH*, *LAPTMB4*, *NSEP1* and *CCNE1*
ERBB2+ subtype	High expression of *ERBB2*, all genes within HER2 amplicon (including *GRB7*) and *TRAP100, FGFR4, EGFR*
Basal-like	Negative expression for ER cluster and HER2, high expression of *KRT5, KRT1, ANXA8, CX3CL1, TRIM29, AKT3, MYC* and gene amplification of *CCNE1, FGFR1, FGFR2, IGFR1, KIT, MET ,PDGFRA, MYC*

These molecular subtypes are representative of the biology behind different stages of epithelial cell development of the human breast with luminal A and luminal B falling under more differentiated tumors compared to the other two subtypes [7]. Luminal A and luminal B subtypes are classified as estrogen receptor positive (ER+), with luminal A associated with the best prognosis compared to all other subtypes of breast cancer [1]. The status of estrogen receptor determined by immunohistochemistry is the most relevant independent prognostic and predictive factor for responsiveness to endocrine therapy in breast cancer [8]. Estrogen receptor negative (ER-) breast cancer, which comprises of ERBB2+ or HER2 enriched and basal subtypes is characterized by the absence of estrogen receptor expression [5, 9]. In contrast to estrogen receptor positive tumors, estrogen negative tumors do not require estrogen hormone for continual growth, and can thus not be treated with standard endocrine therapy, for example tamoxifen or aromatase inhibitors [10]. ER negative group of breast cancer also differs from ER+/luminal clusters in expression of several additional transcription factors [3]. About 30% of breast tumors are estrogen receptor negative [5]. Out of these, breast tumors that express HER2 can be treated with trastuzumab or lapatinib (effective also against EGFR overexpressing breast tumors) [11, 12].

Basal-like tumors are mostly referred to as triple negative breast cancers (TNBCs) due to the lack of expression for ER, PR, and HER2 and constitute 10%-25% of all breast tumors [6, 13]. However, only 75% of TNBCs are indeed basal-like tumors [6]. The rest includes all other molecular subtypes emphasizing the heterogeneity of triple-negative group of tumors [13]. Due to the lack of targeted therapy options in case of basal-like tumors, this subtype is associated with poor overall survival and clinical outcome [9, 10]. Although TNBCs or basal-like tumors are responsive to chemotherapy, still this is associated with disease recurrence and progression [13].

Despite major improvements in diagnosis and treatment, breast cancer is still the second leading cause of tumor associated death among women worldwide [14]. This emphasizes the need to better understand the gene regulation networks deregulated in estrogen receptor negative or basal-like tumors to come up with strategies for improved therapy and diagnosis.

1.2. NF-κB signaling

NF-κB signaling is a key pathway regulating inflammatory responses, cell proliferation, innate immune responses and involved in organogenesis [15]. NF-κB is an evolutionary conserved family of transcription factors with 5 members that are structurally related and can form homo- or hetero-dimers: RelA (p65), RelB, c-Rel, NF-κB1 (p105 and p50), and NF-κB2 (p100 and p52) [15, 16]. RelA (p65), RelB, and c-Rel are produced in mature form and have a transactivation domain [17]. NF-κB1 and NF-κB2 are translated as large precursors, p105 and p100, respectively. These are processed to mature active forms, p50 and p52 respectively [15]. All the 5 members of the family share an 300 amino acid domain known as Rel homology region (RHR) responsible for nuclear localization, binding to the DNA, dimerization and association with inhibitor proteins [17]. In an unstimulated or inactive state, NF-κB proteins reside in cytoplasm through non covalent interactions with inhibitory proteins like, IκBβ, IκBα, IκBε, IκBζ, Bcl-3, IκBNS and inactive precursor forms of proteins [17, 18]. Upon stimulation with appropriate ligand, NF-κB proteins translocate to the nucleus and, as homo or hetero dimers, bind to κB DNA sequence motifs thus regulating gene expression [16].

In response to stimuli such as tumor necrosis factor-α (TNF-α), CD40 ligand (CD40L), interleukin-1 (IL-1), or lipopolysaccharide (LPS) canonical signaling is activated through the IKK (inhibitor of NF-kappa B kinase) complex. This complex consists of three protein subunits IKKα, IKKβ (catalytic subunit) and IKKγ (regulatory subunit) [15]. An activated complex can then phosphorylate and mark IκB proteins for ubiquitination via SCF-type E3 ubiquitin-protein ligase and finally cause degradation by the 26S proteasome [19-21]. The classical inhibitor proteins IκBβ, IκBα, IκBε contain ankyrin repeat domain and two serine residues within the consensus sequence DSGXXS at the N-terminal end of the proteins that are sites for phosphorylation [17]. Upon degradation of the inhibitor proteins, nuclear translocation of activated NF-κB to the nucleus occurs resulting in gene expression activation [21].

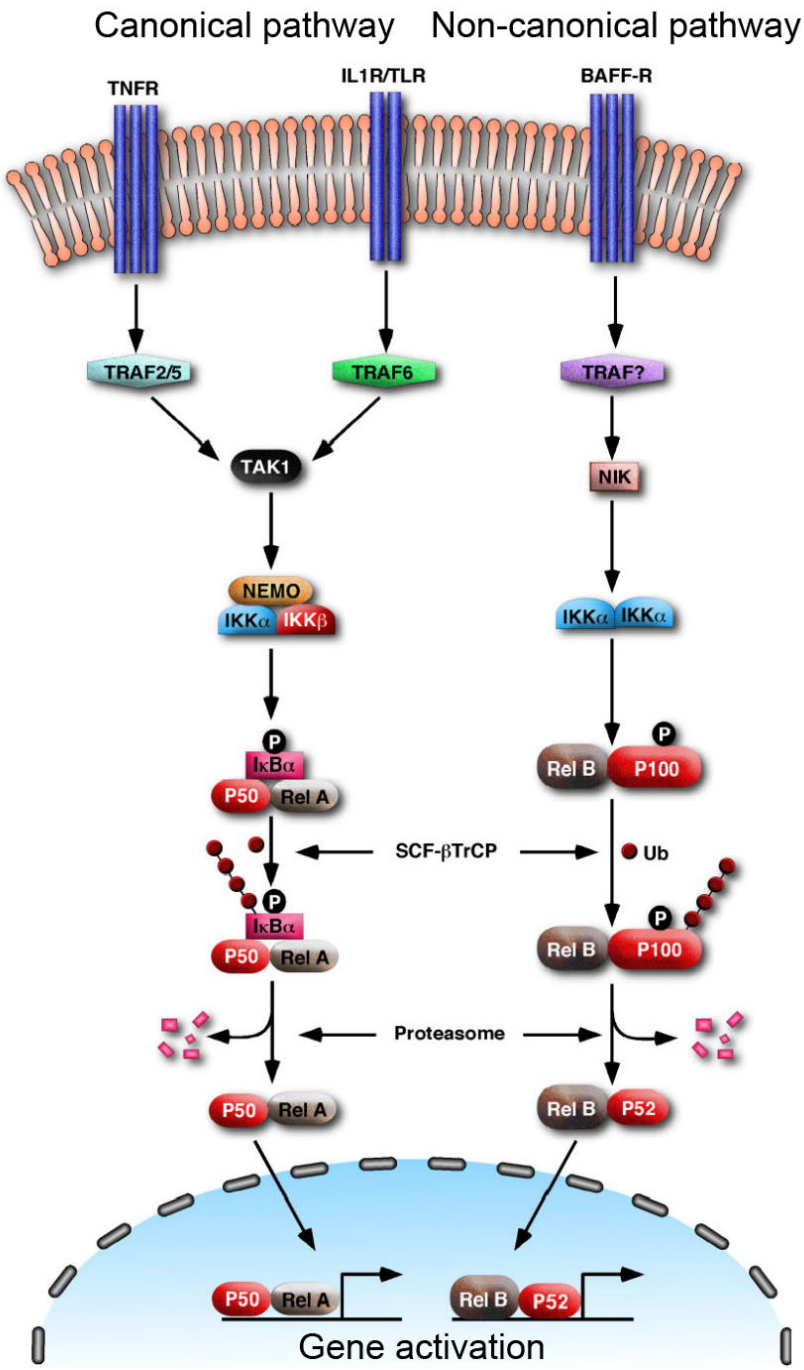

Figure 1: Alternative routes for NF-kB activation. Interaction of TNF receptors (TNFRs) with ligand such as TNF-α or LPS causes activation of IKKβ subunit. This subsequently leads to formation of heterodimers consisting of RelA and p50 which can translocate to nucleus and activate gene expression through canonical pathway. A class of TNFRs known as B-cell receptor for BAFF (BAFF-R) can interact with ligands such as BAFF and initiate NF-κB activation through IKKα subunit. This ultimately results in formation of heterodimers consisting of RelB and p52 which translocate to nucleus leading to gene expression activation through non-canonical pathway for genes involved in B cells function. Figure taken and adapted from [20].

There are two types of NF-κB activation pathways, the canonical and the non-canonical activation pathway (Figure 1). Canonical pathway mainly activates NF-κB dimers consisting of RelA or c-Rel in response to stimuli such as IL-1, TNF-α and LPS [17]. These ligands activate TNF receptor–associated factor 2 (TRAF) proteins and eventually kinase TAK1, which phosphorylates and activates IKKβ subunit of IKK kinase [20]. The signaling activation in response to B-cell-activating factor (BAFF) ligand, CD40 ligand or lymphotoxin-β leads to processing of p100 to p52 and is called non-canonical NF-κB activation pathway which is mostly active in B-cells [20, 22]. In this pathway, IKKα subunit is phosphorylated by NF-κB-inducing kinase (NIK) which in turn phosphorylates p100 that form p52 [22]. The activating stimuli such as TNF-α and IL-1 also lead to expression of signaling inhibitor proteins such as IκBα, IκBε which function to suppress NF-κB activity in a negative feedback loop [17]. Also deubiquitinating enzymes like, CYLD (cylindromatosis (turban tumor syndrome)) and A20 (tumor necrosis factor, alpha-induced protein 3, TNFAIP3) can act as a negative regulators of the signaling [23] to maintain cellular homeostasis.

1.2.1. TNF-α mediated NF-κB signaling

TNF-α is a key stimulator for canonical, or classical, NF-κB signaling and a member of the TNF superfamily [24]. The TNF superfamily comprises 19 ligands including lymphotoxins (LT), receptor activator of nuclear factor-κB (NF-κB) ligand (RANKL), and TNF-related apoptosis-inducing ligand (TRAIL). These can interact with 29 receptors from the TNFR superfamily [24]. Most members of the TNF superfamily are transmembrane proteins that are released from cell surface through the process of proteolysis carried out by proteases [24]. For example, TNF-α is released from the surface of cells by the enzyme TACE (TNF-alpha-converting enzyme) [25].

TNF-α is a proinflammatory factor present in the tumor microenvironment that has been implicated in diverse roles like cell proliferation, inflammation, regulation of immune response and anti-viral response [26, 27]. It can bind to TNF receptors (TNFR1 and TNFR2) that are expressed in most cells and tissues [16, 24], and can also bind the HER2 receptor tyrosine kinase to activate the MAPK signaling pathway [28]. TNFR1

(p55) and TNFR2 (p75) belong to a superfamily of proteins collectively called TNF/Nerve Growth Factor (NGF) receptor [29]. The family members of this superfamily of proteins are characterized by cytoplasmic domains that lack a distinct enzymatic activity and interact with other cytoplasmic proteins to convey biological signals [30]. The characteristic response of cells to TNF-α (Figure 2) is mediated through involvement of an 80 residue long motif called death domain (DD) [31]. Proteins like TNF receptor 1-associated protein (TRADD), Fas-associated death domain (FADD) and receptor interacting protein (RIP1) contain this death domain and can interact with the cytoplasmic domain of the TNFR1 receptor [32-34].

TRADD overexpression leads to two main cellular responses, activation of NF-κB signaling and apoptosis [32]. Interaction of TNF-α with TNFR can also initiate apoptosis by engagement of FADD and caspase 8 [16, 35]. However NF-κB signaling has a protective role against TNF-α induced apoptosis through expression of survival genes such as BCL2L, inhibitors of apoptosis (IAPs), and activation of the AP-1 transcription factor [16, 36, 37]. This anti apoptotic effect is caused by recruitment of TRADD as an adaptor molecule to the cytoplasmic domain of TNFR1. TRADD then recruits TRAF2 which in turn interacts with RIP, this cascade ultimately triggering NF-kB signaling via activation of the IKK complex [16].

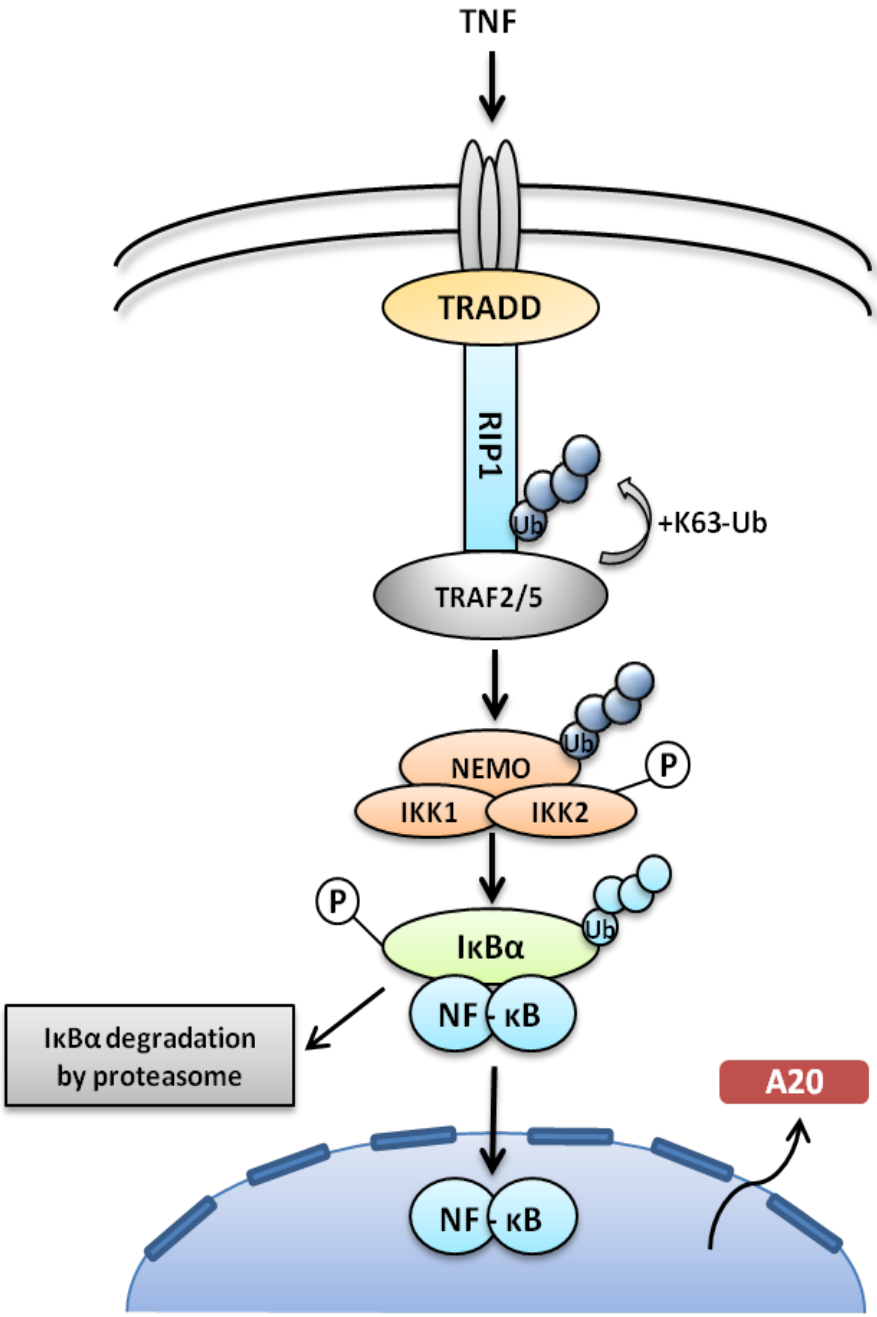

Figure 2: TNF-α mediated activation of cellular signaling. TNF-α activates NF-κB signaling by engaging the TRADD–RIP1–TRAF2–TRAF5 complex to TNFR1. This leads to TRAF mediated K63-linked ubiquitination of RIP1 which induces association with the IKK complex. This in turn leads to phosphorylation and K-63 linked ubiquitination of the IKK complex. This ulimately leads to proteasome mediated degradation of IκB proteins and translocation of NF-κB dimers to the nucleus and activation of gene expression. Figure taken and adapted from [38].

1.2.2. Role of NF- κB signaling in breast tumorigenesis

NF-κB signaling plays an important role in mammary gland development, especially during proliferation of mammary epithelial cells that occurs during pregnancy, differentiation at the time of lactation, and apoptosis of the secretory epithelial cells during involution [39-41]. These effects are mainly mediated in response to RANKL through non-canonical signaling activation [41]. Furthermore, experimental evidence from genetically modified mice that have altered NF-κB, IκB, or IKK proteins show defects in mammary gland development [15]. Deregulation, i.e. constitutive activation of this tightly regulated pathway can lead to tumor initiation and transformation by various mechanisms (Figure 3). These include unregulated proliferation of cells, evasion of apoptosis, and increased tumor metastasis and angiogenesis [42]. Activated NF-κB is mainly responsible for cancer development and is not associated with genetic alterations in NF-κB, IKK or other upstream members of signaling [43]. The consequence is an excessive production of survival proteins like BCL2L, BCL2 and proinflammatory cytokines like IL8, IL6 and CXCL1 which are part of the tumor microenvironment. Thus, this signaling also forms a critical link between cancer and inflammation [43].

Activation of NF-κB signaling through the canonical (dimers of p65/p50) and non-canonical pathways (dimers of p50, p52 and c-Rel) has been shown both in breast tumor samples and breast cancer cell lines [44, 45]. Frequently, NF-κB signaling is constitutively active, particularly in ER negative breast tumors [46, 47]. This is associated with increased cell proliferation, inhibition of apoptosis, metastasis and tumor progression thus making NF-κB signaling an attractive target for therapeutic intervention. NF-κB signaling has also been implicated in malignant transformation of ER positive breast cancer [48]. The hormone independence of ER negative tumors is associated with increased NF-κB activity primarily through increased p50 dimers and higher Bcl-3 expression which can replace estrogen by providing survival and growth signals to the cells [49]. Estrogen receptor mediated signaling on the other hand suppresses NF-κB activation and has an anti-inflammatory role, underlining the relation between these two signaling pathways in the context of breast cancer [50]. This

crosstalk can explain the resistance to antiestrogen therapy including tamoxifen and aromatase inhibitors seen in clinics [51].

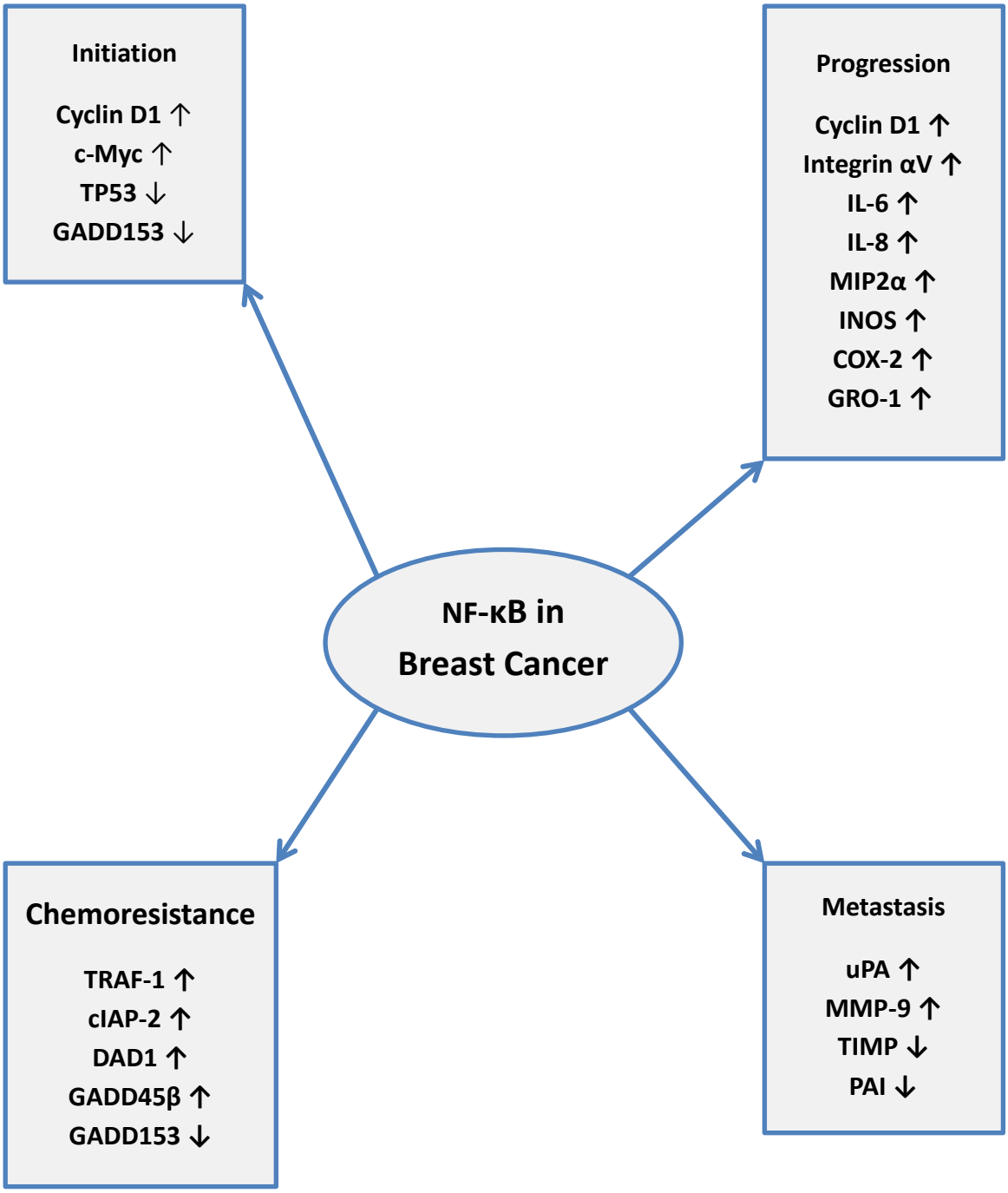

Figure 3: NF-κB signaling is implicated in breast cancer by regulating phenotypes like tumor initiation, progression, chemoresistance and metastasis. Figure taken and adapted from [40].

1.3. Cell cycle regulation

The cell cycle in eukaryotes is a highly regulated biological process and has four distinct phases: mitosis (M-phase), DNA replication (S-phase), gaps G1 and G2 [52]. During the G1 and G2 gap phases, cells synthesize biomolecules such as RNA and proteins and perform metabolism, the DNA is replicated in S-phase, while cell division occurs during M-phase [53]. The mammalian cell cycle is more complex with five distinct cell cycle phases with an additional G0 phase in which cells are in quiescent or non-dividing state. Mammalian cells remain in the G0 phase until they receive a growth stimulus to activate signaling pathways like MAPK pathway [53]. In the late G1 phase, the restriction (R) point defines a critical point in the commitment of cells to the cell cycle and after this point cells are no longer sensitive to presence or absence of growth factors [54]. There are a number of checkpoints in the course of the cell cycle to maintain the integrity of the genome during cell cycle progression [53]. The most important member of this system is the TP53 tumor suppressor protein, which either causes cell cycle arrest to allow DNA repair to occur in response to DNA damage or apoptosis if the damage is too strong [55].

1.3.1. Cyclins and CDKs in cell cycle control

Cyclin-dependent kinases (CDKs) are a conserved family of molecules that coordinate the events in the cell cycle of eukaryotes [52]. These CDKs work in association with proteins named cyclins, because of their oscillating levels in dividing embryonic stem cells [56]. There are 9 CDKs (CDK1 - CDK9) and many cyclins (cyclin A - cyclin T) known [57]. In mammals four different types of CDKs (CDK1/CDC2, CDK2, CDK4 and CDK6) combine with four different families of cyclins: cyclin D (D1, D2 and D3), E (E1 and E2), A (A1 and A2) and B (B1, B2 and B3) [58]. Different combinations of cyclins and CDKs are involved in cell cycle progression (Table 2). The activity of CDKs is kept in check by association with negative regulators known as cyclin-dependent kinase inhibitors (CDKIs). These CDKIs are produced in response to anti mitogenic signals and belong to two main classes of proteins: Cips (CDK interacting protein) and INK4 (inhibitor of CDK4) [59]. These proteins are allosteric competitors of cyclins for binding to CDKs [58].

Table 2: Cell cycle phases and their associated cyclin/CDK complexes during cell cycle progression. Information taken from [53].

Cell cycle phase	cyclin/CDK complexes
Progression through G1 phase	cyclin D/CDK4 (CDK6)
G1/S transition	cyclin E/CDK2
Progression through S phase	cyclin A/CDK2
Progression through G2 phase	cyclin A/CDC2
Progression through M phase	cyclin B/CDC2

In the absence of mitogens, the activity of CDKs is off. As a result of this, the CDK substrate, retinoblastoma protein (Rb) is hypo-phosphorylated, which leads to inhibition of E2F transcriptional activators [60]. However, in the presence of mitogens the synthesis of D-type cyclins and their assembly with CDK4/CDK6 lead to phosphorylation and release from the Rb tumor suppressor protein, resulting in the activation of E2F transcriptional activators [54, 60]. Activated E2F can then induce the expression of cyclin E and other proteins that enhance kinase activity of CDK2 thus leading to further phosphorylation of Rb [54, 61]. Subsequent degradation of CDK activity inhibitor, p21 further drives G1 to S transition [62]. Nuclear p21 can inhibit the activity of transcription factors MYC, E2F1, STAT3 involved in cell cycle [62]. Cytoplasmic p21 can be phosphorylated by IKKβ (inhibitor of nuclear factor-κB kinase-β), preventing nuclear translocation and promoting its anti-apoptotic effects [63]. This showed direct connection between NF-κB signaling and cell cycle control. Phosphorylation of cyclin E by the cyclin E/CDK2 complex leads to proteasome-dependent degradation of cyclin E once S phase is initiated, this favors association of CDK2 with cyclin A [64]. Different combination of CDC2 with cyclin A or cyclin B drives the cells through rest of the cell cycle.

1.3.2. Role of cyclins in breast tumorigenesis

Cell cycle regulation is frequently deregulated during tumorigenesis with cancer cells exhibiting self-sufficiency of growth signals [65]. CDKs and cyclins are often overexpressed in tumor cells as revealed by molecular analysis of human tumors [58]. For example, D-cyclins are found to be overexpressed and associated with alterations like gene amplification and chromosomal translocations in breast tumors which frequently show a high occurrence of cyclin D1 (CCND1) overexpression [58]. Transgenic mice overexpressing cyclin D1 in mammary cells undergo abnormal cell proliferation including formation of mammary adenocarcinoma [66]. Similar to these observations, overexpression of cyclin D2 has been shown to induce cell proliferation and to be oncogenic during mammary gland development [67]. This collectively showed that long term expression of these two cyclins is involved in breast tumorigenesis in mice. Furthermore, the role of cyclin D1 in breast tissue proliferation is underlined by the observation that inhibition of cyclin D1 expression selectively prevented tumor development occurring from alterations in the Ras and Wnt signaling pathways [58].

E-type cyclins (cyclin E1 and cyclin E2) in combination with CDK2 regulates essential processes at G1 to S transition of the cell cycle [68]. The expression of cyclin E is higher than the physiological levels in many types of human tumors, and the genomic locus (19q12-q13) is frequently amplified [68-70]. Higher levels of cyclin E have been implicated in breast tumorigenesis through inactivation of the pRb pathway and increased kinase activity causing unrestrained growth [71]. These observations underline the importance of both cyclin D and cyclin E in breast tumor formation.

The role of cyclin A1 in formation and progression of tumors has also been studied through transgenic mouse models. Overexpression of cyclin A1 proteins in the mammary gland of transgenic mouse models leads to an increased cyclin A1 associated CDK2 kinase activity [72]. These transgenic mice exhibited abnormalities of nucleus like multinucleation and karyomegaly which indicate preneoplastic alterations [72].

1.4. RNA interference

RNA interference (RNAi) is a mechanism of gene expression regulation in eukaryotes which was first discovered in *Caenorhabditis elegans* in response to double-stranded RNA (dsRNA), causing downregulation of complementary target genes [73]. In plants, RNAi is a defense mechanism against RNA viruses to stop their replication [74-76]. Similar downregulation of gene expression in response to dsRNA is also observed in species, such as *Drosophila*, and many mammals [77-80].

RNAi is operational at the post transcriptional level to repress and regulate gene expression. This observation was made in *C.elegans* where ds RNA resulted in loss of expression in corresponding messenger RNAs (mRNA) leaving other regulatory elements such as promoters sequences unaltered [73]. At the molecular level, gene expression is repressed by small interfering RNA (siRNA) which is either produced endogenously or can be artificially introduced into the cell [81]. Endogenous siRNAs are typically up to 23 nucleotides long and are cleavage products of dsRNAs which correspond to mRNAs and result in post transcriptional silencing of these genes (PTGS) [82, 83]. The components of the RNAi pathway were discovered initially in *Drosophila* [84]. A ribonucleoprotein complex called RNA Induced Silencing Complex (RISC) was found to be responsible for sequence guided degradation of mRNA [85]. This complex consists of Dicer, a ribonuclease III family enzyme, for processing long dsRNAs into approximately 22-nucleotide siRNAs, and Argonaute2 protein which is responsible for cleavage of target mRNAs and the siRNAs [85]. The RNAi machinery has been exploited in a number of studies to specifically repress gene expression in mammals [86, 87]. However, introduction of long dsRNA in mammalian cells elicits apoptosis and inhibition of protein synthesis due to activation of the PKR (protein kinase R) and RNAseL pathway [83, 88]. This effect can be circumvented by introducing only 23 nucleotide long double stranded siRNAs into mouse or human cells [89].

1.4.1. miRNA

MicroRNAs (miRNAs) are a class of non protein-coding RNAs that can modulate gene expression at the post transcriptional level. As a result, miRNAs regulate key biological processes like embryonic development [90]. In contrast to most siRNAs, miRNAs are encoded in the genome and transcribed by RNA polymerases II or III [91]. The first step of miRNA biogenesis involves transcription of miRNA genes to form primary or pri-miRNA [91]. This pri-miRNA is then cleaved by RNase III endonuclease Drosha to form a ~70 nucleotide precursor or pre-miRNA which has a stem loop structure [92]. This is then transported into the cytoplasm. There, the second important step during miRNA biogenesis is the cleavage by enzyme Dicer RNase III of pre-miRNA to form mature double stranded miRNA of ~22 nucleotide in length [93].

The first miRNA was discovered in *Caenorhabditis elegans*, where it was shown that *lin-4* negatively regulates the translation of *lin-14* mRNA by binding to complementary sequences within the 3´UTR via antisense RNA-RNA interactions [94]. This translational inhibition was found to be important during larval development [94]. This was followed by the discovery of miRNA *let-7* which, along with *lin-4*, regulates the developmental timing in *Caenorhabditis elegans* [95]. Since then many more miRNAs have been reported in other species as well. In humans, there are currently 2578 mature miRNAs and 1872 precursor miRNAs reported to be encoded in the genome [96].

1.4.2. Mechanism of gene regulation

Processed mature miRNAs are between 21-24 nucleotides long and bind mostly within the 3´UTRs of their target mRNAs [93, 97]. This interaction is mediated by the RNA induced silencing complex (RISC) and leads to degradation or translational repression of the mRNAs depending on the level of complementarity between miRNA or siRNA and mRNA (Figure 4A and B) [84, 93]. This interaction is mediated by involvement of Argonaute (Ago) proteins [98]. After mediating the cleavage of target mRNA, the corresponding miRNA or siRNA can then modulate expression of other mRNAs [93, 99]. Another proposed model of regulation is through siRNA mediated transcriptional silencing of DNA (Figure 4C) [93]. miRNAs bind regions in the 3´UTR of target

mRNAs through the so-called seed sequence of 2-8 nucleotides at the 5´ of every miRNA [100]. This binding specifies target specificity of the miRNA. More than half of the human protein coding genes (approximately 60%) are predicted to be regulated by miRNAs [101]. These targets of miRNAs cover a broad range of biological, molecular and cellular processes [93].

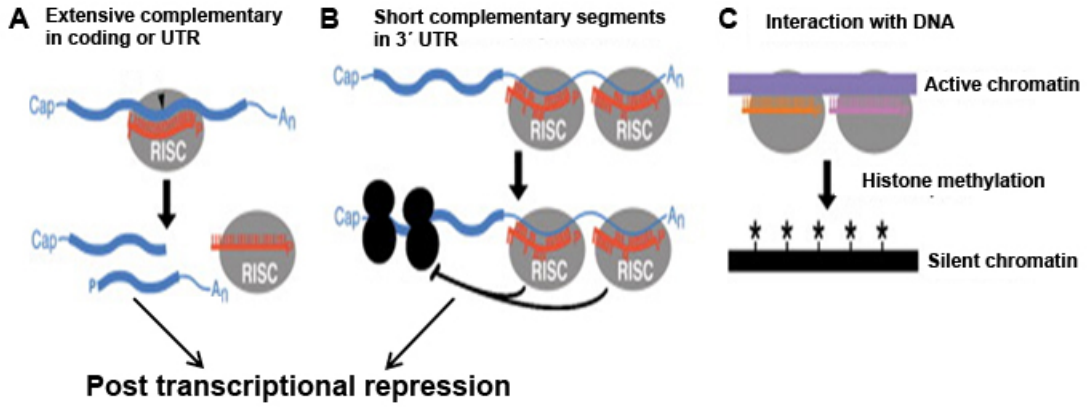

Figure 4: Mechanisms of miRNA/siRNA mediated gene regulation.(A) Cleavage of complementary mRNA caused by both miRNA or siRNA. (B) Repression of mRNA translation caused by both miRNA or siRNA. (C) Transcriptional silencing mediated by siRNA. Figure taken and adapted from[93].

1.4.3. miRNAs and their role in breast cancer

miRNA mediated regulation plays an important role in development and progression of cancer [98]. They can act both as tumor suppressors or oncogenes, depending upon the spectrum of targets regulated by the respective miRNAs [98]. For example miR-21 acts as an oncogene and promotes breast cancer via regulation of anti-apoptotic factor BCL-2 [102]. Frequently, altered expression of miRNA genes has been found in a number of tumor types and between normal and neoplastic tissues. Their role in carcinogenesis and specifically in breast cancer is increasingly studied [103-105]. Moreover, miRNAs have distinct expression patterns across different subtypes of breast cancer and play an important role in defining the associated gene expression pattern [106]. Recently, Ward et al. showed that miR-519a acts as a master regulator of cell cycle in ER positive breast cancer patients by targeting key proteins of cell cycle like RB1, PTEN and p21 [107].

miRNAs have also been implicated to induce or revert drug resistance against standard chemotherapy and targeted therapies [98]. Trastuzumab is a part of targeted drug against overexpressed HER2. miR-21 has been known to be upregulated in trastuzumab resistance in both *in vitro* and *in vivo* conditions which is associated with poor response of patients [108]. Taking into consideration their central role as negative regulators of biological processes, miRNAs can be used as biomarkers or targets in cancer therapy.

1.5. Aim of the study

The aim of my PhD study was to find and characterize novel miRNA regulators of NF-κB signaling that can be potentially used as biomarker or in miRNA based therapy in breast cancer patients. This included elucidation of the mode of gene regulation and cellular phenotypes affected by the miRNA. This consisted of two main parts:

1) Identifying and validating target genes responsible for the phenotype caused by the miRNA.
2) Establishing clinical relevance of *in vitro* findings by analyzing breast cancer patient datasets.

In addition to the primary focus of my research project that is outlined in this thesis, I contributed to several other projects that were related to breast cancer, some of which have already been published while others are still underway (see chapter 5 “Own publications” for details). I have not included any of this work in the thesis because these studies were not along the main focus of my PhD research project.

2. Materials and Methods

2.1. Materials

2.1.1. Instruments

Table 3: Instruments used during this study.

Instrument	Company
ABI Prism 7900HT	Applied Biosystems
Axiovert 25 light microscope	Carl Zeiss
Bacterial incubator (37^{o}C)	Memment
Balance	Kern, EW
Cell counter CASY	Casy, Innovatis
Cell culture hood HERA Safe	Thermo Scientific
Cell culture incubator (37^{o}C)	Heraeus, BBD6220
Centrifuges	Eppendorf, Heraeus
DNA gel apparatus	Renner GmbH
Electrophoresis Power Supply	Pharmacia
Flow Cytometer FACS Calibur	Becton-Dickenson
Gel documentation system	Herolab
Infinite M200 microplate reader	TECAN
Light Microscope	Hund, Wetzlar
Microwave	Panasonic
Nanodrop ND-1000 spectrophotometer	Nanodrop
Odyssey Infrared Imaging System	Li-Cor Biosciences
Olympus Scan^R microscope	Olympus
pH meter	HANNA, Kehl
Pipetteboy	Integra Biosciences

Pipetteman	Gilson
Protein Gel Apparatus	Invitrogen
Sentrix Human HT-12 v4 BeadArrays	Illumina
Shaking bacterial incubator (37^{o}C)	HT INFOS Minitron
Thermocycler	Applied Biosystems
Trans-Blot SD Semi-Dry Electrophoretic	Bio-Rad
Trans-Blot® Electrophoretic Transfer Cell	Bio-Rad
Vortex mixer	NeoLab
Waterbath	Grant SUB14
xCelligence Real-time cell analyzer (RTCA)	Roche

2.1.2. Molecular biology kits

Table 4: Molecular biology kits used and during this study.

Reagents and kits	Company
ABSOLUTE qPCR ROX mix	Thermo Scientific
A protein assay reagent	Pierce
beta-glo® Luminescent Assay Kit	Promega
Caspase-Glo 3/7 Assay	Promega
cDNA synthesis kit	Thermo Scientific
Cell titer blue	Promega
Dual luciferase assay	Promega
miRCURY LNA™ Universal RT microRNA PCR	Exiqon

miRNeasy Mini kit	Qiagen
MiniElute® PCR purification kit	Qiagen
QIAprep Spin Midiprep Kit	Qiagen
QIAprep Spin Miniprep Kit	Qiagen
QIAquick Gel Extraction Kit	Qiagen
QuikChange Lightning Site-Directed Mutagenesis kit	Stratagene
RevertAid™H Minus First Strand cDNA synthesis kit	Fermentas
RNeasy Mini Kit	Qiagen
TA-Cloning Kit	Invitrogen
Wizard® SV Gel and PCR Clean-Up System	Promega

2.1.3. Chemicals, reagents and enzymes

Table 5: Chemicals used during this study.

Chemical	Company
7 Aminoactinomycin D (7-AAD)	BD Pharmingen
Acrylamide/bisacrylamide 37.5:1	Roth
Agarose	Roth
Agar	Sigma-Aldrich
Ammoniumperoxodisulfate (APS)	Roth
Ampicillin	Sigma-Aldrich
Anti- phosphatase PhosSTOP	Roche

Bacto-Trypton	Difco
Blue Prestained Protein Molecular Weight Marker Mix	Pierce
Biozym Sieve GP Agarose	Biozym
BSA	PAA Laboratorien
Coelenterazine	Sigma
CoenzymeA	AppliChem
Chloroform	Merck
Cytofix/Cytoperm Buffer	BD Pharmingen
Dimethylsulfoxide (DMSO)	Sigma
D-luciferin	AppliChem
6x DNA loading dye	Fermentas
DNA Molecular Weight Marker PeqGold Leitermix	PeqLab
DNase, RNase free	Qiagen
deoxynucleoside triphosphate (dNTPS)	New England Biolabs
EDTA	Merck
Ethanol	Merck
Glycerol	Roth
Glycine	Gerbu
Hoeschst-33258	Sigma
HCl	Sigma
Isopropanol	Sigma
Lipofectamine2000 ™	Invitrogen

Methanol	Sigma-Aldrich
$MgSO_4$	Sigma-Aldrich
M-PER lysis buffer	Thermo Scientific
Na_2HPO_4	Sigma
NaCl	AnalaR NORMAPUR
NaH_2PO_4	Sigma
NaOH	Fluka
non-DEPC treated nuclease-free water	Ambion
Paraformaldehyde	Sigma-Aldrich
Perm/Wash buffer	BD Pharmingen
Phusion® Hot Start DNA Polymeras	New England Biolabs
protease inhibitor Complete Mini	Roche
4× Roti Load	Roth
Restriction enzymes	NEB
SDS	Roth
Skimmed milk powder	Roth
SOC medium	Invitrogen
sodium citrate tribasic dehydrate	AppliChem
sodium deoxycholate	Sigma
SYBR Green master mix, Universal RT, 25ml	Exiqon
TEMED	Roth
T4 DNA ligase	NEB
Tricine	Roth
Tris HCl	Sigma

Tris-base	Sigma
Triton X-100	Sigma
Tween 20	Sigma
WST-1 proliferation assay	Roche

2.1.4. Consumables

Table 6: Consumables used during this study.

Name	Company
1.5 mL microcentrifuge tube	Eppendorf
10cm Petri dish	TPP
15mL conical tube	BD Falcon
2 mL microcentrifuge tube	Eppendorf
50mL conical tube	BD Falcon
6-well plate, flat bottom, transparent	Nunc
96-well plate, flat bottom, transparent	BD Falcon
96-well plate, flat bottom, white	Perkin Elmer
384-well plate	Applied Biosystems
Blotting paper	Whatman
Cell Culture Flasks, T-25, T-75	TPP
Cell Scraper	Corning
Cryovials 1.8mL	Nunc
Facs tubes	BD Bioscience
Falcon tubes	Corning
Filter tips, 10µL, 20µL, 100µL, 200µL, 1000µL	Neptune
PCR strips	Steinbrenner
PVDF membrane (0.45µm)	Amersham
RTCA CIM-plates	Roche
RTCA E-plates	Roche
Serological pipettes 2.5mL, 5mL, 10mL, 25mL	BD Falcon

Adhesive Optically Clear Plate Seal	Thermo Scientific
PVDF membrane Immobilon-P	Millipore
Sentrix Human HT-12 v4 BeadArrays	Illumina
Whatman 3 MM filter paper	GE Healthcare

2.1.5. Bacterial strains and media

E. coli DH5alpha strain from Invitrogen and XL10-Gold ultracompetent cells from Stratagene were used in molecular cloning experiments.

Table 7: Bacterial media composition.

Bacteria culture media	
Luria-Bertani (LB)	10 g Bacto-trypto, 5 g yeast extract, 10g NaCl Dissolved in water up to 1L and autoclaved.
LB agar	15g of LB agar in 1L of the LB medium and autoclaved.

2.1.6. Cell lines

Table 8: Cell lines used in this study and their sources.

Human cell line	**Cancer type**	**Cell type/disease**	**Purchased from**
HEK293FT	Embryonic kidney	Epithelial	Invitrogen
MCF10A	Non-tumorigenic breast	Mammary epithelial	ATCC
SKBR3	Breast cancer	Adenocarcinoma	ATCC
MDA-MB-231	Breast cancer	Adenocarcinoma	ATCC

T47D	Breast cancer	Ductal adenocarcinoma	ATCC
UACC812	Breast cancer	Ductal carcinoma	ATCC
BT474	Breast cancer	Ductal carcinoma	ATCC
ZR7530	Breast cancer	Ductal carcinoma	ATCC

2.1.7. Cell culture media

Table 9: Cell culture media components and their manufacturing companies.

Name	Company
0.25% trypsin EDTA solution	GIBCO, Invitrogen
bovine insulin	Sigma
Choleratoxin	Sigma
DMEM	GIBCO, Invitrogen
DMEM F12	GIBCO, Invitrogen
DMSO	PAN Biotech
DPBS	GIBCO, Invitrogen
Fetal Bovine Serum	GIBCO, Invitrogen
Geniticin	Sigma
Horse serum	GIBCO, Invitrogen
Hydrocortisone	Sigma

Leibovitz's L-15	GIBCO, Invitrogen
L-glutamine, 200mM	GIBCO, Invitrogen
McCoy´s 5A medium	GIBCO, Invitrogen
MEM	GIBCO, Invitrogen
Non-essential amino acids (100x)	GIBCO, Invitrogen
OptiMEM	GIBCO, Invitrogen
Phosphate buffered Saline (PBS)	GIBCO, Invitrogen
Penicillin/Streptamycin	GIBCO, Invitrogen
Recombinant human EGF	BD Biosciences
Recombinant human LPS	Sigma
Recombinant human TNF-α	Sigma
RPMI 1640 (A10491-01)	GIBCO, Invitrogen
Sodium pyruvate, 100mM	GIBCO, Invitrogen
Streptomycin sulfate	GIBCO, Invitrogen

2.1.8. Plasmids

Table 10: Plasmids used during this study.

Name	Source
3xKBL	Kindly provided by Prof. George Mosialos

pMIR-REPORT β-gal vector	Ambion
psiCHECK2	Promega

2.1.9. Software and databases

Software

Adobe Photoshop CS3, Adobe

CellQuest Pro, BD Biosciences

GraphPad Prism, GraphPad Software, Inc

Lasergene, DNAstar

Odyssey software, Li-cor biosciences, Lincoln

SDS 2.2, Applied Biosystems

xCelligence Real Time Cell Analyzer (RTCA) software 1.2

Databases

GEO, http://www.ncbi.nlm.nih.gov/geo/

KEGG pathway database, http://www.genome.jp/kegg/pathway.html

miRWalk, http://www.umm.uni-heidelberg.de/apps/zmf/mirwalk/

MetaCore™, http://thomsonreuters.com/metacore/

NCBI, http://www.ncbi.nlm.nih.gov/

PrimerX, http://www.bioinformatics.org/primerx/

DAVID, http://david.abcc.ncifcrf.gov/

2.1.10. Primers

All primers used for sequencing, cloning or qRT-PCR were purchased from Sigma-Aldrich.

Sequencing primers

psiCHECK_seq_fwd: 5´ CCAGGATTCTTTTCCAATGC 3´

psiCHECK_seq_rev: 5´ CGAGGTCCGAAGACTCATTT 3´

Table 11: Sequences of PCR primers used for cloning and mutagenesis of TRADD and CCNE1 3´ UTR.

Name	Sequence(5´->3´)
TRADD_UTR-for	CTCGAGTCTGCGGCTATTGCTGAAC
TRADD_UTR-rev	GCGGCCGCTTCTCACATCAAAATCCGTG
TRADD_MUT-for	GAGATCAGCCTCACCAAGACCCATCCCAGAAGCGG
TRADD_MUT-rev	CCGCTTCTGGGATGGGTCTTGGTGAGGCTGATCTC
CCNE1_UTR-for	CTCGAGCCACGTTCTCTTCTGTCTGTTG
CCNE1_UTR-rev	GCGGCCGCAATGGATAGATATAGCAGCACTTAC
CCNE1_MUT-for	GCTACTTGACCTAAGGGACCGGGACAACAACAAAAGCTTGAAG
CCNE1_MUT-rev	CTTCAAGCTTTTGTTGTTGTCCCGGTCCCTTAGGTCAAGTAGC

Table 12: Sequences and Universal Probe Library (UPL) probe numbers of genes analyzed by Taqman qRT-PCR.

Name	Sequence (5'->3')	UPL Probe
GAPDH_L	AGCCACATCGCTCAGACAC	#60
GAPDH_R	GCCCAATACGACCAAATCC	#60

IL8_L	AGACAGCAGAGCACACAAGC	#72
IL8_R	ATGGTTCCTTCCGGTGGT	#72
CXCL1_L	TCCTGCATCCCCCATAGTTA	#52
CXCL1_R	CTTCAGGAACAGCCACCAGT	#52
IL6-L	GCCCAGCTATGAACTCCTTCT	#45
IL6-R	GAAGGCAGCAGGCAACAC	#45
HPRT-1_L	TGACCTTGATTTATTTTGCATACC	#73
HPRT-1_R	CGAGCAAGACGTTCAGTCCT	#73
TRADD_L	CAGAAGGTGGCAGTGTACAGG	#53
TRADD_R	CAGCATCTGCAGCACGTC	#53
CCNE1_L	GGCCAAAATCGACAGGAC	#36
CCNE1_R	GGGTCTGCACAGACTGCAT	#36
MMP-9_L	GAACCAATCTCACCGACAGG	#53
MMP-9_R	GCCACCCGAGTGTAACCATA	#53
MYC_L	CACCAGCAGCGACTCTGA	#43
MYC_R	GATCCAGACTCTGACCTTTTGC	#43
CSF2_L	TCTCAGAAATGTTTGACCTCCA	#1
CSF2_R	GCCCTTGAGCTTGGTGAG	#1

CCND1_L	GAAGATCGTCGCCACCTG	#67
CCND1_R	GACCTCCTCCTCGCACTTCT	#67

Primers for miRNA detection

miRNA specific primer sets for miR-30c-2-3p, SNO38b and SNO48 were purchased from Exiqon. SNO38b and SNO48 were used for normalization of miRNA expression analysis.

2.1.11. siRNAs and miRNAs

Table 13: siRNA and miRNAs used during this study

Name	Company
miRCURY LNA microRNA inhibitors	Exiqon
miRNA mimics	Dharmacon
siRNA oligos	Ambion

Table 14: Sequences of siRNAs used for targeting and knocking down the expression of RELA, TRADD, CCNE1.

Gene	siRNA ID	Sequence	
		Sense	Antisense
RELA	s11914	CCCUUUACGUCAUCCCUGAtt	UCAGGGAUGACGUAAAGGGAt
TRADD	s16607	GCGCAUACCUGUUUGUGGAtt	UCCACAAACAGGUAUGCGCtg
CCNE1	118605	CCGGGUUUACCCAAACUCAtt	UGAGUUUGGGUAAACCCGGtc

2.1.12. Antibodies

Table 15: Primary antibodies used in this study.

Detected protein	Catalog no.	Host	Company
Actin (20-33)	A5060	Rabbit	Sigma
NF-κB p105/p50	3035	Rabbit	Cell signaling
Phospho NF-κB p105/p50 (Ser933)	18E6	Rabbit	Cell signaling
Phospho-IKKα (Ser176)/IKKβ (Ser177)	C84E11	Rabbit	Cell signaling
IKKβ	2C8	Rabbit	Cell signaling
IKKα	3G12	Mouse	Cell signaling
GAPDH	14C10	Rabbit	Cell signaling
TRADD	sc-7868	Rabbit	Santa Cruz Biotechnologies
CCNE1	sc-247	Mouse	Santa Cruz Biotechnologies

Table 16: Secondary antibodies used in this study.

Detected protein	Catalog no.	Company
IRDye®680_rabbit	926-68071	Li-COR
IRDye®680_mouse	926-68070	Li-COR
IRDye®800_rabbit	926-32211	Li-COR
IRDye®800_mouse	926-32210	Li-COR

2.2. Methods

2.2.1. Cell Culture

Cell lines were cultured in media compositions (Table 17) according to ATCC recommendation.

Table 17: Media composition used for cell culture of different cell lines

Cell line	Base medium	Supplements
HEK293FT	DMEM	10%FCS, 1%L-Glu, 1% non-essential aminoacids, 1% Penicillin/Streptomycin, 1% Geneticin
MCF10A (growth)	DMEM-F12	5% Horse serum, 20ng/ml EGF, 0.5µg/ml Hydrocortisone, 100ng/ml Cholera toxin, 0.01mg/ml bovine insulin
MCF10A (resuspension)	DMEM-F12	20% Horse serum
SKBR-3	Mc Coy´s 5A	10%FBS, 1% Penicillin/Streptomycin
MDA-MB-231	Leibovitz´s L-15	10% FCS, 1% non-essential amino acids, 15g/L NaHCO3, 1% Penicillin/Streptomycin
T47D	RPMI-1640	10%FBS, 0.2 Units/ml bovine Insulin, 1% Penicillin/Streptomycin
ZR-75-30	RPMI-1640	10%FBS, 1% Penicillin/Streptomycin
UACC812	Leibovitz´s L-15	20% FBS, 1% Penicillin/Streptomycin, 20ng/ml of EGF, 2 mM L-glutamine
BT 474	DMEM	10%FBS, 1% Penicillin/Streptomycin;

Cell lines were checked for mycoplasma contamination and verified at the cell line authentication service at the DKFZ Core Facility. Human recombinant TNF-α was purchased from Sigma-Aldrich (St. Louis, MO, USA) and used at a final concentration of 20 ng/ml. Lipopolysaccharides from *Escherichia coli* 0127:B8 (Sigma-Aldrich) and used at a final concentration of 10 ng/ml.

2.2.2. Transfections

All transfections were performed in antibiotic free media using Lipofectamine 2000 (LF 2000) transfection reagent from Invitrogen (CA, USA). LF 2000 is a formulation of cationic lipid which forms complexes with DNA/RNA which can deliver these nucleic acids to adherent cells. Cells were seeded in full growth media and transfected when they reached 70-90% confluency. Short interfering (si) RNAs for TRADD, RELA and CCNE1 were used to knockdown respective proteins and mRNA. Si negative control (NTC) was used as a non-targeting control. miRNA-30c-2-3p mimic and mimic control (mimic CTRL) was used to overexpress miRNAs. siRNAs and miRNAs were used at a final concentration of 30 nM each using Lipofectamine 2000 transfection reagent.

2.2.3. NF-κB reporter luciferase assay

NF-κB reporter assay was used to study the effect of miRNA overexpression or gene knockdown on activation of signaling pathway. For performing NF-κB reporter assay, HEK293FT cells were seeded at a density of 6000 cells per well in 96-well plates. 24 hours later cells were transfected with miRNA mimic or siRNAs, together with the NF-κB reporter 3xKBL plasmid which contains 3 consensus NF-κB binding sites upstream of the firefly gene (provided by Prof. Mosialos) and pMIR-REPORT β-gal vector. Cells were stimulated with TNF-α (20 ng/ml) or LPS (10 ng/ml) 48 hours after transfection, and luciferase activity was measured after 5 hours. β-galactosidase which is driven by CMV promoter activity was used for normalization, and measured by beta-glo® Luminescent Assay Kit (Promega, Madison, WI, USA). For measuring luminescence, medium was aspirated from wells and cells were washed with PBS. Later cells were lysed in 100 µl per well of M-PER or lysis buffer for mammalian cells for 10 min at

room temperature. Cells were carefully resuspended in order to insure complete lysis. Luminescence intensity of each well was measured by the plate reader (TECAN infinite200 microplate reader). For data analysis, the ratio of firefly over β-galactosidase readouts was evaluated for each well.

2.2.4. 3´UTR targeting luciferase assay

To prove direct targeting by miR-30c-2-3p, 3´UTRs of TRADD (NM_003789) and CCNE1 (NM_001238) were cloned downstream of *Renilla* luciferase into psiCHECK2 vector using *XhoI* and *NotI* restriction sites. 3´UTR was PCR amplified from human genomic DNA of the HEK293 cell line. For introducing mutation in miRNA binding site, QuikChange Lightning Site-Directed Mutagenesis kit was used. The master mix was made as given in Table 18. Primers were designed using PrimerX tool (http://www.bioinformatics.org/primerx/). The PCR program used was: 95°C for 2 minutes, 18 cycles of 95°C for 20 seconds, 60°C for 10 seconds and 68°C for 3 minutes. This was followed by a final extension for 68°C 5 minutes. The PCR product was then digested with 2 µl of *DpnI* restriction enzyme for 5 minutes at 37°C. XL10-Gold ultracompetent cells were transformed with the PCR product using the heat shock method. Bacterial cells were later plated onto ampicillin resistant agar plates and incubated at 37°C overnight. Next day colonies were picked and inoculated in LB medium with ampicillin. 24 hours later DNA was purified using midi prep kit and sent for sequencing.

Table 18: Master mix composition per reaction.

Master mix for mutagenesis	Volume
10x reaction buffer	5 µl
DNA template (50 ng)	1 µl
Primer_mut-forward (10 µM)	2 µl
Primer_mut-reverse (10 µM)	2 µl
dNTP mix (10 mM)	1 µl
QuikSolution reagent	1,5 µl
Water	37,5 µl
QuikChange Lightning Enzyme	1 µl

For performing the assay, cells were co-transfected with mimic miRNAs and psicheck vectors (wild type or mutated) in MDA-MB-231 cells. 48 hours after transfection *Renilla* and firefly luciferase activities were determined using plate reader (TECAN infinite200 microplate reader). No stimulation was used for these experiments. For data analysis, the ratio of *Renilla* over firefly (used for normalization) readouts was computed for each well.

2.2.5. Whole transcriptome profiling

MDA-MB-231 cells were transfected with miR-30c-2-3p or mimic control in 6-well plates. Cells were harvested 48 hours later and total RNA was isolated using the RNeasy Mini Kit (Qiagen, Hilden, Germany) according to the manufacturer's protocol. miRNA overexpression was confirmed using qRT-PCR. Quality control of total RNA (Agilent bioanalyzer, Santa Clara, CA, USA) and gene expression profiling (Illumina whole genome Bead Chip® Sentrix arrays HumanHT-12 v4, San Diego, CA, USA) were performed by the DKFZ microarray core facility. Expression profiling data was

normalized and analyzed for changes in expression levels using the vsn bioconductor package in R (http://www.bioconductor.org/packages/2.12/bioc/html/vsn.html).

2.2.6. Quantitative Real-Time PCR

For protein coding genes, primers and probes for TaqMan® qRT-PCR were designed using the Universal Probe Library (UPL) site (https://lifescience.roche.com/shop/home). UPL technology from Roche (Roche, Penzberg, Germany) is based on short hydrolysis probes whose 5´ end is labelled with fluorescein (FAM) and 3´ end has a quencher dye. These probes (165 in total) are 8-9 nucleotides long and have Locked Nucleic Acids (LNAs) incorporated into them. Primer sequences used for genes of interests and corresponding probes from the Universal Probe Library are listed in materials section. For mRNA qRT-PCR, RevertAid™H Minus First Strand cDNA synthesis kit from Fermentas (Karlsruhe, Germany) was used for the synthesis of cDNA according to the manufacturer's instructions. For the quantification of mRNA of interest, 10 ng of cDNA made from equivalent RNA was used per well of 348 plate. 5µl of cDNA (2ng/µl) was added with 6µl of enzymatic master mix (Table 19), with 11µl of total volume in each well.

Table 19: Master mix composition per reaction.

Master mix composition	Volume
ABsolute QPCR Mix	5.5µl
Forward primer (10 µM)	0.11µl
Reverse primer (10 µM)	0.11µl
UPL probe	0.11µl
Nuclease free water	0.17µl

This master mix was then pipetted on 384 well plate along with cDNAs in triplicates. The PCR program used for the qRT-PCR was 2 minutes at 50°C followed by 15 minutes at 95°C to activate the master mix. This was followed by 45 cycles of 15

seconds at 95°C and 60 seconds at 60°C. After finishing the PCR run, raw Ct value data was retrieved using the SDS software v2.1. GAPDH and HPRT were used as normalizing controls for mRNA expression analysis. Results were analyzed using 2(-Delta Delta C(T)) method [109].

For miRNA quantification using TaqMan®, first miRNA was isolated using the miRNeasy Mini kit (from Qiagen) according to the manufacturer's recommendations. Exiqon miRNA Universal Reverse Transcription kit was used for miR-30c-2-3p detection. In the first step for reverse transcription, the template RNA samples were adjusted to a final concentration of 5 ng/µl using nuclease free water. Then, a master mix (Table 20) was prepared.

Table 20: Master mix composition per reaction.

Master mix composition per reaction	Volume
5x Reaction Buffer	4 µl
Nuclease-free water	10 µl
Enzyme mix	2 µl
template RNA (5 ng/µl)	4 µl

The reaction mixture was incubated for 60 minutes at 42°C. Later, the reverse transcriptase was heat inactivated at 95°C for 5 minutes and immediately transferred to 4°C. All reactions were diluted with nuclease-free water to a 1:20 ratio. miR-30c-2-3p, SNO38b and SNO48 specific primer sets were purchased from Exiqon (Vedbaek, Denmark). For the quantitative miRNA expression studies using the Exiqon miRNA qRT-PCR assay, 4 µl of the 1:20 diluted RT reaction were mixed with 5 µl SYBR green master mix and 1 µl of primer mix, yielding 10 µl total sample volume (per reaction). A 384-well plate layout document was prepared using the SDS software. The PCR program of the RT-PCR followed by a melting curve analysis was 10 minutes at 95°C to activate the master mix. This was followed by 45 cycles of 10 seconds at 95°C and 60 seconds at 60°C. After finishing the PCR, raw data was evaluated using the SDS

software v2.1. SNO38b and SNO48 were used for normalization in miRNA expression analysis.

2.2.7. Immunoblotting

For cell lysate collection, cells were transfected previously in 6-well plates. 48 hours after transfection with miRNA or siRNA, medium was aspirated from the cells and they were washed with ice-cold PBS. Cells were then lysed in M-PER supplemented with protease inhibitor (Complete Mini EDTA-free proteinase inhibitor, Roche) and phosphatase inhibitor (Phospho-Stop, Roche). 70µl of this mixture was added on cells, and cells were detached by scraping. Cell lysate was then incubated in 4°C for 20 minutes on a vertical rotor. Later the lysate was centrifuged at 13,000 rpm for 15 minutes at 4°C and clear supernatant was transferred to a new 1.5 ml tube which was stored at -80°C. Protein concentration of samples was quantified using Thermo Scientific™ Pierce™ BCA™ Protein Assay according to the manufacturer's instructions.

SDS-PAGE (sodium dodecyl sulphate-polyacrylamide gel electrophoresis) was used to separate proteins according to their molecular weights. 15 µg of total protein lysate was mixed with protein loading buffer (4x Roti Load) and denatured for 5 minutes at 95 °C. Denatured proteins were loaded unto mini polyacrylamide gel (3% stacking gel/12% separating gel) along with the molecular weight protein marker (Precision Plus Protein^{TM} Dual Color Standard). The gel was run at 120 Volt for 70 minutes allowing separation of proteins, tracked with the help of Protein^{TM} Dual Color Standard marker.

Separated proteins were then transferred onto Immobilon-P membrane (Millipore) using semi dry transfer. The membrane was activated in absolute ethanol for 1 min and later transferred to anode solution II for 10 minutes. Whatman filter papers were soaked and equilibrated in blotting solutions. Four filter papers were soaked in anode solution I, two in anode solution II and six in cathode solution. The gel was placed on top of the activated membrane, and placed in between soaked whatman filter papers. Semi-dry

transfer was performed in the Trans-Blot SD Semi-Dry Electrophoretic Transfer Cell for 1 hour at 25 Volt.

The membrane was blocked after completion of transfer for 1 hour at room temperature with 5% non-fat milk made in in 1x TBST buffer. Later the membrane was incubated overnight with respective primary antibody at 4°C, using a 1:1000 dilution in 1xTBST. Next day, the membrane was washed 3x 5 minutes with 1xTBST, incubated for 1 hour at RT with the secondary antibody (IRDye®680 or IRDye®800), using a 1:10000 dilution in 1xTBST and later washed 3x5 minutes with 1x TBST. The bands were visualized using an Odyssey scanner (LI-COR).

2.2.8. Cell proliferation and apoptosis assays

Cells were transfected in 96-well white plates in 100µl of full growth media. 72 hours after transfection with miRNAs/siRNAs, cell viability and proliferation was measured using either WST reagent from Roche (Penzberg, Germany) or Celltiter Blue from Promega (Madison, WI, USA). WST measures the levels of NAD(P)H in viable and metabolically active cells. 10 µl of WST was added to each well. After 3 hours of incubation, absorbance was measured at 460 nm. Celltiter Blue on the other hand measures the ability of viable cells to reduce resazurin to resorufin, a fluorescence product that can be read at 560Ex/590Em. 20 µl of Celltiter Blue was added to each well and incubated for 3 hours before the measurement. Apoptosis was measured using caspase glo 3/7 assay kit from Promega (Madison, WI, USA). It is a luminescence based assay that measures the activities of caspase 3 and caspase 7. The luminescence measured is proportional to the amount of active caspase3/7. 100µl of reagent was added to each well and luminescence was measured in a plate reader after one hour incubation at room temperature. All experiments were performed according to the manufacturer's recommendations.

7-AAD (7-Aminoactinomycin D) and BrdU (5-bromo-2'-deoxyuridine) staining for cell cycle assays were carried out according to the manufacturer's protocol (BD Pharmingen San Diego, CA, USA). 7-AAD is a DNA intercalating dye and florescent in nature. It is

excluded from live cells and therefore cells need to be fixed and permeabilized, to allow binding with 7-AAD. BrdU is a chemical analogue of thymidine and can get incorporated specifically in cells in S-phase of cell cycle. Monoclonal antibodies directed against BrdU can then be used to detect and differentiate dividing from not dividing population of cells. For performing the assay, cells were seeded in 24-wells plate in full growth media. 72 hours after transfection with miRNA/siRNAs the cells were incubated with BrdU at a final concentration of 1 µM for 1 hour at 37ºC temperature. Cells were then harvested and treated with DNase1 for one hour at 37ºC. Later, cells were washed and resuspended in anti-BrdU FITC-conjugated antibody purchased from BD Pharmingen (San Diego, CA, USA). Half an hour later cells were washed and resuspended in 7-AAD solution for another half an hours. Stained cells were then measured by flow cytometry using a FACS Calibur (BD Biosciences, Heidelberg, Germany) and Cell Quest Pro software (BD Biosciences, Heidelberg, Germany) was used for data analysis. No stimulation was used for cell viability, apoptosis and cell cycle progression experiments.

For direct cell counting of cells, Olympus ScanR high-content screening microscope was used. Cells were seeded in glass bottom square well MatriPlates and transfected with miRNA or mimic control. Hoeschst-33258 diluted to 1:5000 in starvation medium was used to stain DNA of cells. After 30 minutes, cells were washed with PBS and replaced by starvation media. The florescence intensity was used to count the DNA content of cells. Analysis of the images was performed using ScanR analysis software.

2.2.9. Invasion assay

Invasion experiments were performed using a Real Time Cell Analyzer (RTCA, xCELLigence, Roche, Germany). This instrument detects changes in electric cell impedance upon cell attachment or cell doubling. Cell index (CI) is measured as a function of electrical impedance and gives a measure of cell number. CIM plates were used to record the impedance of the invading cells. MDA-MB-231 cells were transfected in 6-well plates. 24 hours after transfection, cells were starved overnight in 0.5% FBS medium. The next day, cells were trypsinized, washed once with starvation

medium, counted using a CASY cell counter and adjusted to a cell number of 75,000 cells/100 µL in starvation medium. The upper chamber was coated with growth factor reduced matrigel matrix from Corning (Tewksbury, MA, USA) at a dilution of 1:30 in starvation media. Matrigel was allowed to solidify in the upper chamber of CIM plate for 4 hours at 37°C. The cell suspension was then seeded on top of the matrigel. The lower compartment was filled with 175 µl full growth medium. CIM plates were placed in RTCA instrument and cell index values were recorded with a time-interval of 15 minutes for a total of 15 hours.

2.2.10. Wound healing assay

MCF-10A cells were seeded in glass bottom plate at a density of 55,000 cells per well in full growth medium. Next day, cells were transfected with siRNAs or miRNAs in antibiotic free medium. 24 hours after transfection the full growth medium was removed and replaced with starvation medium. After over 16 hours of starvation, cells were stained with CMFDA (5-Chloromethylfluorescein Diacetate), cell tracker green dye (MW 464.86). This dye has absorption at 492 nm wavelength and emission at 517 nm. The dye was used at a final concentration of 0.5-25 µM (1:5000) in starvation medium. Cells were incubated with dye for 30 minutes and later the medium was removed. This was replaced then with starvation medium without the dye and incubated for another 30 minutes. Later, a uniform wound was made on monolayer of cells using Beckman Coulter robot. The medium of cells was then changed back to full growth media. Olympus ScanR high-content microscope was then used to take pictures of cells before they started migrating. Cells were then allowed to migrate for 14 hours in presence of EGF present in full growth media and images were taken using Olympus ScanR high-content microscope. The average distance migrated (A.M.D) by the cells was then calculated using qCMA software [110].

2.2.11. Patient Data Analysis

Breast cancer patient dataset analysis was performed by Ashwini Kumar Sharma from the Division of Theoretical Bioinformatics, DKFZ. Normalized mRNA and miRNA

expression data from the METABRIC study [106, 111] was used to analyze differential expression of target genes in ER subgroups. To investigate this, dataset consisting of 781 patients whose ER status was known and who had both mRNA and corresponding miRNA expression data available (N = 781) was analyzed. Welch's t-test was performed to detect significant differential expression changes between the two ER subgroups. MiRNA expression levels were categorized based on distribution quartiles into low (<Q1), medium (Q1-Q3) and high (>Q3) expression group. To evaluate association between mRNA and miRNA, a linear regression analysis was performed on scale normalized miRNA and mRNA expression data according to Spearman rank correlation. Fisher's exact test was used to test association between miRNA groups and categorical clinico-pathological factors. Kruskal-Wallis test was used to test association between miRNA groups and quantitative clinico-pathological factors. For outcome analysis, disease-specific survival (DSS) was analysed as in [106], with disease-unrelated deaths being censored. Univariate and multivariate Cox regression was used to assess the prognostic impact of miRNA expression levels and clinico-pathological factors for DSS. This analysis was performed by Thomas Hielscher from the Division of Biostatistics, DKFZ. Survival analysis was done using R package, from CRAN (http://CRAN.R-project.org/package=survival). All analyses were carried out using software R 3.0.1 (http://www.R-project.org) or GraphPad Prism 5.0 software. All *t* tests were two-sided tests. P-values below 0.05 are considered statistically significant.

3. Results

3.1. miR-30c-2-3p negatively regulates NF-κB signaling and is down-regulated in ER negative breast cancer patients

A genome wide miRNA screen had been carried out previously to identify novel miRNA regulators of NF-κB signaling [103]. This screen had been based on a NF-κB reporter construct with three binding sites for NF-κB cloned in the promoter upstream of the luciferase ORF [103]. miRNA mimics were individually co-transfected with the NF-κB reporter construct together with β-galactosidase vector into HEK293FT cells. At 48 hours after transfection, cells were treated with TNF-α for 5 hours to stimulate NF-κB signaling, luminescence was then quantified. β-galactosidase was used for normalization of luciferase signal. In this screen, miR-30c-2-3p was as the third strongest negative regulator of the signaling pathway with a z-score of -2.031 among the 810 miRNAs screened (Figure 5A). To validate the result from screening, I repeated the NF-κB luciferase reporter assay again in the HEK293FT cell line and found that miR-30c-2-3p overexpression reproducibly abrogated NF-κB activity, which was similar to RNAi induced knockdown of RelA which was used as a positive control (Figure 5B). To study the role of miR-30c-2-3p in NF-κB regulation in the context of breast cancer, I next overexpressed the miRNA in the MDA-MB-231 cell line, an established model for ER- breast cancer [112]. miR-30c-2-3p overexpression decreased phosphorylation of NF-κB1 precursor compared to mimic control upon TNF-α stimulation, proving that indeed miR-30c-2-3p inhibited activation of NF-κB signaling also in the context of breast cancer (Figure 5C).

To ascertain the role of miR-30c-2-3p in breast cancer patients, I next investigated whether endogenous expression levels of miR-30c-2-3p were associated with the ER status of patients, since NF-κB signaling is known to be constitutively active in ER negative breast cancer tumors [44, 46]. To investigate this, dataset from the METABRIC (Molecular Taxonomy of Breast Cancer International Consortium) study was analyzed, which has miRNA expression data from a cohort of 781 breast tumors [106]. This analysis identified miR-30c-2-3p as a significantly downregulated miRNAs in ER negative versus ER positive breast cancer patients (Figure 5D and E). The same

relation between miR-30c-2-3p expression and ER status was verified (Figure 6A) in an independent cohort of 432 breast tumors from The Cancer Genome Atlas (TCGA) [6]. This was further validated *in vitro* in a panel of seven breast epithelial cell lines where the endogenous expression of miR-30c-2-3p was lower in ER negative compared to ER positive cell lines (Figure 6B). However, from cell line data only a trend was observed ($P = 0.057$).

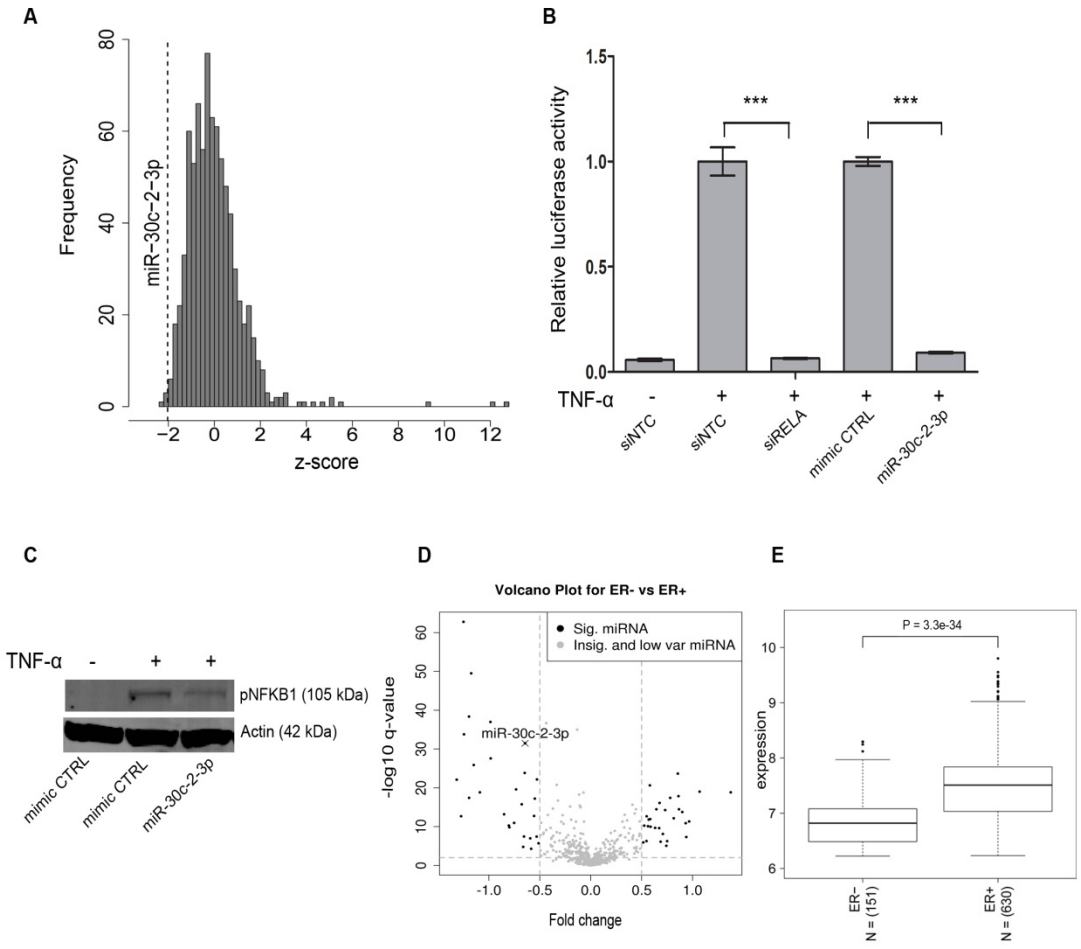

Figure 5: miR-30c-2-3p regulates NF-κB signaling in breast cancer. (A) z-score distribution of 810 miRNAs screened for effects on NF-κB signaling based on 3xKBL luciferase assay where miR-30c-2-3p was the third strongest negative regulator with a z-score of -2.031 [103]. (B) Validation of the screen results where miR-30c-2-3p strongly reduced the luciferase signal in HEK293FT cell line to measure NF-κB activity upon stimulation of the signaling by TNF-α (20 ng/ml). β-galactosidase was used for normalization. siRELA was used as a positive control (***p≤0.001 compared to respective stimulated control, *t* test). Data are shown as mean±s.d of two biological and three technical replicates. (C) phospho-NF-κB1 protein levels are downregulated upon treatment of MDA-MB-231 with 20 ng/ml of TNF-α for 10 minutes in cells transfected with miR-30c-2-3p mimic compared to mimic CTRL. Cells were harvested 48h after transfection. Actin was used as a loading control. (D) Volcano plot showing miR-30c-2-3p as one of the most deregulated miRNA based on the fold change and q value (P value corrected for multiple testing, Benjamini-Hochberg) out of the 853 miRNAs analyzed in the METABRIC study [106]. Black dots represent significant genes miRNA and gray dots represent insignificant and low variance miRNAs. (E) miR-30c-2-3p was downregulated in ER negative compared to ER positive breast cancer patients in the METABRIC dataset [106] (P = 3.3e-34).

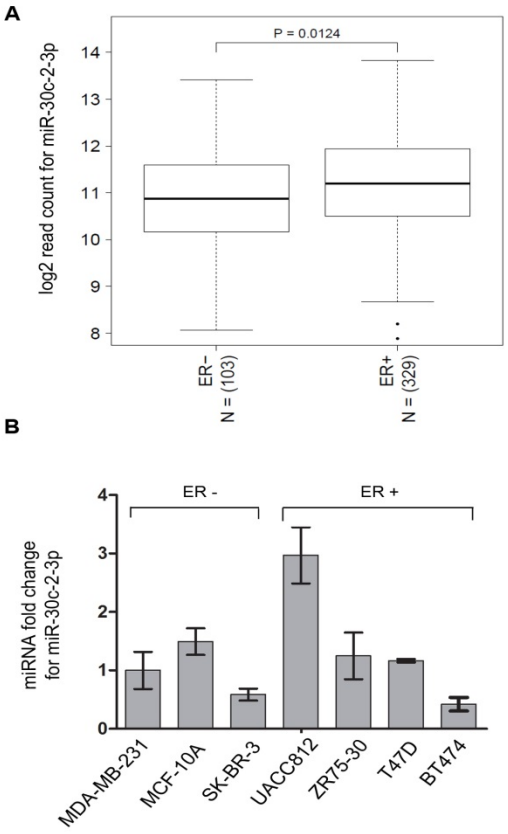

Figure 6: Expression levels of miR-30c-2-3p in an independent breast cancer patient dataset and breast epithelial cell lines. (A) miR-30c-2-3p was found to be lower expressed in ER negative compared to ER positive breast cancer patients (P = 0.0124) in TCGA study [6]. (B) Validation of miR-30c-2-3p expression in a panel of seven breast epithelial cell lines. The expression of miR-30c-2-3p showed a trend of higher level in ER positive compare to ER negative breast cell lines (P = 0.057). Data are shown as mean±s.d of two biological and three technical replicates.

3.2. Expression of miR-30c-2-3p significantly correlates with clinico-pathological features in breast cancer patients

Since miR-30c-2-3p is significantly associated with the ER status in breast cancer, I hypothesized that its expression might also correlate with additional clinico-pathological parameters in patients like tumor grade, tumor size, age at diagnosis, lymph node invasion, HER2 expression, progesterone receptor (PR) status and TP53 status. To test this hypothesis, the METABRIC dataset [106] was analyzed by Thomas Hielscher from the Division of Biostatistics, DKFZ.

To investigate this, miRNA expression levels were categorized based on distribution quartiles into low (<Q1), medium (Q1-Q3) and high (>Q3) expression groups of patients. These groups were then tested for association between miRNA groups and categorical clinico-pathological factors. Indeed, a significant correlation between low expression levels of miR-30c-2-3p and the presence of adverse prognostic factors was found (Table 21). Furthermore, disease-specific survival was significantly better in patients with medium (HR = 0.64, P = 0.005) and high (HR = 0.43, P<0.0001) miR-30c-2-3p expression levels in univariate analysis (Table 22). However in multivariate analysis, miR-30c-2-3p expression did not remain an independent prognostic factor of disease specific survival in breast cancer patients (Table 22).

Table 21: Association of miR-30c-2-3p expression with clinico-pathological features in breast cancer patients. Breast cancer patient data from METABRIC study [106].

	Parameter	P value
1	Tumor grade	< 1e-04
2	Tumor size	0.01910
3	Age at diagnosis	< 1e-04
4	Lymph nodes positive	< 1e-04
5	ER	< 1e-04
6	HER2	< 1e-04
7	PR	< 1e-04
8	TP53 mutation status	< 1e-04

Table 22: Univariate and multivariate Cox proportional hazard regression analysis in breast cancer patients to evaluate prognostic impact of miR-30c-2-3p expression. Breast cancer patient data from METABRIC study [106].

ref: Reference, HR: Hazard ratio, LCL: Lower confidence limit, UCL: Upper confidence limit, low , mid and high levels refers to the expression level of miR based on distribution quartile, tumor grade 1, 2 , 3 refers to differentiation status, +/- indicate presence or absence of receptor, WT: wild type, MUT: mutated type.

				Univariate analysis				Multivariate analysis			
	covariate	level	ref	HR	LCL	UCL	P value	HR	LCL	UCL	P value
1.	miR-30c-2-3p expression in 3 groups	mid	low	0.64	0.46	0.87	0.00505	0.97	0.65	1.45	0.89594
		high	low	0.43	0.28	0.66	< 1e-04	0.84	0.49	1.45	0.53023
2.	Tumor grade	2	1	1.10	0.53	2.32	0.79486	0.99	0.42	2.35	0.97807
		3	1	2.44	1.19	4.98	0.01451	1.57	0.66	3.71	0.30951
3.	Tumor size			1.02	1.02	1.03	< 1e-04	1.01	1.00	1.02	0.00805
4.	Age at diagnosis			1.00	0.98	1.01	0.42995	1.00	0.99	1.02	0.74225
5.	Lymph nodes positive			1.11	1.08	1.14	< 1e-04	1.07	1.04	1.11	< 1e-04
6.	ER	+	-	0.44	0.32	0.60	< 1e-04	0.75	0.47	1.21	0.24080
7.	HER2	+	-	2.50	1.74	3.58	< 1e-04	1.80	1.18	2.76	0.00632
8.	PR	+	-	0.49	0.37	0.65	< 1e-04	0.87	0.58	1.30	0.49510
9.	TP53 mutation status	WT	MUT	0.35	0.24	0.51	< 1e-04	0.50	0.33	0.75	0.00098

3.3. Ectopic expression of miR-30c-2-3p reduces expression of genes relevant in inflammation, decreases cell proliferation, and invasion/migration

To investigate the role of miR-30c-2-3p in the regulation of NF-κB signaling, I evaluated the expression of NF-κB targets genes in response to TNF-α stimulation in miR-30c-2-3p transfected MDA-MB-231 cells. Expression of proinflammatory cytokines *IL8*, *IL6*, and *CXCL1* was strongly downregulated in cells transfected with miR-30c-2-3p compared to mimic control transfected cells upon induction of signaling with TNF-α (Figure 7A). Next, I checked expression of *MYC*, *CCND1* and *CSF2* which are also known NF-κB transcriptional targets involved in promoting cell proliferation [48, 113, 114]. Indeed, qRT-PCR showed that these genes were significantly reduced in miR-30c-2-3p over-expressing cells (Figure 7B). To test the effects of miR-30c-2-3p overexpression on basal level of cell proliferation, I performed cell proliferation assays in absence of any stimulation. This showed that miR-30c-2-3p significantly decreased cell proliferation in MDA-MB-231 cells (Figure 7C). Finally, to study the effects on cell cycle progression, I performed BrdU and 7-AAD staining on miR-30c-2-3p and mimic control transfected cells. Overexpression of miR-30c-2-3p significantly blocked cell cycle progression in MDA-MB-231 cells with only 2.65(+/-0.73) % cells in S-phase of cell cycle compared to 17.10(+/-2.6) % in the control (Figure 7D).

Since NF-κB signaling also positively regulates cell invasion, and MDA-MB-231 is a highly invasive cell line [115], I wanted to investigate if miR-30c-2-3p was also capable of abrogating cell invasion. Indeed, a decreased invasive capacity of MDA-MB-231 cells was observed upon miR-30c-2-3p overexpression as measured in Real Time Cell Analyzer (RTCA) (Figure 7E). Since NF-κB signaling has previously been shown to facilitate cell invasion/migration through the regulation of metalloproteinases (MMPs), like MMP-9 [116], I hypothesized that decreased invasion might be accompanied by decreased MMP-9 levels upon miR-30c-2-3p overexpression. Indeed, downregulation of MMP-9 was observed at the mRNA level in the presence of miR-30c-2-3p upon TNF-α stimulation (Figure 7F).

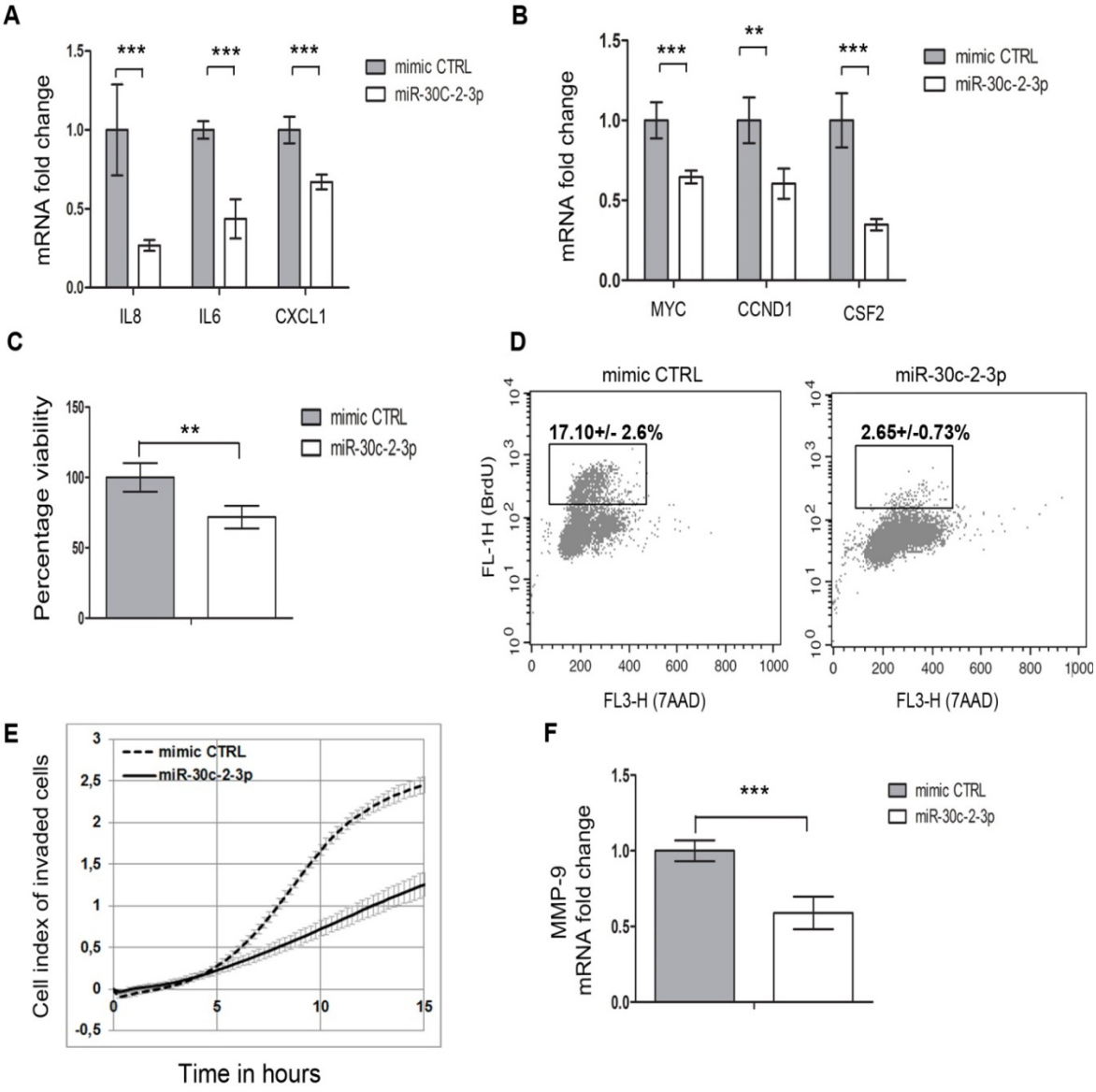

Figure 7: Effect of miR-30c-2-3p overexpression on expression of cytokines, cell proliferation and cell invasion in MDA-MB-231 breast cancer cell line. (A) mRNA expression of inflammatory cytokines *IL8, IL6* and *CXCL1* is reduced upon miR-30c-2-3p overexpression. To activate NF-κB signaling, cells were treated with TNF-α **(**20 ng/ml**)** for 5 hours before being harvested. (***p≤0.001 compared to stimulated control, *t* test). (B) In the same experimental setup, reduced mRNA levels of proliferation related genes *MYC, CCND1* and *CSF2* was observed (***p≤0.001, **p≤0.01 compared to stimulated control, *t* test). (C) miR-30c-2-3p reduced cell viability compared to mimic CTRL measured 72 hours after transfection. (**p≤0.01 compared to control, *t* test). (D) 7-AAD and BrdU staining was measured 72 hours after transfection with mimic CTRL or miR-30c-2-3p to measure cell cycle phases. A reduced S-phase population, gated for BrdU positive cells was observed upon miR-30c-2-3p overexpression (***p≤0.001 compared to control, *t* test). (E) miR-30c-2-3p reduced the invading capability of MDA-MB-231 cells. Significance was tested at the 15 hour time point measured in Real-Time Cell Analyzer (RTCA), which was 48 hours after transfection with miRNA (***p≤0.001 compared to control, *t* test). (F) Concordantly, reduced level of mRNA level of MMP-9 by miR-30c-2-3p upon TNF-α **(**20 ng/ml**)** treatment of cells for 5 hours to activate the signaling. Cells were harvested 48 hours after transfection with miRNA (***p≤0.001 compared to stimulated control, *t* test). Data are shown as mean±s.d of two biological and three technical replicates.

To further study the effect on cell proliferation, I did direct cell counting of cells after transfection of MDA-MB-231 cells with mimic control or miR-30c-2-3p. After 72 hours of transfection, miR-30c-2-3p overexpressing cells were fewer in number as seen in bright field microscope (Figure 8A). When cells were counted and analyzed after Hoechst staining in Olympus ScanR microscope, the cell number was significantly reduced compared to mimic control transfected cells (Figure 8B).

Next, I wanted to investigate if miR-30c-2-3p is capable of inducing apoptosis in cells. To this effect, I measured the caspase 3/7 activity in cells transfected with miR-30c-2-3p or mimic control. MDA-MB-231 cells overexpressing miR-30c-2-3p had higher caspase3/7 activity, 72 hours post transfection (Figure 8C). These effects on proliferation and apoptosis were independently verified in another the ER negative breast cell line, MCF10A (Figure 9A and B).

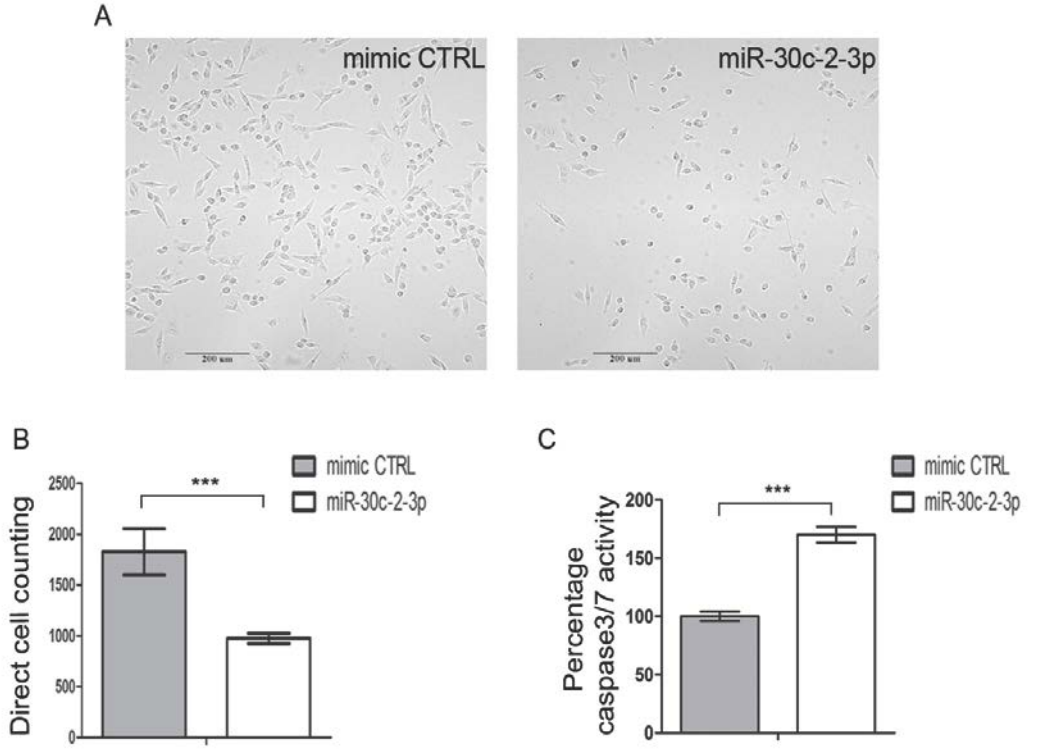

Figure 8: miR-30c-2-3p overexpression reduced cell number and increased apoptosis in MDA-MB-231 cells. (A) MDA-MB-231 cells were seeded in 96-well glass bottom plates and transfected with miR-30c-2-3p or mimic CTRL. After 72 hours of transfection, miR-30c-2-3p transfected cells were more round in shape and fewer cell were attached to the surface compared to mimic control transfected cells. Images were taken at 10x magnification with bright field microscope. (B) For quantification cells were stained with Hoechst dye and counted using Olympus ScanR microscope**.** miR-30c-2-3p overexpressing cells were significantly reduced compared to the control (***p≤0.001 compared to control, *t* test). (C) miR-30c-2-3p increases apoptosis compared to mimic control in MDA-MB-231 cell line 72 hours after transfection (***p≤0.001 compared to control, *t* test). Data are shown as mean from two biological and three technical replicates ±s.d.

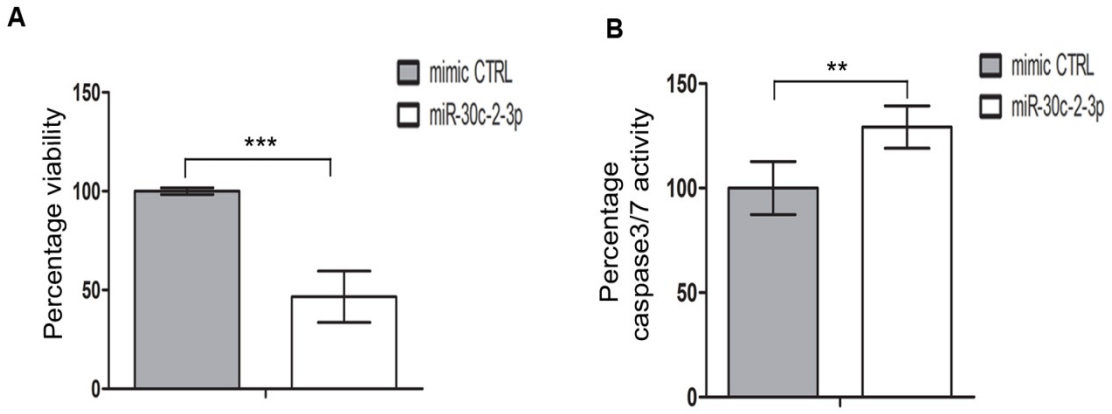

Figure 9: Effects of miR-30c-2-3p overexpression in MCF-10A cells. (A) Decreased cell viability (B) and increased apoptosis in MCF-10A was observed compared to mimic CTRL, 72 hours after transfection. (***p≤0.001 compared to control, *t* test). Data are shown as mean from two biological and three technical replicates ±s.d.

To study the effect of miR-30c-2-3p on cell migration, I used MCF-10A as the cell line system because it is a non-tumorigenic breast epithelial cell line, with strong migration ability in response to EGF and the ability to form an epithelial sheet when confluent [117]. This confluent sheet can be scratched and used to study cell migration using a scratch-wound assay (Figure 10). This assay is well recognized for measuring epithelial cell motility [118]. For evaluating the Average Migratory Distance (A.M.D) covered by the cells during the migration assay, generic merge software program was used [110].

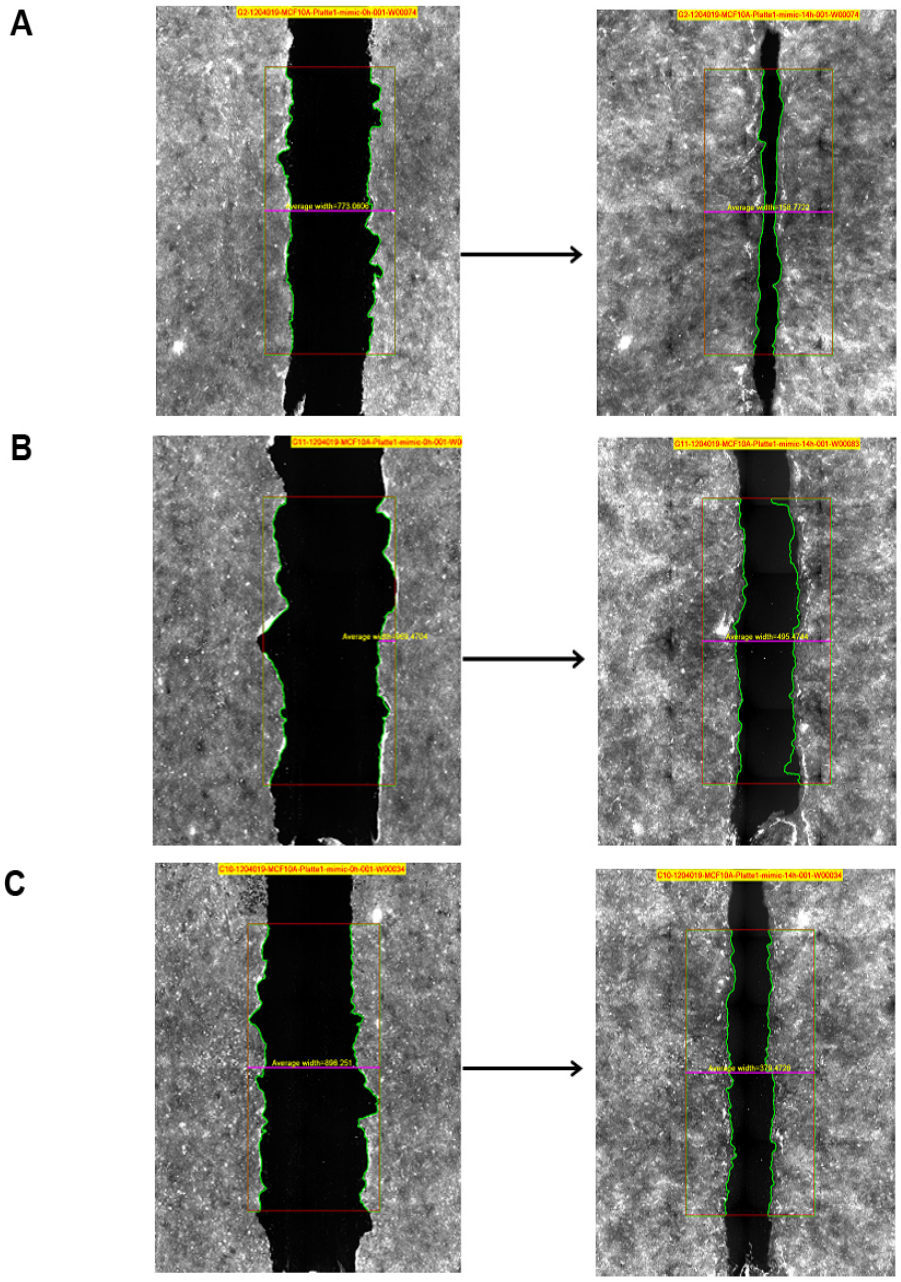

Figure 10: miR-30c-2-3p is an inhibitor of migration in MCF-10A cell line. An artificial wound was introduced on monolayer of cells 48 hours after transfection with (A) negative (non-targeting controls) (B) positive controls (siEGFR) and (C) miR-30c-2-3p. Cells were then induced to migrate with full growth media containing 20 ng/ml of EGF. The average distance migrated by the cells was then calculated 14 hours post EGF stimulation. Data are shown as mean from two biological and three technical replicates ±s.d.

miR-30c-2-3p transfected cells showed reduced migratory capability in response to EGF (Figure 10) compared to control transfected cells. Upon quantification of the distance migrated by cells, miR-30c-2-3p transfected cells had 60% lower migratory ability compared to control transfected cells (Figure 11). siEGFR was used as a positive control for the experiments.

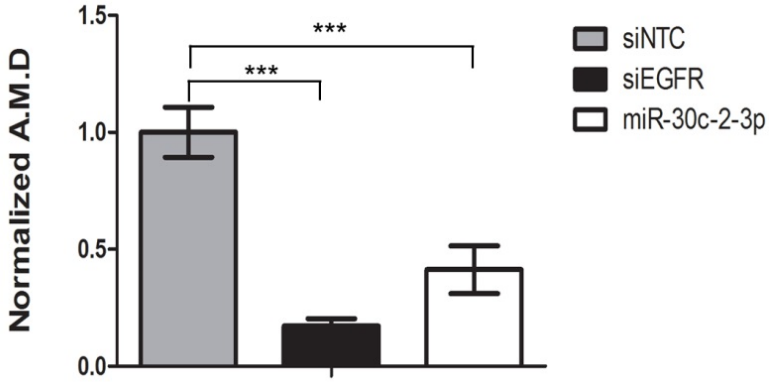

Figure 11: Quantification of MCF-10 A cell migration upon miR-30c-2-3p overexpression. Cell migration was significantly reduced upon miR-30c-2-3p overexpression in response to EGF. Data are shown as mean from two biological and three technical replicates ±s.d.

3.4. miR-30c-2-3p directly targets TRADD

Next, I wanted to uncover the molecular mechanism of regulation by miR-30c-2-3p to explain the different observed phenotypes in breast cancer cells. To this end, I performed a whole transcriptome mRNA expression analysis of MDA-MB-231 cells transfected with miR-30c-2-3p compared to cells transfected with mimic control. Ectopic expression of miR-30c-2-3p resulted in 38 fold higher expression of this miRNA (Supplementary figure 1) and to a distinctly different gene expression profile compared to mimic control transfected cells (Figure 12). Bioinformatic analysis performed by Ashwini Kumar Sharma identified 370 genes (given in Supplementary table 1) which were downregulated at the mRNA level upon miR-30c-2-3p

overexpression with a corrected P value of less than 0.05. This approach can identify mRNA targets affected at post transcriptional level by miRNA. However targets affected on protein level or post translational level cannot be identified by this approach.

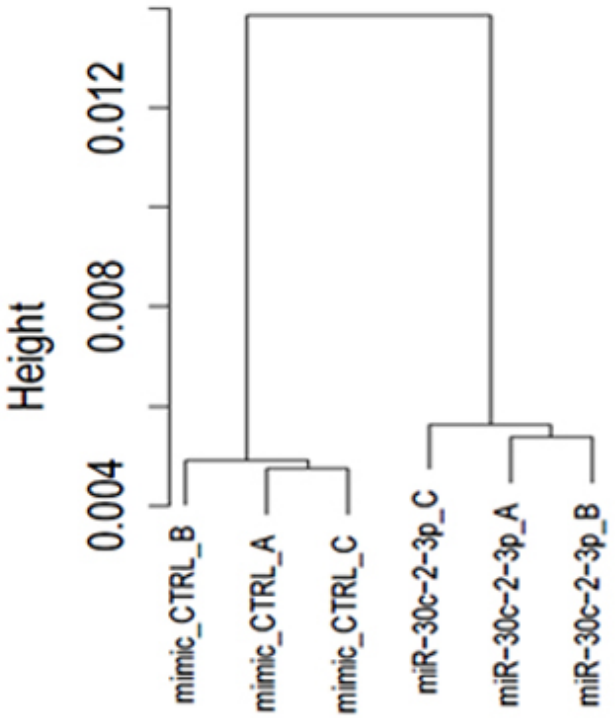

Figure 12: Dendogram showing clustered gene expression analysis. MDA-MB-231 cells were transfected with miR-30c-2-3p or mimic control. Cells were harvested 48 hours after transfection. Gene expression profiling data revealed 370 genes that are downregulated at mRNA level upon miR-30c-2-3p overexpression. Figure is representative of 3 biological replicates represented by A, B & C.

To identify potential target genes of miR-30c-2-3p within the NF-κB signaling pathway, I intersected these 370 genes with a list of NF-κB related genes (obtained from KEGG pathway database, http://www.genome.jp/kegg/pathway.html). This analysis identified TRADD as a potential target gene which is involved in TNF-α induced NF-κB activation. Gene Ontology (GO) term analysis identified biological processes in which TRADD is involved, including NF-κB signaling activation (Table 23). To explore the possibility of TRADD as a direct target, I verified the result from gene expression analysis using qRT-PCR taqman which showed that the mRNA level of TRADD was significantly reduced upon miR-30c-2-3p overexpression compared to mimic control transfected cells (Figure 13A). *In silico* analysis using miRWalk (http://www.umm.uni-heidelberg.de/apps/zmf/mirwalk/) revealed that TRADD is also a predicted target of miR-30c-2-3p (Figure 13B) with one putative target site in the 3´UTR. Immunoblotting revealed the same downregulation at the protein level (Figure 13C).

To prove direct targeting of TRADD by miR-30c-2-3p, I cloned the wild type 3´UTR of TRADD, or the mutant version containing four point mutations within the miRNA target site downstream of the *Renilla* luciferase open reading frame, in the dual luciferase vector psiCHECK2. A significant down regulation of *Renilla* luciferase signal in the presence of miR-30c-2-3p compared to mimic control was observed when using the wild type 3´UTR of TRADD in the MDA-MB-231 cell line. In contrast, this effect was abrogated when the mutated 3´UTR vector was used (Figure 13D). These results put together suggested that TRADD is a direct target of miR-30c-2-3p. For further validation, METABRIC data was analyzed [106, 111] to establish a correlation between mRNA of TRADD and miR-30c-2-3p expression in patients. Indeed, a significant anti-correlation ($P = 0.03$) in patients was found (Figure 13E) revealing the pathological significance of targeting that I initially discovered *in vitro*.

Table 23: GO term analysis for biological processes regulated by TRADD.

GO_id	Term
GO:0051291	protein heterooligomerization
GO:2001239	regulation of extrinsic apoptotic signaling pathway in absence of ligand
GO:0035666	TRIF-dependent toll-like receptor signaling pathway
GO:0002756	MyD88-independent toll-like receptor signaling pathway
GO:0034138	toll-like receptor 3 signaling pathway
GO:0043122	regulation of I-kappaB kinase/NF-kappaB signaling
GO:0033209	tumor necrosis factor-mediated signaling pathway
GO:0034142	toll-like receptor 4 signaling pathway
GO:0034612	response to tumor necrosis factor
GO:0006915	apoptotic process
GO:0043123	positive regulation of I-kappaB kinase/NF-kappaB signaling
GO:0045651	positive regulation of macrophage differentiation
GO:0051259	protein oligomerization
GO:2000116	regulation of cysteine-type endopeptidase activity
GO:0006461	protein complex assembly

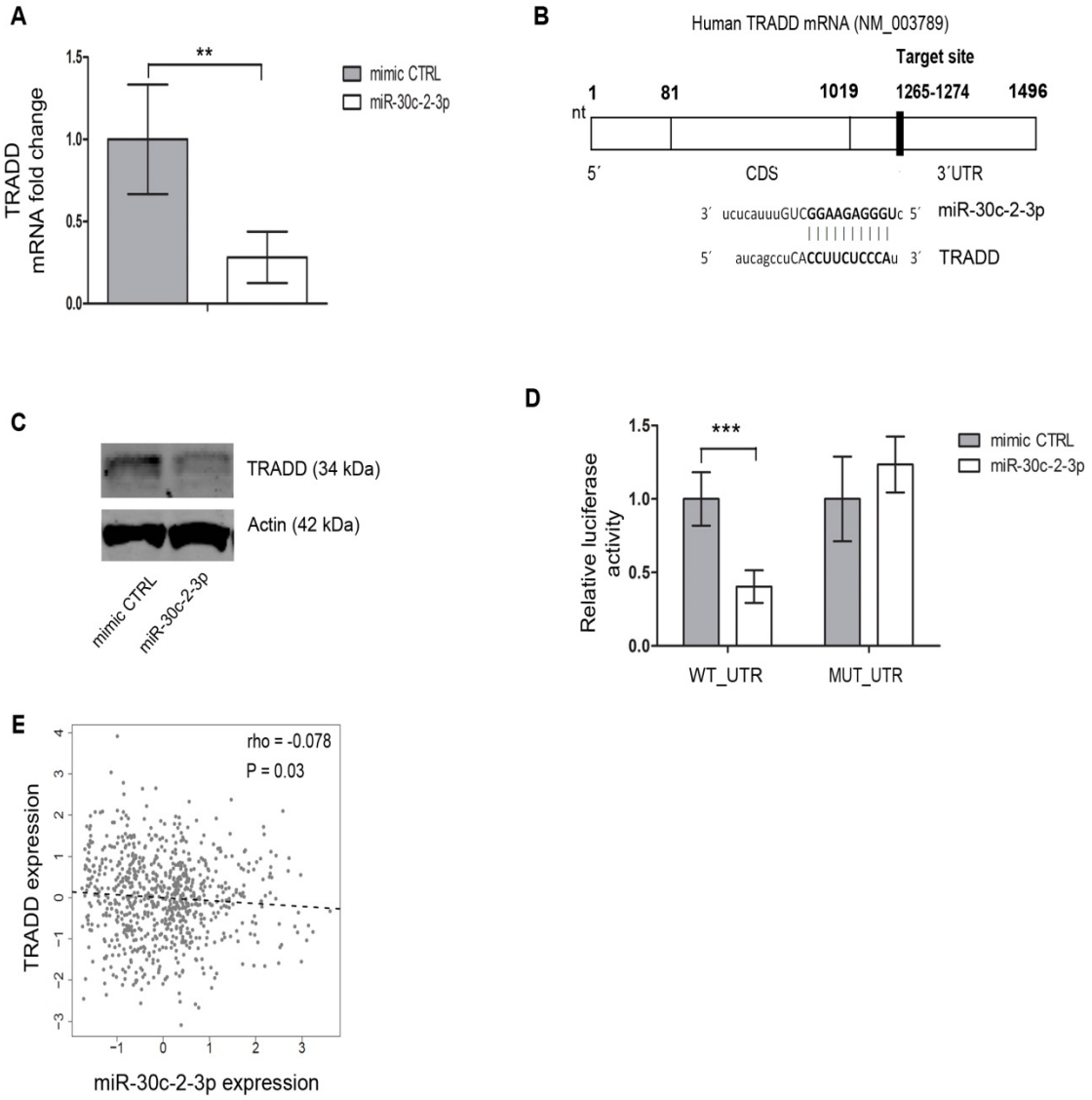

Figure 13: TRADD is a direct target of miR-30c-2-3p: (A) Downregulation of TRADD at mRNA upon miR-30c-2-3p overexpression 48 hours after transfection with miRNA (**p≤0.01 compared to control, *t* test). (B) Alignment of miR-30c-2-3p with target site within TRADD 3´UTR. (C) Downregulation of TRADD protein level upon overexpression of miR-30c-2-3p compared to mimic CTRL 48 hours after transfection with miRNA. Actin was used as a loading control. (D) Reduced *Renilla* luciferase signal in cells transfected with 3´UTR of TRADD and miR-30c-2-3p compared to mimic CTRL 48 hours after transfection with miRNA (**p≤0.01 compared to control, *t* test). This effect was lost when the binding site in 3´UTR was mutated. *Renilla* luciferase values were normalized to an internal firefly luciferase control and the values reported as fold expression compared to mimic control. Data are shown as mean±s.d of two independent biological and three technical replicates. (E) A negative correlation (based on Spearman rank correlation) between scale normalized miR-30c-2-3p and TRADD mRNA levels is seen in breast cancer patients (N = 781) from the METABRIC study [106, 111].

3.5. TRADD regulates NF-κB signaling in breast cancer cells

To assess the influence of TRADD on NF-κB signaling and to investigate if TRADD as a target can explain the effects caused by miR-30c-2-3p, I used siRNA to knockdown TRADD expression in MDA-MB-231 cells. Knockdown of TRADD by siRNA was confirmed both at mRNA and protein levels (Figure 14 A and B). To study the effect of TRADD knockdown on NF-κB signaling, I repeated the NF-κB reporter assay after TRADD knockdown to assess the effect on NF-κB signaling activation. Indeed, the knockdown of TRADD reduced NF-κB signaling despite TNF-α stimulation (Figure 15A) at a level similar to that of elevated miR-30c-2-3p (Figure 5B). Next, I evaluated the effects on expression of inflammatory cytokines. Similar to effects seen upon overexpression of miR-30c-2-3p, proinflammatory cytokines like *IL8*, *IL6* and *CXCL1* were down regulated upon TRADD inhibition in MDA-MB-231 cells at mRNA level (Figure 15B). Further, both overexpressing miR-30c-2-3p and inhibiting TRADD reduced the phosphorylation of NF-κB precursor (p105) upon stimulation with TNF-α (Figure 15C). The precursor p105 is processed to p50 which can act in the nucleus as homodimers or heterodimers along with p65 and c-Rel to regulate gene expression [119].

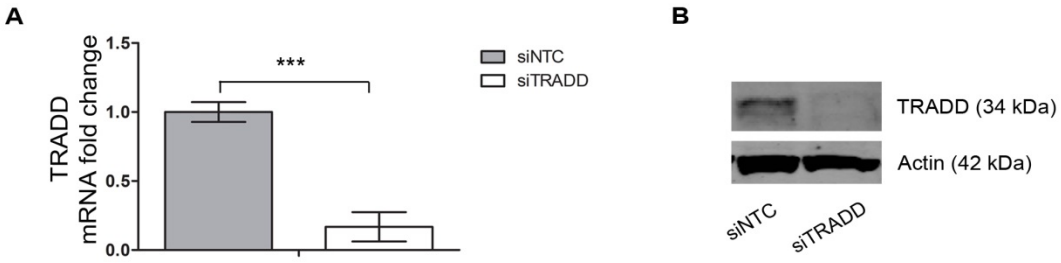

Figure 14: TRADD knockdown efficiency with siTRADD in the MDA-MB-231 cell line. (A) Significantly reduced expression was seen at the mRNA level 48 hours after transfection (***p≤ 0.001 compared to control, *t* test). Data are shown as mean±s.d of two biological and three technical replicates. (B) Protein level of TRADD was similarly reduced by siTRADD. Actin was stained as a loading control.

To ascertain the effect of TRADD on proliferative capability, I performed 7-AAD and BrdU staining of MDA-MB-231 cells transfected with siTRADD or non targeting control. However, unlike miR-30c-2-3p, TRADD knockdown only mildly reduced S-phase of the cell cycle (Figure 15D). Next, I checked the role of TRADD knockdown on the invasive capability of MDA-MB-231 cells. Indeed, similar to miR-30c-2-3p overexpression, TRADD knockdown significantly blocked cell invasion (Figure 15E) and reduced MMP-9 mRNA levels upon TNF-α stimulation (Figure 15F). To further investigate the effect of ectopic expression of miR-30c-2-3p as well as of TRADD knockdown on NF-κB signaling activation by TNF-α, I checked the phosphorylation of levels IKKα/IKKβ (important kinases of the pathway). Indeed, in both cases, a decrease in phosphorylation levels were observed compared to stimulated non targeting controls (Figure 16). This observation provided further evidence for the regulation of NF-κB signaling by miR-30c-2-3p through TRADD targeting.

These results suggested that TRADD, as a direct target, was only able to phenocopy the effects of miR-30c-2-3p on NF-κB signaling. The effects on cell proliferation were not completely phenocopied by TRADD, indicating that there are additional targets of miR-30c-2-3p.

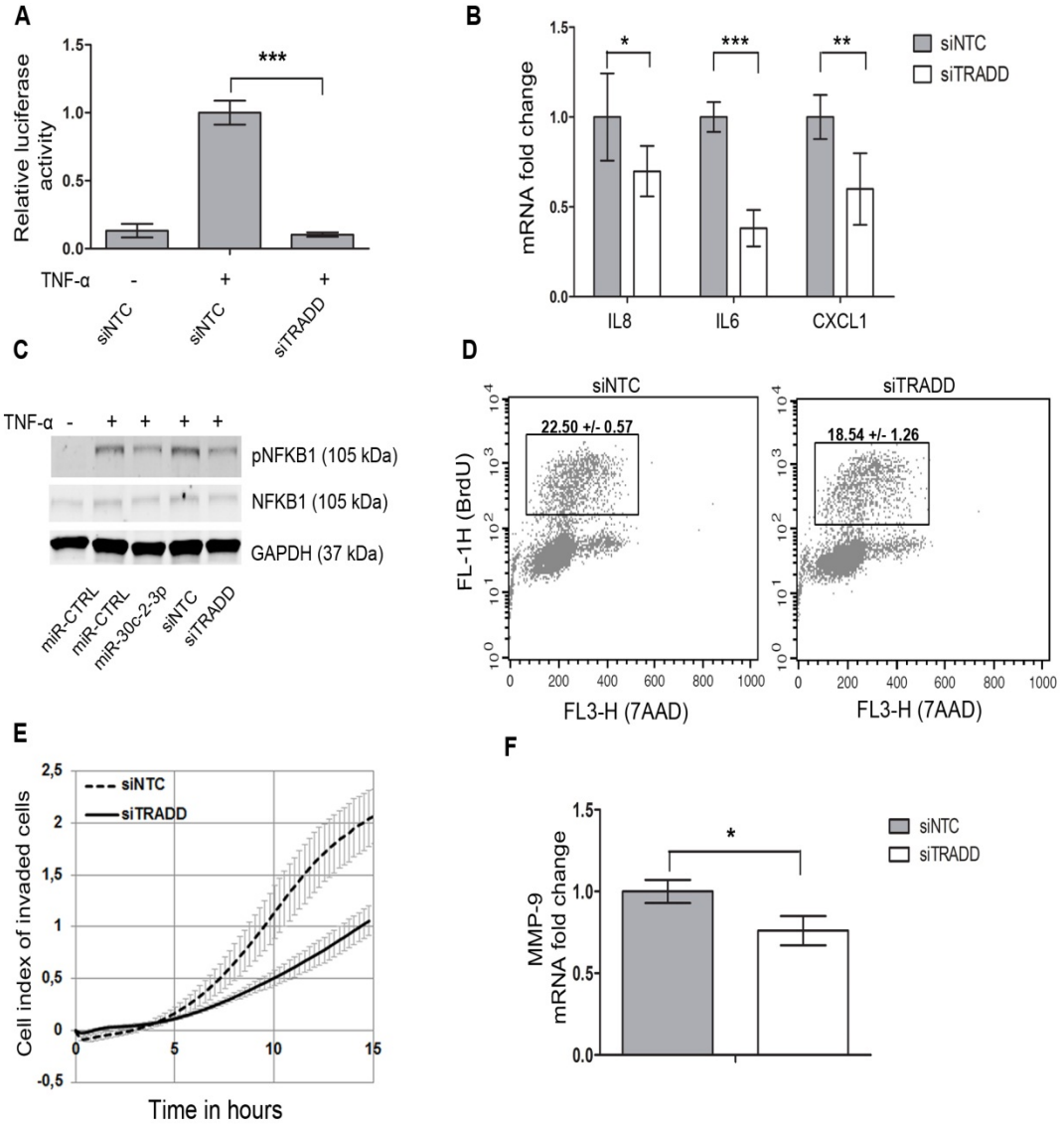

Figure 15: miR-30c-2-3p regulates NF-kB signaling by TRADD targeting. (A) Downregulation of TRADD with siRNA significantly decreased the luciferase signal measuring NF-κB activity upon activation of signaling with TNF-α **(**20 ng/ml**)** for 5 hours. This was similar to reduction seen upon miR-30c-2-3p overexpression (***p≤0.001 compared to stimulated control, *t* test). (B) mRNA expression of proinflammatory cytokines *IL-8, IL-6* and *CXCL-1* was reduced upon TRADD knockdown and activation of signaling with TNF-α (cells treated for 5 hours) (***p≤0.001, **p≤0.01,*p≤0.05 compared to stimulated control, *t* test). (C) Reduced phospho NFκB1 protein levels were observed upon treatment with 20 ng/ml TNF-α for 10 min after 48 hours of transfection with miR-30c-2-3p or siTRADD compared to controls. No change in total protein level was seen. GAPDH was used as a loading control. (D) Knockdown of TRADD did not have a significant effect on S-phase of the cell cycle compared to control, 72 hours after transfection. (E) siTRADD reduced invasion in the highly invasive MDA-MB-231 breast cell line (***p≤0.001 compared to control, *t* test). (F) In addition, siTRADD reduced MMP-9 at the mRNA levels after treatment of cells with TNF-α **(**20 ng/ml**)** for 5 hours after 48 hours of transfection. (*p≤0.05 compared to control, *t* test). Data are shown as mean±s.d of two biological and three technical replicates.

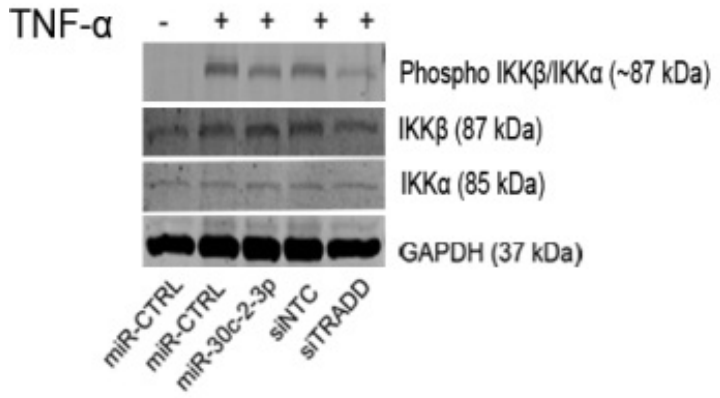

Figure 16: Effect of miR-30c-2-3p ectopic expression and TRADD knockdown on activation of NF-κB signaling. Reduced phospho-IKKα (Ser176)/IKKβ (Ser177) protein levels were observed upon treatment with 20 ng/ml of TNF-α for 10 minutes after 48 hours of transfection with miR-30c-2-3p or siTRADD compared to controls. No change in total protein level was seen. GAPDH was used as a loading control.

To study the effect of TRADD knockdown on expression of genes involved in cell proliferation like *MYC*, *CCND1* and *CSF2*, I performed qRT-PCR to quantify the mRNA changes in MDA-MB-231 cells stimulated with TNF-α. TRADD knockdown downregulated *CSF2* significantly upon TNF-α stimulation (Figure 17). However, expression of *MYC* and *CCND1* was slightly but not significantly upregulated in the same experimental setup (Figure 17).

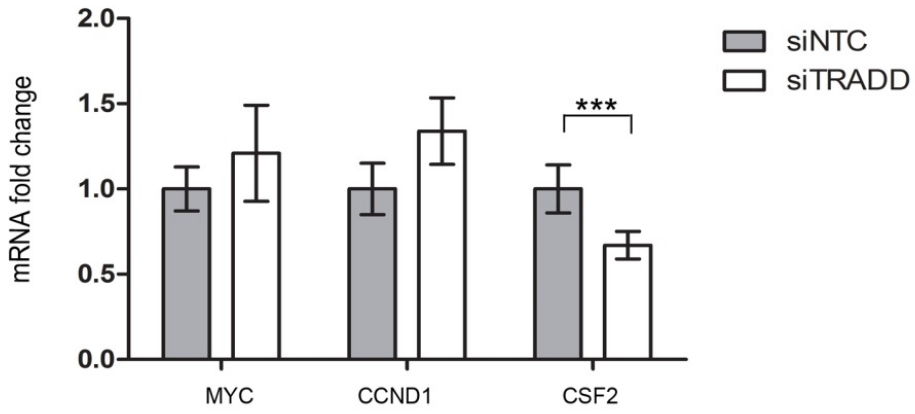

Figure 17: Effect of TRADD knockdown on expression of proliferation genes TRADD knockdown did not reduce mRNA expression of *MYC* and *CCND1* upon treatment of MDA-MB-231 cells with TNF-α (20 ng/ml) for 5 hours. However, a significant reduction in mRNA levels of *CSF2* was observed. All experiments were made 48 hours after transfection. (***p≤0.001 compared to stimulated control, *t* test). Data are shown as mean±s.d of two biological and three technical replicates.

I next tested the effect of miR-30c-2-3p overexpression or TRADD knockdown on NF-κB activation using lipopolysaccharide (LPS) to stimulate NF-κB signaling instead of TNF-α. To investigate this, I again performed the 3xKBL luciferase assay. NF-κB activation was similarly reduced (Figure 18) as after TNF-α stimulation, underlining the role of TRADD and miR-30c-2-3p in regulation of canonical NF-κB signaling.

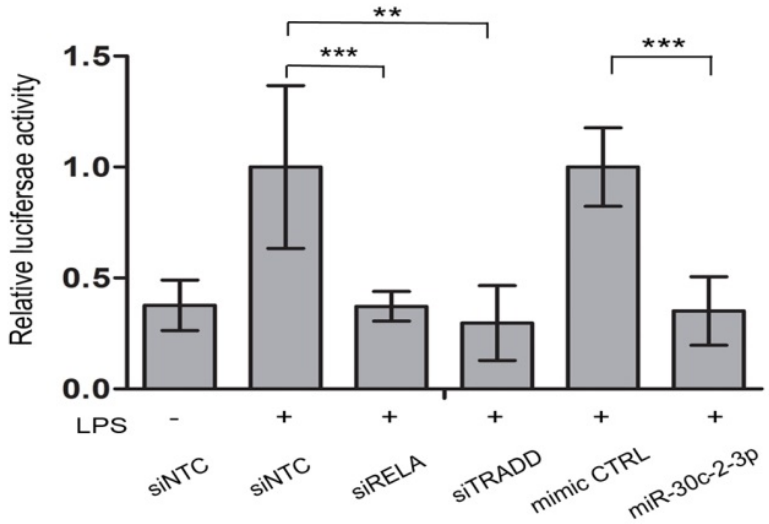

Figure 18: Effect of TRADD knockdown or miR-30c-2-3p overexpression on LPS induced NF-κB activation. RelA and TRADD knockdown as well as miR-30c-2-3p overexpression inhibited LPS induced NF-κB activation measured with NF-κB reporter plasmid in HEK293FT cell line (***p≤0.001, **p≤0.01 compared to stimulated control, *t* test). Cells were treated with 10 ng/ml of LPS for 5 hours. Data are shown as mean±s.d of two biological and three technical replicates.

3.6. miR-30c-2-3p regulates cell cycle progression by directly targeting CCNE1

To further investigate the potential target genes which are responsible for the observed reduction in S-phase of the cell cycle, I performed pathway enrichment analysis on the mRNAs that are downregulated upon miR-30c-2-3p overexpression using MetaCore™ (http://thomsonreuters.com/metacore/). This identified the most deregulated signaling pathways upon miR-30c-2-3p overexpression (Table 24).

Table 24: Top 10 significantly downregulated pathways from Metacore pathway enrichment analysis upon miR-30c-2-3p overexpression.

FDR: False discovery rate

	Signaling Pathways	Total genes	P value	FDR	Genes in data
1.	Cell cycle: Start of DNA replication in early S-phase	32	8.745E-07	3.682E-04	7
2.	Cell cycle: Role of SCF complex in cell cycle regulation	29	7.772E-06	1.636E-03	6
3.	Cell cycle: Influence of Ras and Rho proteins on G1/S Transition	53	2.680E-04	3.671E-02	6
4.	Cell cycle	21	3.924E-04	3.671E-02	4
5.	Cell cycle: Regulation of G1/S transition	38	4.360E-04	3.671E-02	5
6.	Cytoskeleton remodelling: Role of PDGFs in cell migration	24	6.695E-04	4.698E-02	4
7.	Transcription: Androgen Receptor nuclear signaling	45	9.642E-04	5.723E-02	5
8.	Glutathione metabolism / Rodent version	70	1.206E-03	5.723E-02	6
9.	Cell cycle: Transition and termination of DNA replication	28	1.223E-03	5.723E-02	4
10.	Some pathways of EMT in cancer cells	51	1.708E-03	7.190E-02	5

In line with the effects shown by miR-30c-2-3p on inhibition of cell proliferation, pathways involved in cell cycle regulation were highly enriched upon miR-30c-2-3p overexpression. Cyclin E1 (CCNE1), a cell cycle regulatory protein involved in G1 to S transition [120] and frequently overexpressed in breast cancer [121], was down regulated at the mRNA level (Figure 19A) and also a predicted target of miR-30c-2-3p (Figure 19B) by miRWalk. Down regulation of CCNE1 at the protein level upon miR-30c-2-3p overexpression was confirmed using immunoblotting (Figure 19C). In summary, CCNE1 (known oncogene in breast cancer) was downregulated both at the mRNA and protein levels upon ectopic over-expression of miR-30c-2-3p.

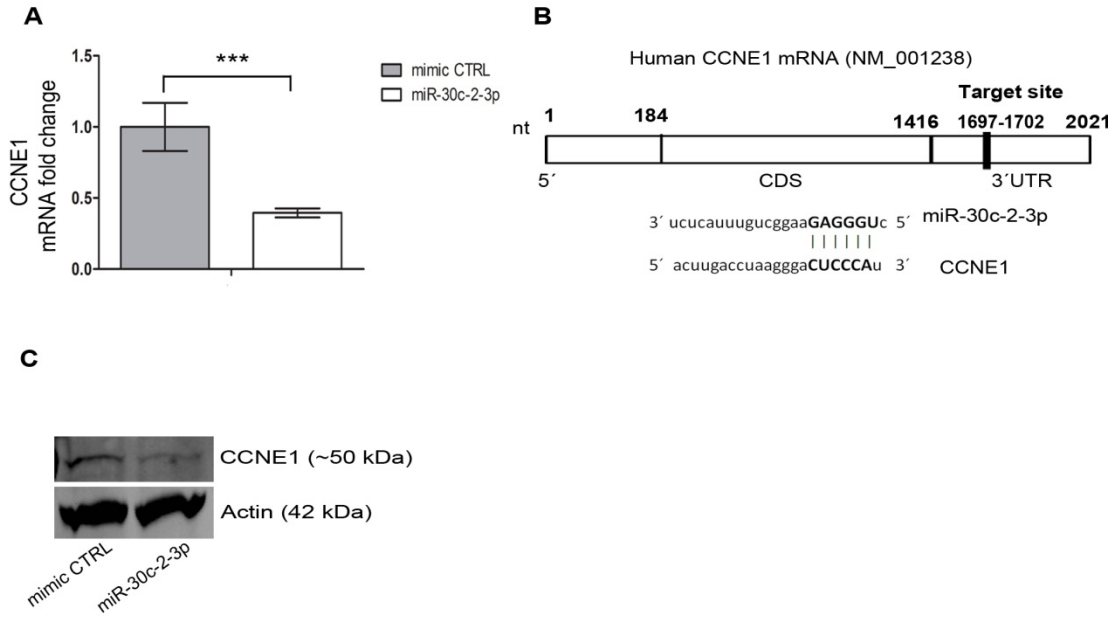

Figure 19: miR-30c-2-3p directly targets CCNE1. (A) mRNA levels of CCNE1 are significantly downregulated upon miR-30c-2-3p overexpression 48 hours after transfection with miRNA (***p≤0.001 compared to control, *t* test). Data are shown as mean±s.d of two biological and three technical replicates.. (B) CCNE1 is a predicted target of miR-30c-2-3p. (C) miR-30c-2-3p reduced CCNE1 at protein level compared to control. Actin was used a loading control.

Gene Ontology (GO) term analysis identified biological processes in which CCNE1 is involved (Table 25) that include regulation of cell cycle at G1 to S transition.

Table 25: GO term analysis for biological processes regulated by CCNE1

GO_id	Term
GO:0000082	G1/S transition of mitotic cell cycle
GO:1901990	regulation of mitotic cell cycle phase transition
GO:0010564	regulation of cell cycle process
GO:1901987	regulation of cell cycle phase transition
GO:0044772	mitotic cell cycle phase transition
GO:0044770	cell cycle phase transition
GO:0007093	mitotic cell cycle checkpoint
GO:0007346	regulation of mitotic cell cycle
GO:1901991	negative regulation of mitotic cell cycle phase transition
GO:1901988	negative regulation of cell cycle phase transition
GO:0000075	cell cycle checkpoint
GO:0090068	positive regulation of cell cycle process
GO:0051726	regulation of cell cycle
GO:0072431	signal transduction involved in mitotic G1 DNA damage checkpoint
GO:1902400	intracellular signal transduction involved in G1 DNA damage checkpoint

To study the effects of CCNE1 on cell cycle, I used siRNA against CCNE1 to block its expression. The efficiency of knockdown was confirmed both at mRNA and protein levels (Figure 20). Effect on cell cycle progression was then evaluated using 7-AAD and BrdU staining. As expected, CCNE1 knockdown phenocopied reduction in S-phase of cell cycle (Figure 21) that was also seen with miR-30c-2-3p overexpression (Figure 7D).

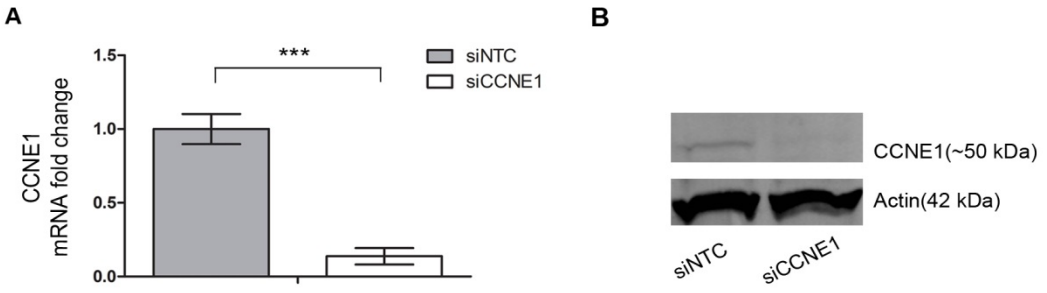

Figure 20: CCNE1 knockdown efficiency with siCCNE1 in the MDA-MB-231 cell line. (A) Significantly reduced expression of CCNE1 upon knockdown with siCCNE1 was seen at the mRNA level 48 hours after transfection (***p≤ 0.001 compared to control, t test). Data are shown as mean±s.d of two biological and three technical replicates. (B) Protein level of CCNE1 was similarly reduced by siCCNE1. Actin was used as a loading control.

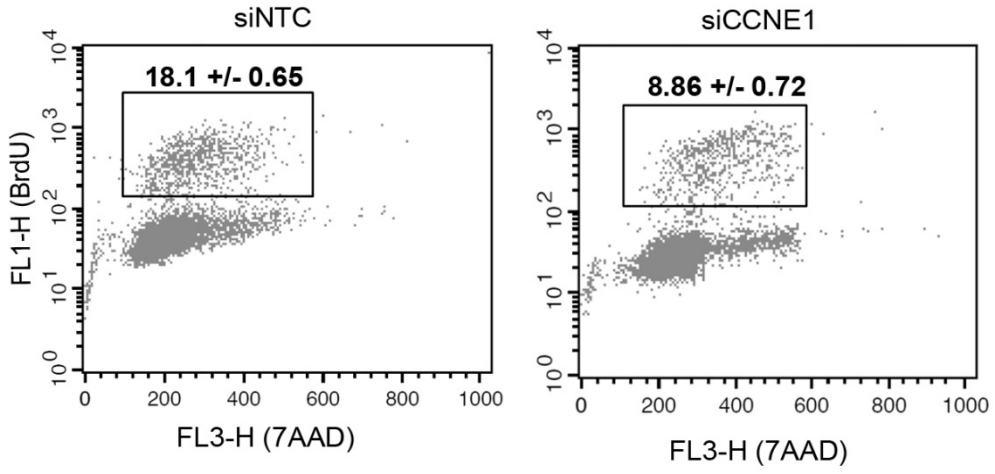

Figure 21: CCNE1 knockdown reduces the population of MDA-MB-231 cells in S-phase of cell cycle. Reduced S-phase population of MDA-MB-231 cells was seen 72 hours after transfection with siCCNE1 (***p≤0.001 compared to control, *t* test). Data are shown as representative of two biological and three technical replicates.

Using a reporter gene construct, I confirmed direct targeting of CCNE1 by miR-30c-2-3p (Figure 22A). Similar to the observations made for TRADD, the expression of CCNE1 and miR-30c-2-3p was significantly anticorrelated in the METABRIC cohort of breast cancer patients [106, 111] (Figure 22B), suggesting clinical relevance of this targeting.

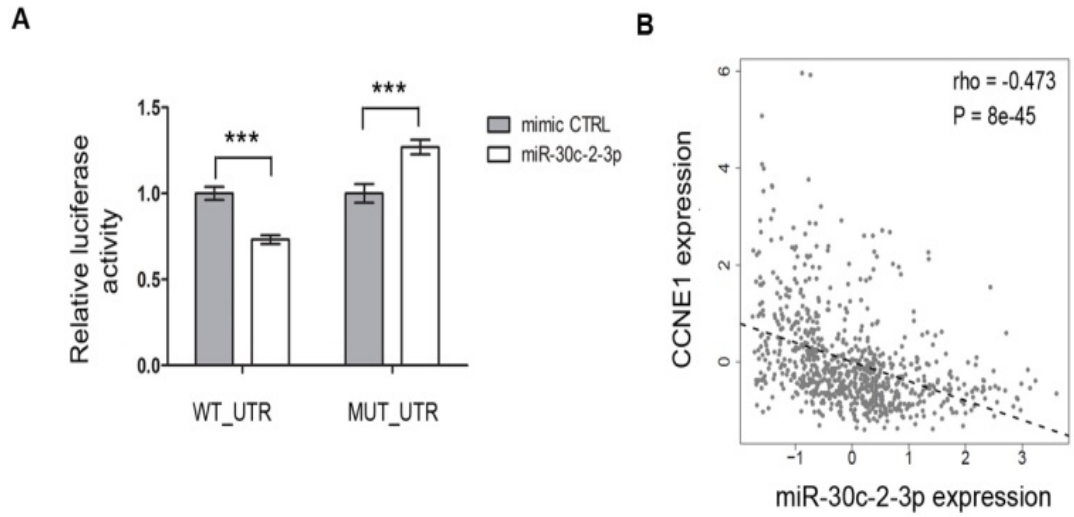

Figure 22: CCNE1 is a direct target of miR-30c-2-3p. (A) The luciferase assay with 3´UTR of CCNE1 upon overexpression of miR-30c-2-3p showed a significant decrease in *Renilla* luciferase signal compared to mimic CTRL transfected cells. This effect was abolished when the miR-30c-2-3p seed region within the 3´UTR of CCNE1 was mutated. (***p≤0.001 compared to control, *t* test). *Renilla* luciferase values were normalized to an internal firefly luciferase control and the values reported as fold expression compared to mimic control. Data are shown as mean±s.d of two biological and three technical replicates. (B) A negative correlation (Spearman rank correlation) between scale normalized miR-30c-2-3p and CCNE1 mRNA levels is seen in breast cancer patients (N = 781) from the METABRIC study [106, 111].

3.7. TRADD and CCNE1 are up regulated in ER negative breast cancer patients

To further ascertain the relation between TRADD, CCNE1 and miR-30c-2-3p in breast cancer patients, the METABRIC data was analyzed [106, 111]. TRADD and CCNE1 expression was found to be significantly up regulated (P<0.005) in ER negative patients

compared to ER positive breast cancer patients (Figure 23A and B), which corroborated with *in vitro* findings of my study. Next, the expression of miR-30c-2-3p was analyzed among the different subtypes of breast cancer in the METABRIC cohort of breast cancer patients [106]. In this dataset miR-30c-2-3p was found to be significantly lower expressed in basal-like and HER2 positive subtypes compared to the luminal subtypes (Figure. 23C). Finally, to assess the prognostic potential of miR-30-c-2-3p expression in patients, a survival analysis was performed. miR-30c-2-3p was found to be significantly associated with better survival in all three groups based on miRNA expression level distribution quartiles into low (<Q1), medium (Q1-Q3) and high (>Q3) expression groups (Figure 23D), further supporting a direct role in breast cancer and a tumor suppressive role for this miRNA.

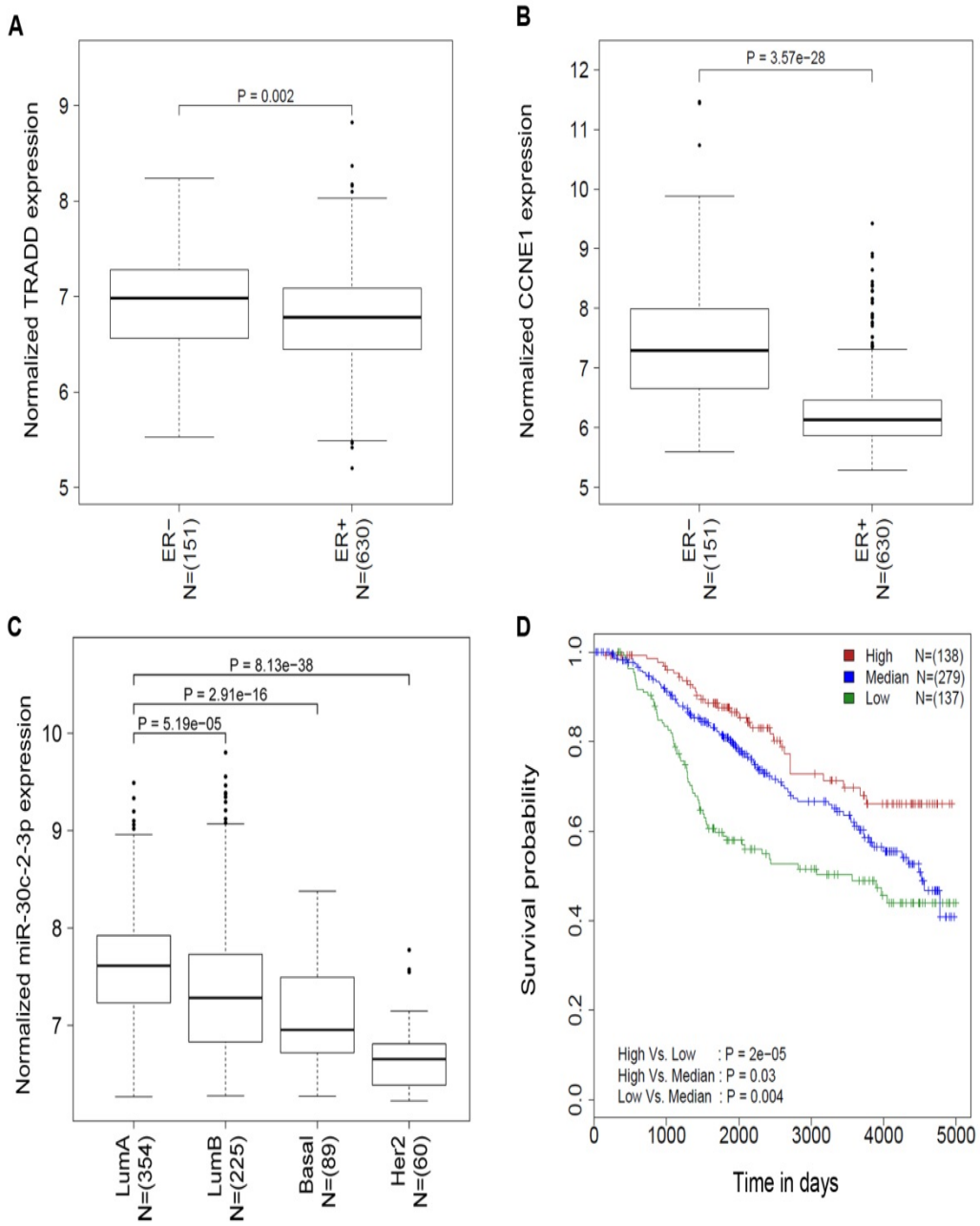

Figure 23: Expression of TRADD, CCNE1 and miR-30c-2-3p in breast cancer patients. (A&B) The mRNA expression of both TRADD and CCNE1 is significantly higher in ER negative breast cancer patients [111]. (C) Across different molecular subtypes of breast cancer, the expression levels of miR-30c-2-3p are lower in basal and HER2 enriched subtype [106]. (D) Higher expression of miR-30c-2-3p is associated with long term disease specific survival in patients for over 13 years [106]**.**

4. Discussion

4.1. miR-30c-2-3p expression analysis in breast cancer patients

To validate the expression of miR-30c-2-3p in breast cancer patients, RNA sequencing data from the TCGA (The Cancer Genome Atlas) study [6] and microarray gene expression data from the METABRIC (Molecular Taxonomy of Breast Cancer International Consortium) study [106] were analyzed. This was done to confirm expression levels of miR-30c-2-3p from independent platforms and two independent cohorts of breast cancer patients (Figure 5E and 6A). The two independent cohorts showed similar results for miR-30c-2-3p expression, with lower expression in ER- compared to ER+ breast cancer patients. This observation was recapitulated *in vitro* in a panel of 7 breast cell lines using miRNA qRT-PCR (Figure 6B). The validation for miRNA expression was critical in light of wrong miRNA annotations reported and to show that miR-30c-2-3p is a high confidence miRNA [96, 122]. miR-30c-2-3p has also been found in more than 2200 reads in miRBase (Version 21, accessed July 29, 2014) thus further supporting the relevance of this miRNA.

4.2. miR-30c-2-3p mediated regulation of NF-κB signaling

miRNAs are important regulators of gene expression during carcinogenesis, and the current project was aimed at elucidating the tumor suppressive activities of miR-30c-2-3p in breast cancer patients. This established NF-κB signaling and cell cycle progression to be directly regulated by miR-30c-2-3p. These processes in turn regulate hallmarks of cancer like proliferation, invasion, and inflammation [65]. miR-30c-2-3p negatively regulates these phenotypes in breast cancer cells.

The role of NF-κB signaling in cancer development and specifically in breast cancer progression is increasingly studied [28, 42, 43, 46, 123]. Constitutively active NF-κB signaling is detected both in mammary carcinoma cell lines and primary human breast cancer tissues [15]. It has also been implicated in development of resistance against anti-estrogen therapy e.g. tamoxifen with resistant cells expressing high levels of p50, RelB and increased phosphorylation of p65 [124]. Additionally, inhibiting NF-κB

signaling can re-sensitize these resistant cells to tamoxifen and could be expoited for the development of effective novel drugs for treatment of breast cancer patients [124]. This underlines the importance of studying constitutive activation of NF-κB signaling and effective ways to inhibit this in the context of breast cancer.

The biological mechanisms of miRNAs to regulate or inhibit NF-κB signaling in breast cancer are currently being explored. The work by Kekikoglou et.al. on the miRNA-520/373 family showed the negative regulation of NF-κB signaling by direct targeting of RelA in ER negative breast cancer patients [103]. Similarly, miR-31 has been shown to regulate NF-κB signaling by targeting protein kinase C epsilon and sensitizing human breast cells to apoptosis [104]. In the current study, TRADD was identified as a direct target gene of miR-30c-2-3p (Figure 13). TRADD is a member of tumor necrosis factor receptor superfamily characterized by the presence of a death domain (DD) and on the one hand, plays an important role in inducing proinflammatory responses by interacting with TNFR1 upon TNF-α activation [125]. On the other hand, TNFα can also initiate apoptosis and necrosis, through recruitment of another death domain containing protein known as FADD [126]. However, TNF-α induced NF-κB activation is attenuated in TRADD deficient cells as has been shown by somatic knockout of TRADD in a human B cell line [127], demonstrating the importance of TRADD in NF-κB signaling. These findings are further supported by results in TRADD deficient mice where TNF-α induced activation of NF-κB, ERK and JNK signaling has been found to be defective [128]. Upon TNF-α activation, TRADD interacts with other DD containing kinase protein like RIP1 (receptor-interacting protein-1) and the ubiquitin ligase, TRAF2 (TNF receptor–associated factor 2) [125]. These interactions ultimately activate signaling pathways like NF-κB and MAPK (Mitogen activated protein kinase) [125].

This study confirmed that TRADD is required for TNF-α mediated activation of NF-κB signaling in breast cancer as well as its effect on expression of known NF-κB target genes like pro inflammatory cytokines *IL8, IL6* and *CXCL1* (Figure 15B). These cytokines contribute to the shaping of the tumor microenvironment by promoting inflammation in most solid tumors, including breast cancer [123, 129]. Other inflammation mediators part of the tumor microenvironment include chemokines and

prostaglandins [123]. All these mediators can then activate transcription factors, like NF-κB, in stromal cells and tumor cells which can in turn generate more inflammatory mediators and thus form an inflammatory microenvironment [123]. miR-30c-2-3p potently inhibited the expression of these inflammatory cytokines in MDA-MB-231 cells (Figure 7A) suggesting that this miRNA could be a central factor in the regulation of tumor inflammatory processes that could be executed also via its direct target TRADD. Furthermore, TRADD knockdown inhibited the phosphorylation of NF-κB1 and IKKα/IKKβ upon TNF-α stimulation, thus phenocopying the effect observed upon miR-30c-2-3p overexpression (Figure 15C and 16). Hence, miR-30c-2-3p inhibits activation of NF-κB signaling and as a result affects a number of downstream phenotypes.

TRADD is also known to play a role in regulating TLR signaling by formation of a complex with TLR4 upon stimulation with TNF-α [128]. Moreover, TRADD deficiency inhibits cellular response like TNF-α production in response to LPS induction [128]. TLR signaling has been shown to support tumor growth by activating inflammatory response and supporting oncogenesis in the breast by activating NF-κB, MAPKs including JNK, p38 and ERK pathways [130]. These findings are in line with the results from my study showing that TRADD knockdown can inhibit LPS induced canonical NF-κB signaling and miR-30c-2-3p also shows this effect (Figure 18).

TNF-α has been shown to have mitogenic function in breast cancer cells thereby promoting malignancy via NF-κB signaling activation [27, 28]. This finding is supported by *in vitro* data showing that TNF-α promotes proliferation in cancer cells (specifically breast cancer cells) [131] and *in vivo* data from experiments with murine breast cancer growth [28]. Interestingly, TNF-α is also a transcriptional target of NF-κB. Activated signaling can thus lead to increased expression of TNF-α in a feed forward loop [123]. Moreover, TNF-α is known to promote tumor invasion by upregulating important extracellular matrix (ECM) degrading enzymes which are involved in metastasis and progression of a number of cancers [132]. Matrix metalloproteinases (MMPs), and specifically MMP-9 which has been shown to have potent basement degrading capability [133], was down regulated upon miR-30c-2-3p

overexpression (Figure 7E and F) as well as by knockdown of TRADD (Figure 15E and F). Taking these results together, the mode of regulation of NF-κB signaling by miR-30c-2-3p can be well explained via TRADD targeting. Furthermore the anticorrelation between expression of TRADD mRNA and miR-30c-2-3p (Figure 13E) was also seen in the METABRIC cohort of breast cancer patients [106, 111].

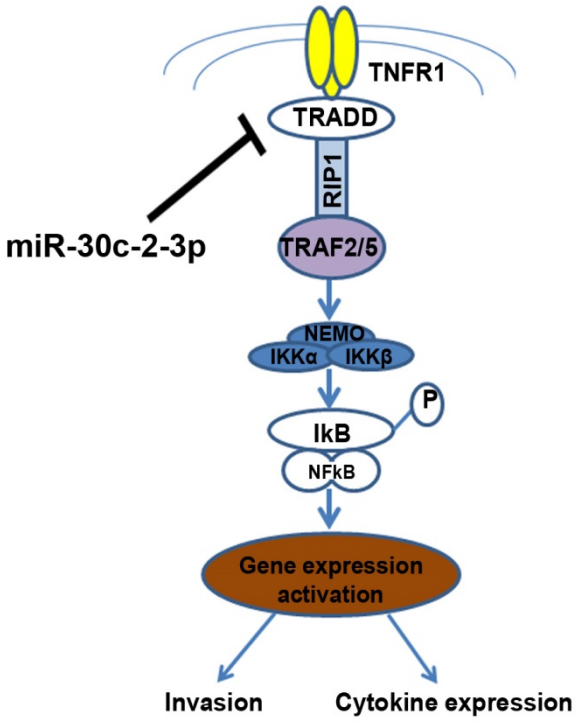

Figure 24: Molecular mechanism underlying the regulation of NF-κB signaling by miR-30c-2-3p in breast cancer cells. miR-30c-2-3p regulates invasion and cytokine expression by directly targeting TRADD. Idea of the figure adapted from [38].

In summary, TRADD can explain the effects of miR-30c-2-3p on phenotypes like cytokine expression and invasion that are regulated by NF-κB signaling (Figure 24). TRADD as a direct target however cannot explain the effects of miR-30c-2-3p on cell cycle inhibition. This can be explained by the ability of miRNAs to have multiple mRNA targets [98]. It was observed that, miR-30c-2-3p overexpression resulted in downregulation of 370 mRNAs. Pathway enrichment analysis on these mRNAs showed

that miR-30c-2-3p downregulated key biological pathways related to cell proliferation (Table 24). miRNAs can therefore regulate many biological processes and have pleiotropic effects.

4.3. Cell cycle inhibition by miR-30c-2-3p

Cyclin E1 (CCNE1) was identified to be another direct target of miR-30c-2-3p (Figure 19) which could explain the reduced proliferation capacity of breast cancer cells that was observed upon overexpression of this miRNA. CCNE1 interacts with cyclin dependent kinase CDK2 (Figure 25), and cell cycle inhibitors like CDKN1A, CDKN1B to regulate cell cycle. Both overexpression of miR-30c-2-3p (Figure 7D) or CCNE1 knockdown (Figure 21) caused a decreased population of MDA-MB-231 cells in S-phase of cell cycle. This effect was not seen upon knockdown of TRADD (Figure 15D), showing that miR-30c-2-3p regulates cell cycle progression and NF-κB signaling through targeting of different genes.

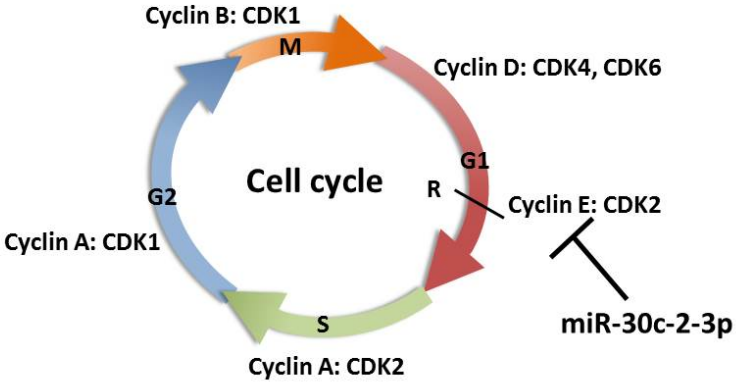

Figure 25: miR-30c-2-3p inhibits cell cycle by directly targeting CCNE1 which is a central player of cell cycle network. CCNE1 regulates G1 restriction point (R) in cell cycle**.** By directly targeting CCNE1, miR-30c-2-3p inhibits cell proliferation in breast cancer cells. Idea of the figure adapted from [134].

CCNE1 is a cell cycle regulatory protein that, along with CDK2, drives the cell cycle from G1 to S phase by CDK2 mediated phosphorylation of Rb protein and release of the transcription factor, E2F [120]. The complex of CCNE1 with CDK2 acts like a master switch for initiation of S-phase and the regulation of processes such as DNA synthesis, duplication of centrosome and chromatin assembly [58]. CCNE1 is frequently deregulated or undergoes gene amplification in breast cancer and higher expression is associated with poor overall survival compared to patients with lower expression [135].

In the dataset published by the METABRIC study [106], CCNE1 was found to be upregulated in ER negative breast cancer patients compared to ER positive patients (Figure 23B). This is in line with the finding that miR-30c-2-3p is lower expressed in the ER negative group. Also, the expression of miR-30c-2-3p and CCNE1 is strongly anticorrelated (Figure 22B) in a cohort of 781 breast cancer patients [106, 111] showing the clinical relevance of the targeting by miR-30c-3p.

The results found during my PhD work, are in line with a previous study on the tumor suppressive role of miR-30c-2-3p in ovarian cancer, where Jia and coworkers showed BCL9 as a direct target gene of the miRNA and proved its anti-proliferative effect [136]. Another report in clear cell renal cell carcinoma showed that lower expression of miR-30c-2-3p was associated with increased tumor growth through enhanced activity of hypoxia inducible factor (HIF2)α [137]. From the microarray gene expression data upon overexpression of miR-30c-2-3p, I observed that both BCL9 and HIF2α were not downregulated pointing towards tissue specific mode of regulation for this interaction. When the METABRIC data [106, 111] was analyzed to evaluate correlation between miR-30c-2-3p and BCL9 or HIF2α, it was found that there is a weak positive correlation between miR-30c-2-3p and BCL9 (Supplementary figure 2). However, in case of miR-30c-2-3p and HIF2α a weak anti-correlation was observed (Supplementary figure 3).

The precursor pre-miR-30c-2 is processed asymmetrically to form mature hsa-miR-30c-5p (miR-30c) and hsa-miR-30c-2-3p (mir-30c-2*) from the 5´and 3´ arms of the precursor miRNA, respectively. miR-30c-5p has been shown to regulate

chemoresistance in breast tumors through direct targeting of the cytoskeleton gene TWF1 and indirect regulation of IL-11 [138]. In combination with my results this is an interesting finding as the two mature forms of the same precursor have different seed sequences and, therefore, different sets of target genes, but function as important regulators of gene expression in breast cancer. Both miRNAs appear to confer similar functions by the regulation of different target genes. A linear regression analysis identified the expression of miR-30-5p to be positively correlated to miR-30c-2-3p expression (Supplementary figure 4) in METABRIC study [106] emphasizing their co-regulation and likely coordinated activities in breast cancer patients. However from the screening data for regulators of NF-κB signaling [103], miR-30c-2-3p had a strong negative effect on activation of NF-κB signaling (z score of -2.013) compared to the insignificant effect of miR-30c-5p (z-score of -0.258).

In summary, miR-30c-2-3p affected key cellular phenotypes in breast cancer cells by regulating NF-κB signaling and cell cycle regulation. The effects on cell proliferation, invasion, migration and expression of inflammatory cytokines can be explained by CCNE1 and TRADD as direct targets in breast cancer. This molecular mechanism can be exploited to come up with better treatment options for ER negative as well as basal subtypes of breast cancer.

4.4. Conclusions and outlook

Treatment of the basal-like subtype of breast cancer remains a big clinical challenge, with chemotherapy and radiation therapy in neoadjuvant therapy as the major options for treatment. Due to the lack of expression of ER, PR, HER2, or other targetable drivers of these tumors, no targeted therapies have been identified yet. This aggressive subtype of breast cancer is known to have aberrant NF-κB activation [139]. Effective inhibition of the aberrantly active NF-κB signaling cascade by targeted therapy in ER negative or basal-like tumors could be a solution to this problem. Initial efforts in this direction have already been made for the treatment of breast cancer [46]. miR-30c-2-3p was shown in this study to inhibit NF-κB signaling in case of ER negative breast cancer cells. Xenograft tumor mouse models, will allow testing of the efficacy of miR-30c-2-3p to serve in cancer therapeutics.

The property of miRNAs to inhibit a range of targets and affect signaling pathways is one way to overcome resistance caused by targeted or chemo therapies in cancer treatment. Moreover, tumors are associated with distinct expression patterns of miRNAs and mRNAs also known as expression signatures [140]. These can be used to study pathways which are deregulated specifically in cancer cells as opposed to the adjacent normal tissue. In the present study miR-30c-2-3p was shown to regulate two central pathways in breast cancer development, NF-κB signaling and cell cycle progression. However, there are a number of challenges that have to be tackled before miRNAs can potentially be used as effective therapeutic tools in treatment of cancer. These challenges include effective *in vivo* delivery, escape from enzymatic or blood clearance and off-targets repressed by miRNAs [141, 142]. Nevertheless, the future for miRNA in clinics as therapeutic drugs and as biomarkers to predict clinical outcomes looks promising with miR-34 mimic being tested in clinical trials for miRNA replacement therapy in cancer treatment because of its tumor suppressive role [143]. Another candidate, miR-122 inhibitor (also known as miravirsen) is in phase 2 clinical trials for the treatment of hepatitis C virus (HCV) infection [144]. In this case, locked nucleic acid (LNA) based oligonucleotides are used for targeting of endogenous expression of miR-122 [144].

The work from my PhD study contributed to a novel understanding of miR-30c-2-3p mediated regulation in breast cancer by combining *in vitro* results with publically available breast cancer patients datasets that had long term follow up data of patients. This established miR-30c-2-3p as a tumor suppressor in breast cancer.

5. Own publications

Publication No. 5 is about the work that I describe in the present thesis and is thus based mostly on my own work. I have described in the thesis where others have contributed. In all other publications, I contributed both scientifically and technically. This included discussion about respective projects and performing functional assays which contributed to the publication.

Publications (in peer-reviewed Journals):

1. A. Ward, **K. Shukla**, A. Balwierz, Z. Soons, R. Konig, O. Sahin, S. Wiemann, **MicroRNA-519a is a novel oncomir conferring tamoxifen resistance by targeting a network of tumour-suppressor genes in ER+ breast cancer**. *The Journal of pathology*, (2014). 233(4):368-379. PMID: 24752803

2. W. J. Kostler, A. Zeisel, C. Korner, J. M. Tsai, J. Jacob-Hirsch, N. Ben-Chetrit, **K. Sharma**, H. Cohen-Dvashi, A. Yitzhaky, E. Lader, U. Tschulena, G. Rechavi, E. Domany, S. Wiemann, Y. Yarden**, Epidermal growth-factor-induced transcript isoform variation drives mammary cell migration.** *PloS one* **8**, e80566 (2013)10.1371/journal.pone.0080566). PMID: 24324612

3. S. Srivastava, **K. Sharma**, N. Kumar, P. Roy, **Bradykinin regulates osteoblast differentiation by Akt/ERK/NFkappaB signalling axis.** *Journal of cellular physiology*, (2014); published online EpubMay 13 (10.1002/jcp.24668). PMID: 24825463

4. Mattia Lauriola, Yehoshua Enuka, Amit Zeisel, Gabriele D'Uva, Lee Roth ,Michal Sharon-Sevilla , Moshit Lindzen , **Kirti Shukla** , Nava Nevo, Morris Feldman , Silvia Carvalho, Hadas Cohen-Dvashi, Merav Kedmi, Nir Ben-Chetrit, Alon Chen , Rossella Solmi, Stefan Wiemann, Fernando Schmitt, Eytan Domany, Yosef Yarden. **Diurnal suppression of EGF-receptor signaling by glucocorticoids: implications for tumor progression and treatment.** Accepted in *Nature Communications.*

Manuscripts under revision and submitted :

5. **Kirti Shukla**, Ashwini Kumar Sharma, Aoife Ward, Thomas Hielscher, Rainer Will, Aleksandra Balwierz, Christian Breunig, Ewald Münstermann, Rainer König, Ioanna Keklikoglou, Stefan Wiemann, **microRNA-30c-2-3p negatively regulates NF-κB signaling and cell cycle progression through downregulation of TRADD and CCNE1 in breast cancer.** Submitted to *Molecular Oncology*.

6. Nir Ben-Chetrit, David Chetrit, Roslin Russell, Cindy Körner, Maicol Mancini, Silvia Carvalho, Hadas Cohen-Dvashi, Wolfgang Köstler, **Kirti Shukla**, Moshit Lindzen, Merav Kedmi, Mattia Lauriola, Ziv Shulman, Haim Barr, Dalia seger, Daniela A. Ferraro, Fresia Pareja, Hava Gil-Henn, Tsvee Lapidot , Ronen Alon, Fernanda Milanezi, Marc Symons , Rotem Ben-Hano , Sol Efroni , Fernando Schmitt , Stefan Wiemann , Carlos Caldas , Marcelo Ehrlich, Yosef Yarden. **Synaptojanin 2, a druggable metastasis driver, is overexpressed and amplified in breast cancer**. Under revision in *Science Signaling.*

Other publications

Aleksandra Balwierz, Alexander Bott, Christian Breunig, Nese Erdem, Chiara Giacomelli, Cindy Körner, Omar Salem, **Kirti Shukla**, Stefan Wiemann. **microRNAs – kleine Moleküle ganz groß**. *Biologie in unserer Zeit*, (2014); Doi:10.1002/biuz.201410543

6. References

1. Parker, J.S., et al., *Supervised risk predictor of breast cancer based on intrinsic subtypes.* J Clin Oncol, 2009. **27**(8): p. 1160-7.
2. Perou, C.M., et al., *Molecular portraits of human breast tumours.* Nature, 2000. **406**(6797): p. 747-52.
3. Sorlie, T., et al., *Gene expression patterns of breast carcinomas distinguish tumor subclasses with clinical implications.* Proc Natl Acad Sci U S A, 2001. **98**(19): p. 10869-74.
4. Hu, Z., et al., *The molecular portraits of breast tumors are conserved across microarray platforms.* BMC Genomics, 2006. **7**: p. 96.
5. Sorlie, T., *Molecular portraits of breast cancer: tumour subtypes as distinct disease entities.* Eur J Cancer, 2004. **40**(18): p. 2667-75.
6. Cancer Genome Atlas, N., *Comprehensive molecular portraits of human breast tumours.* Nature, 2012. **490**(7418): p. 61-70.
7. Prat, A. and C.M. Perou, *Mammary development meets cancer genomics.* Nat Med, 2009. **15**(8): p. 842-4.
8. Bentzon, N., et al., *Prognostic effect of estrogen receptor status across age in primary breast cancer.* Int J Cancer, 2008. **122**(5): p. 1089-94.
9. Engstrom, M.J., et al., *Molecular subtypes, histopathological grade and survival in a historic cohort of breast cancer patients.* Breast Cancer Res Treat, 2013. **140**(3): p. 463-73.
10. Hammond, M.E., et al., *American Society of Clinical Oncology/College Of American Pathologists guideline recommendations for immunohistochemical testing of estrogen and progesterone receptors in breast cancer.* J Clin Oncol, 2010. **28**(16): p. 2784-95.
11. Slamon, D.J., et al., *Studies of the HER-2/neu proto-oncogene in human breast and ovarian cancer.* Science, 1989. **244**(4905): p. 707-12.
12. Stebbing, J., et al., *The efficacy of lapatinib in metastatic breast cancer with HER2 non-amplified primary tumors and EGFR positive circulating tumor cells: a proof-of-concept study.* PLoS One, 2013. **8**(5): p. e62543.
13. Perou, C.M., *Molecular stratification of triple-negative breast cancers.* Oncologist, 2011. **16 Suppl 1**: p. 61-70.
14. Siegel, R., D. Naishadham, and A. Jemal, *Cancer statistics, 2012.* CA Cancer J Clin, 2012. **62**(1): p. 10-29.
15. Cao, Y. and M. Karin, *NF-kappaB in mammary gland development and breast cancer.* J Mammary Gland Biol Neoplasia, 2003. **8**(2): p. 215-23.
16. Barkett, M. and T.D. Gilmore, *Control of apoptosis by Rel/NF-kappaB transcription factors.* Oncogene, 1999. **18**(49): p. 6910-24.
17. Huxford, T., A. Hoffmann, and G. Ghosh, *Understanding the logic of IkappaB:NF-kappaB regulation in structural terms.* Curr Top Microbiol Immunol, 2011. **349**: p. 1-24.

18. May, M.J. and S. Ghosh, *Rel/NF-kappa B and I kappa B proteins: an overview.* Semin Cancer Biol, 1997. **8**(2): p. 63-73.
19. Chen, Z., et al., *Signal-induced site-specific phosphorylation targets I kappa B alpha to the ubiquitin-proteasome pathway.* Genes Dev, 1995. **9**(13): p. 1586-97.
20. Chen, Z.J., *Ubiquitin signalling in the NF-kappaB pathway.* Nat Cell Biol, 2005. **7**(8): p. 758-65.
21. Karin, M. and Y. Ben-Neriah, *Phosphorylation meets ubiquitination: the control of NF-[kappa]B activity.* Annu Rev Immunol, 2000. **18**: p. 621-63.
22. Senftleben, U., et al., *Activation by IKKalpha of a second, evolutionary conserved, NF-kappa B signaling pathway.* Science, 2001. **293**(5534): p. 1495-9.
23. Sun, S.C., *Deubiquitylation and regulation of the immune response.* Nat Rev Immunol, 2008. **8**(7): p. 501-11.
24. Aggarwal, B.B., *Signalling pathways of the TNF superfamily: a double-edged sword.* Nat Rev Immunol, 2003. **3**(9): p. 745-56.
25. Black, R.A., et al., *A metalloproteinase disintegrin that releases tumour-necrosis factor-alpha from cells.* Nature, 1997. **385**(6618): p. 729-33.
26. Jaattela, M., M. Pinola, and E. Saksela, *Heat shock inhibits the cytotoxic action of TNF-alpha in tumor cells but does not alter its noncytotoxic actions in endothelial and adrenal cells.* Lymphokine Cytokine Res, 1991. **10**(1-2): p. 119-25.
27. Garcia-Tunon, I., et al., *Role of tumor necrosis factor-alpha and its receptors in human benign breast lesions and tumors (in situ and infiltrative).* Cancer Sci, 2006. **97**(10): p. 1044-9.
28. Rivas, M.A., et al., *TNF alpha acting on TNFR1 promotes breast cancer growth via p42/P44 MAPK, JNK, Akt and NF-kappa B-dependent pathways.* Exp Cell Res, 2008. **314**(3): p. 509-29.
29. Aggarwal, B.B. and K. Natarajan, *Tumor necrosis factors: developments during the last decade.* Eur Cytokine Netw, 1996. **7**(2): p. 93-124.
30. Darnay, B.G. and B.B. Aggarwal, *Early events in TNF signaling: a story of associations and dissociations.* J Leukoc Biol, 1997. **61**(5): p. 559-66.
31. Tartaglia, L.A., et al., *A novel domain within the 55 kd TNF receptor signals cell death.* Cell, 1993. **74**(5): p. 845-53.
32. Hsu, H., J. Xiong, and D.V. Goeddel, *The TNF receptor 1-associated protein TRADD signals cell death and NF-kappa B activation.* Cell, 1995. **81**(4): p. 495-504.
33. Boldin, M.P., et al., *A novel protein that interacts with the death domain of Fas/APO1 contains a sequence motif related to the death domain.* J Biol Chem, 1995. **270**(14): p. 7795-8.
34. Stanger, B.Z., et al., *RIP: a novel protein containing a death domain that interacts with Fas/APO-1 (CD95) in yeast and causes cell death.* Cell, 1995. **81**(4): p. 513-23.

35. Wong, G.H., et al., *Antiviral activity of tumor necrosis factor is signaled through the 55-kDa type I TNF receptor [corrected].* J Immunol, 1992. **149**(10): p. 3350-3.

36. Pender, S.L., et al., *A p55 TNF receptor immunoadhesin prevents T cell-mediated intestinal injury by inhibiting matrix metalloproteinase production.* J Immunol, 1998. **160**(8): p. 4098-103.

37. Pahl, H.L., *Activators and target genes of Rel/NF-kappaB transcription factors.* Oncogene, 1999. **18**(49): p. 6853-66.

38. Jacque, E. and S.C. Ley, *RNF11, a new piece in the A20 puzzle.* EMBO J, 2009. **28**(5): p. 455-6.

39. Hennighausen, L. and G.W. Robinson, *Signaling pathways in mammary gland development.* Dev Cell, 2001. **1**(4): p. 467-75.

40. Nakshatri, H. and R.J. Goulet, Jr., *NF-kappaB and breast cancer.* Curr Probl Cancer, 2002. **26**(5): p. 282-309.

41. Haffner, M.C., C. Berlato, and W. Doppler, *Exploiting our knowledge of NF-kappaB signaling for the treatment of mammary cancer.* J Mammary Gland Biol Neoplasia, 2006. **11**(1): p. 63-73.

42. Karin, M., et al., *NF-kappaB in cancer: from innocent bystander to major culprit.* Nat Rev Cancer, 2002. **2**(4): p. 301-10.

43. DiDonato, J.A., F. Mercurio, and M. Karin, *NF-kappaB and the link between inflammation and cancer.* Immunol Rev, 2012. **246**(1): p. 379-400.

44. Nakshatri, H., et al., *Constitutive activation of NF-kappaB during progression of breast cancer to hormone-independent growth.* Mol Cell Biol, 1997. **17**(7): p. 3629-39.

45. Cogswell, P.C., et al., *Selective activation of NF-kappa B subunits in human breast cancer: potential roles for NF-kappa B2/p52 and for Bcl-3.* Oncogene, 2000. **19**(9): p. 1123-31.

46. Singh, S., et al., *Nuclear factor-kappaB activation: a molecular therapeutic target for estrogen receptor-negative and epidermal growth factor receptor family receptor-positive human breast cancer.* Mol Cancer Ther, 2007. **6**(7): p. 1973-82.

47. Biswas, D.K., et al., *NF-kappa B activation in human breast cancer specimens and its role in cell proliferation and apoptosis.* Proc Natl Acad Sci U S A, 2004. **101**(27): p. 10137-42.

48. Oida, K., et al., *Nuclear factor-kB plays a critical role in both intrinsic and acquired resistance against endocrine therapy in human breast cancer cells.* Sci Rep, 2014. **4**: p. 4057.

49. Pratt, M.A., et al., *Estrogen withdrawal-induced NF-kappaB activity and bcl-3 expression in breast cancer cells: roles in growth and hormone independence.* Mol Cell Biol, 2003. **23**(19): p. 6887-900.

50. Biswas, D.K., et al., *Crossroads of estrogen receptor and NF-kappaB signaling.* Sci STKE, 2005. **2005**(288): p. pe27.

51. Zhou, Y., et al., *The NFkappaB pathway and endocrine-resistant breast cancer.* Endocr Relat Cancer, 2005. **12 Suppl 1**: p. S37-46.
52. Humphrey, T. and A. Pearce, *Cell cycle molecules and mechanisms of the budding and fission yeasts.* Methods Mol Biol, 2005. **296**: p. 3-29.
53. Harper, J.V. and G. Brooks, *The mammalian cell cycle: an overview.* Methods Mol Biol, 2005. **296**: p. 113-53.
54. Trimarchi, J.M. and J.A. Lees, *Sibling rivalry in the E2F family.* Nat Rev Mol Cell Biol, 2002. **3**(1): p. 11-20.
55. Hanahan, D. and R.A. Weinberg, *The hallmarks of cancer.* Cell, 2000. **100**(1): p. 57-70.
56. Evans, T., et al., *Cyclin: a protein specified by maternal mRNA in sea urchin eggs that is destroyed at each cleavage division.* Cell, 1983. **33**(2): p. 389-96.
57. Dickson, M.A. and G.K. Schwartz, *Development of cell-cycle inhibitors for cancer therapy.* Curr Oncol, 2009. **16**(2): p. 36-43.
58. Santamaria, D. and S. Ortega, *Cyclins and CDKS in development and cancer: lessons from genetically modified mice.* Front Biosci, 2006. **11**: p. 1164-88.
59. Pavletich, N.P., *Mechanisms of cyclin-dependent kinase regulation: structures of Cdks, their cyclin activators, and Cip and INK4 inhibitors.* J Mol Biol, 1999. **287**(5): p. 821-8.
60. Spencer, S.L., et al., *The proliferation-quiescence decision is controlled by a bifurcation in CDK2 activity at mitotic exit.* Cell, 2013. **155**(2): p. 369-83.
61. Massague, J., *G1 cell-cycle control and cancer.* Nature, 2004. **432**(7015): p. 298-306.
62. Abbas, T. and A. Dutta, *p21 in cancer: intricate networks and multiple activities.* Nat Rev Cancer, 2009. **9**(6): p. 400-14.
63. Ping, B., et al., *Cytoplasmic expression of p21CIP1/WAF1 is correlated with IKKbeta overexpression in human breast cancers.* Int J Oncol, 2006. **29**(5): p. 1103-10.
64. Koepp, D.M., et al., *Phosphorylation-dependent ubiquitination of cyclin E by the SCFFbw7 ubiquitin ligase.* Science, 2001. **294**(5540): p. 173-7.
65. Hanahan, D. and R.A. Weinberg, *Hallmarks of cancer: the next generation.* Cell, 2011. **144**(5): p. 646-74.
66. Wang, T.C., et al., *Mammary hyperplasia and carcinoma in MMTV-cyclin D1 transgenic mice.* Nature, 1994. **369**(6482): p. 669-71.
67. Kong, G., et al., *Functional analysis of cyclin D2 and p27(Kip1) in cyclin D2 transgenic mouse mammary gland during development.* Oncogene, 2002. **21**(47): p. 7214-25.
68. Moroy, T. and C. Geisen, *Cyclin E.* Int J Biochem Cell Biol, 2004. **36**(8): p. 1424-39.
69. Akama, Y., et al., *Frequent amplification of the cyclin E gene in human gastric carcinomas.* Jpn J Cancer Res, 1995. **86**(7): p. 617-21.

70. Demetrick, D.J., et al., *Chromosomal mapping of the genes for the human cell cycle proteins cyclin C (CCNC), cyclin E (CCNE), p21 (CDKN1) and KAP (CDKN3).* Cytogenet Cell Genet, 1995. **69**(3-4): p. 190-2.

71. Loden, M., et al., *The cyclin D1 high and cyclin E high subgroups of breast cancer: separate pathways in tumorogenesis based on pattern of genetic aberrations and inactivation of the pRb node.* Oncogene, 2002. **21**(30): p. 4680-90.

72. Bortner, D.M. and M.P. Rosenberg, *Overexpression of cyclin A in the mammary glands of transgenic mice results in the induction of nuclear abnormalities and increased apoptosis.* Cell Growth Differ, 1995. **6**(12): p. 1579-89.

73. Fire, A., et al., *Potent and specific genetic interference by double-stranded RNA in Caenorhabditis elegans.* Nature, 1998. **391**(6669): p. 806-11.

74. Ruiz, M.T., O. Voinnet, and D.C. Baulcombe, *Initiation and maintenance of virus-induced gene silencing.* Plant Cell, 1998. **10**(6): p. 937-46.

75. Angell, S.M. and D.C. Baulcombe, *Consistent gene silencing in transgenic plants expressing a replicating potato virus X RNA.* EMBO J, 1997. **16**(12): p. 3675-84.

76. Dougherty, W.G., et al., *RNA-mediated virus resistance in transgenic plants: exploitation of a cellular pathway possibly involved in RNA degradation.* Mol Plant Microbe Interact, 1994. **7**(5): p. 544-52.

77. Romano, N. and G. Macino, *Quelling: transient inactivation of gene expression in Neurospora crassa by transformation with homologous sequences.* Mol Microbiol, 1992. **6**(22): p. 3343-53.

78. Fire, A., et al., *Production of antisense RNA leads to effective and specific inhibition of gene expression in C. elegans muscle.* Development, 1991. **113**(2): p. 503-14.

79. Dernburg, A.F., et al., *Transgene-mediated cosuppression in the C. elegans germ line.* Genes Dev, 2000. **14**(13): p. 1578-83.

80. Pal-Bhadra, M., U. Bhadra, and J.A. Birchler, *Cosuppression in Drosophila: gene silencing of Alcohol dehydrogenase by white-Adh transgenes is Polycomb dependent.* Cell, 1997. **90**(3): p. 479-90.

81. Bosher, J.M. and M. Labouesse, *RNA interference: genetic wand and genetic watchdog.* Nat Cell Biol, 2000. **2**(2): p. E31-6.

82. Hamilton, A.J. and D.C. Baulcombe, *A species of small antisense RNA in posttranscriptional gene silencing in plants.* Science, 1999. **286**(5441): p. 950-2.

83. Milhavet, O., D.S. Gary, and M.P. Mattson, *RNA interference in biology and medicine.* Pharmacol Rev, 2003. **55**(4): p. 629-48.

84. Hammond, S.M., et al., *An RNA-directed nuclease mediates post-transcriptional gene silencing in Drosophila cells.* Nature, 2000. **404**(6775): p. 293-6.

85. Hammond, S.M., et al., *Argonaute2, a link between genetic and biochemical analyses of RNAi.* Science, 2001. **293**(5532): p. 1146-50.

86. Wianny, F. and M. Zernicka-Goetz, *Specific interference with gene function by double-stranded RNA in early mouse development.* Nat Cell Biol, 2000. **2**(2): p. 70-5.

87. Billy, E., et al., *Specific interference with gene expression induced by long, double-stranded RNA in mouse embryonal teratocarcinoma cell lines.* Proc Natl Acad Sci U S A, 2001. **98**(25): p. 14428-33.

88. Gil, J. and M. Esteban, *Induction of apoptosis by the dsRNA-dependent protein kinase (PKR): mechanism of action.* Apoptosis, 2000. **5**(2): p. 107-14.

89. Elbashir, S.M., et al., *Duplexes of 21-nucleotide RNAs mediate RNA interference in cultured mammalian cells.* Nature, 2001. **411**(6836): p. 494-8.

90. de Pontual, L., et al., *Germline deletion of the miR-17 approximately 92 cluster causes skeletal and growth defects in humans.* Nat Genet, 2011. **43**(10): p. 1026-30.

91. Macfarlane, L.A. and P.R. Murphy, *MicroRNA: Biogenesis, Function and Role in Cancer.* Curr Genomics, 2010. **11**(7): p. 537-61.

92. Lee, Y., et al., *MicroRNA maturation: stepwise processing and subcellular localization.* EMBO J, 2002. **21**(17): p. 4663-70.

93. Bartel, D.P., *MicroRNAs: genomics, biogenesis, mechanism, and function.* Cell, 2004. **116**(2): p. 281-97.

94. Lee, R.C., R.L. Feinbaum, and V. Ambros, *The C. elegans heterochronic gene lin-4 encodes small RNAs with antisense complementarity to lin-14.* Cell, 1993. **75**(5): p. 843-54.

95. Reinhart, B.J., et al., *The 21-nucleotide let-7 RNA regulates developmental timing in Caenorhabditis elegans.* Nature, 2000. **403**(6772): p. 901-6.

96. Kozomara, A. and S. Griffiths-Jones, *miRBase: annotating high confidence microRNAs using deep sequencing data.* Nucleic Acids Res, 2014. **42**(Database issue): p. D68-73.

97. Cullen, B.R., *Transcription and processing of human microRNA precursors.* Mol Cell, 2004. **16**(6): p. 861-5.

98. Raza, U., J.D. Zhang, and O. Sahin, *MicroRNAs: master regulators of drug resistance, stemness, and metastasis.* J Mol Med (Berl), 2014. **92**(4): p. 321-36.

99. Tang, G., et al., *A biochemical framework for RNA silencing in plants.* Genes Dev, 2003. **17**(1): p. 49-63.

100. Lai, E.C., *Micro RNAs are complementary to 3' UTR sequence motifs that mediate negative post-transcriptional regulation.* Nat Genet, 2002. **30**(4): p. 363-4.

101. Friedman, R.C., et al., *Most mammalian mRNAs are conserved targets of microRNAs.* Genome Res, 2009. **19**(1): p. 92-105.

102. Si, M.L., et al., *miR-21-mediated tumor growth.* Oncogene, 2007. **26**(19): p. 2799-803.

103. Keklikoglou, I., et al., *MicroRNA-520/373 family functions as a tumor suppressor in estrogen receptor negative breast cancer by targeting NF-kappaB and TGF-beta signaling pathways.* Oncogene, 2012. **31**(37): p. 4150-63.

104. Korner, C., et al., *MicroRNA-31 sensitizes human breast cells to apoptosis by direct targeting of protein kinase C epsilon (PKCepsilon).* J Biol Chem, 2013. **288**(12): p. 8750-61.

105. Uhlmann, S., et al., *Global microRNA level regulation of EGFR-driven cell-cycle protein network in breast cancer.* Mol Syst Biol, 2012. **8**: p. 570.

106. Dvinge, H., et al., *The shaping and functional consequences of the microRNA landscape in breast cancer.* Nature, 2013. **497**(7449): p. 378-82.

107. Ward, A., et al., *MicroRNA-519a is a novel oncomir conferring tamoxifen resistance by targeting a network of tumour-suppressor genes in ER+ breast cancer.* J Pathol, 2014.

108. Gong, C., et al., *Up-regulation of miR-21 mediates resistance to trastuzumab therapy for breast cancer.* J Biol Chem, 2011. **286**(21): p. 19127-37.

109. Livak, K.J. and T.D. Schmittgen, *Analysis of relative gene expression data using real-time quantitative PCR and the 2(-Delta Delta C(T)) Method.* Methods, 2001. **25**(4): p. 402-8.

110. Zeisel, A., et al., *qCMA: a desktop application for quantitative collective cell migration analysis.* J Biomol Screen, 2013. **18**(3): p. 356-60.

111. Curtis, C., et al., *The genomic and transcriptomic architecture of 2,000 breast tumours reveals novel subgroups.* Nature, 2012. **486**(7403): p. 346-52.

112. Park, B.K., et al., *NF-kappaB in breast cancer cells promotes osteolytic bone metastasis by inducing osteoclastogenesis via GM-CSF.* Nat Med, 2007. **13**(1): p. 62-9.

113. Hynes, N.E. and T. Stoelzle, *Key signalling nodes in mammary gland development and cancer: Myc.* Breast Cancer Res, 2009. **11**(5): p. 210.

114. Li, Y., et al., *NF-kappaB controls Il2 and Csf2 expression during T cell development and activation process.* Mol Biol Rep, 2013. **40**(2): p. 1685-92.

115. Tsai, P.C., et al., *Inhibitory action of naphtho[1,2-b]furan-4,5-dione on hepatocyte growth factor-induced migration and invasion of MDA-MB-231 cells. Mechanisms of action.* Clin Exp Pharmacol Physiol, 2014.

116. Bera, A., et al., *Oncogenic K-Ras and Loss of Smad4 Mediate Invasion by Activating an EGFR/NF-kappaB Axis That Induces Expression of MMP9 and uPA in Human Pancreas Progenitor Cells.* PLoS One, 2013. **8**(12): p. e82282.

117. Simpson, K.J., et al., *Identification of genes that regulate epithelial cell migration using an siRNA screening approach.* Nat Cell Biol, 2008. **10**(9): p. 1027-38.

118. Simpson, K.J., et al., *Identification of genes that regulate epithelial cell migration using an siRNA screening approach.* Nature Cell Biology, 2008. **10**(9): p. 1027-1038.

119. Visekruna, A., et al., *Proteasome-mediated degradation of IkappaBalpha and processing of p105 in Crohn disease and ulcerative colitis.* J Clin Invest, 2006. **116**(12): p. 3195-203.

120. Rosenberg, E., et al., *Expression of cell cycle regulators p57(KIP2), cyclin D1, and cyclin E in epithelial ovarian tumors and survival.* Hum Pathol, 2001. **32**(8): p. 808-13.

121. Spruck, C.H., K.A. Won, and S.I. Reed, *Deregulated cyclin E induces chromosome instability.* Nature, 1999. **401**(6750): p. 297-300.

122. Meng, Y., et al., *Are all the miRBase-registered microRNAs true? A structure- and expression-based re-examination in plants.* RNA Biol, 2012. **9**(3): p. 249-53.

123. Mantovani, A., et al., *Cancer-related inflammation.* Nature, 2008. **454**(7203): p. 436-44.

124. Yde, C.W., et al., *NFkappaB signaling is important for growth of antiestrogen resistant breast cancer cells.* Breast Cancer Res Treat, 2012. **135**(1): p. 67-78.

125. Wilson, N.S., V. Dixit, and A. Ashkenazi, *Death receptor signal transducers: nodes of coordination in immune signaling networks.* Nat Immunol, 2009. **10**(4): p. 348-55.

126. Hsu, H., et al., *TRADD-TRAF2 and TRADD-FADD interactions define two distinct TNF receptor 1 signal transduction pathways.* Cell, 1996. **84**(2): p. 299-308.

127. Schneider, F., et al., *The viral oncoprotein LMP1 exploits TRADD for signaling by masking its apoptotic activity.* PLoS Biol, 2008. **6**(1): p. e8.

128. Chen, N.J., et al., *Beyond tumor necrosis factor receptor: TRADD signaling in toll-like receptors.* Proc Natl Acad Sci U S A, 2008. **105**(34): p. 12429-34.

129. Erez, N., et al., *Cancer associated fibroblasts express pro-inflammatory factors in human breast and ovarian tumors.* Biochem Biophys Res Commun, 2013. **437**(3): p. 397-402.

130. Ahmed, A., H.P. Redmond, and J.H. Wang, *Links between Toll-like receptor 4 and breast cancer.* Oncoimmunology, 2013. **2**(2): p. e22945.

131. Pirianov, G. and K.W. Colston, *Interactions of vitamin D analogue CB1093, TNFalpha and ceramide on breast cancer cell apoptosis.* Mol Cell Endocrinol, 2001. **172**(1-2): p. 69-78.

132. Shin, K.Y., et al., *Effects of tumor necrosis factor-alpha and interferon-gamma on expressions of matrix metalloproteinase-2 and -9 in human bladder cancer cells.* Cancer Lett, 2000. **159**(2): p. 127-34.

133. Kessenbrock, K., V. Plaks, and Z. Werb, *Matrix metalloproteinases: regulators of the tumor microenvironment.* Cell, 2010. **141**(1): p. 52-67.

134. Dehay, C. and H. Kennedy, *Cell-cycle control and cortical development.* Nat Rev Neurosci, 2007. **8**(6): p. 438-50.

135. Keyomarsi, K., et al., *Cyclin E and survival in patients with breast cancer.* N Engl J Med, 2002. **347**(20): p. 1566-75.

136. Jia, W., et al., *MicroRNA-30c-2* expressed in ovarian cancer cells suppresses growth factor-induced cellular proliferation and downregulates the oncogene BCL9.* Mol Cancer Res, 2011. **9**(12): p. 1732-45.

137. Mathew, L.K., et al., *Restricted Expression of miR-30c-2-3p and miR-30a-3p in Clear Cell Renal Cell Carcinomas Enhances HIF2alpha Activity.* Cancer Discov, 2013.

138. Bockhorn, J., et al., *MicroRNA-30c inhibits human breast tumour chemotherapy resistance by regulating TWF1 and IL-11.* Nat Commun, 2013. **4**: p. 1393.

139. Piao, H.L., et al., *alpha-catenin acts as a tumour suppressor in E-cadherin-negative basal-like breast cancer by inhibiting NF-kappaB signalling.* Nat Cell Biol, 2014. **16**(3): p. 245-54.

140. Sempere, L.F., *Integrating contextual miRNA and protein signatures for diagnostic and treatment decisions in cancer.* Expert Rev Mol Diagn, 2011. **11**(8): p. 813-27.

141. Chen, Y., D.Y. Gao, and L. Huang, *In vivo delivery of miRNAs for cancer therapy: Challenges and strategies.* Adv Drug Deliv Rev, 2014.

142. Duchaine, T.F. and F.J. Slack, *RNA interference and micro RNA-oriented therapy in cancer: rationales, promises, and challenges.* Curr Oncol, 2009. **16**(4): p. 61-6.

143. Bader, A.G., *miR-34 - a microRNA replacement therapy is headed to the clinic.* Front Genet, 2012. **3**: p. 120.

144. Lindow, M. and S. Kauppinen, *Discovering the first microRNA-targeted drug.* J Cell Biol, 2012. **199**(3): p. 407-12.

7. Supplementary data

Supplementary Table 1: List of mRNAs downregulated upon miR-30c-2-3p overexpression.

Entrez_Gene_ID	Accession	Symbol	p_value	BH
3399	NM_002167.2	ID3	7.64765559133124e-07	0.01457613
441518	NM_005532.3	IFI27	1.36042739467141e-06	0.01457613
6746	NM_018660.2	ZNF395	1.78118271574823e-06	0.01457613
8030	NM_173156.1	SMG7	2.0272781572215e-06	0.01457613
9235	NM_178868.3	CMTM8	2.66415640914972e-06	0.01532422
684	NM_080916.1	DGUOK	5.5325645082648e-06	0.01677677
2181	NM_199069.1	NDUFAF3	5.57259508373374e-06	0.01677677
51006	NM_018047.1	RBM22	6.88724576961158e-06	0.01677677
152189	NM_001040455.1	SIDT2	6.93058005804733e-06	0.01677677
4641	NM_024649.4	BBS1	7.44269022989081e-06	0.01677677
55696	NM_181353.1	ID1	1.02771169643986e-05	0.01677677
55893	NM_003145.3	SSR2	1.06702054063459e-05	0.01677677
5296	NM_004124.2	GMFB	1.12435095670553e-05	0.01677677
124565	NM_031899.2	GORASP1	1.16688276026016e-05	0.01677677
10606	NM_001048201.1	UHRF1	1.20598314274373e-05	0.01677677
85315	NM_032211.6	LOXL4	1.28364452562564e-05	0.01677677
5147	NM_002601.2	PDE6D	1.33381160141058e-05	0.01677677
723790	NM_004148.3	NINJ1	1.40000862614633e-05	0.01677677
118460	NM_138357.1	CCDC109A	1.49218826909693e-05	0.01716613
1525	NM_001080779.1	MYO1C	1.66997806924935e-05	0.017342
9500	NM_014071.2	NCOA6	1.80366459547189e-05	0.017342
3866	NM_024096.1	DCTPP1	1.80897081157651e-05	0.017342
53371	NM_207309.1	UAP1L1	2.19462273625154e-05	0.01838882
10668	NM_005334.2	HCFC1	2.36166602862947e-05	0.01838882
244	NM_198120.1	EBAG9	2.42863391919032e-05	0.01838882
7027	NM_031905.2	ARMC10	2.66987358277139e-05	0.01838882
582	NM_003786.2	ABCC3	2.69212105359013e-05	0.01838882
51090	NM_005937.3	MLLT6	2.71185849730176e-05	0.01838882
8818	NM_003863.2	DPM2	2.89716965772341e-05	0.01838882
3397	NM_001005332.1	MAGED1	2.97865042589916e-05	0.01838882
8318	NM_004335.2	BST2	3.05238907860973e-05	0.01838882

285704	NM_003789.2	TRADD	3.34473593131219e-05	0.01838882
197259	NM_006452.3	PAICS	3.36349007470087e-05	0.01838882
8459	NM_012302.2	LPHN2	3.40706988204152e-05	0.01838882
64423	NM_031449.3	ZMIZ2	4.09208974373448e-05	0.01838882
9632	NM_001014436.1	DBNL	3.73561750151898e-05	0.01838882
10482	NM_020877.2	DNAH2	3.71439285544299e-05	0.01838882
1728	NM_005027.2	PIK3R2	4.04726930276837e-05	0.01838882
5831	NM_000402.3	G6PD	4.02223146417751e-05	0.01838882
1861	NM_001042432.1	CLN3	3.90233534257564e-05	0.01838882
199990	NM_016817.2	OAS2	3.93538992225112e-05	0.01838882
162989	NM_001025436.1	SPAG16	4.0905715730101e-05	0.01838882
55902	NM_012343.3	NNT	4.20883197582258e-05	0.01862246
1201	NM_001008566.1	TPST2	4.28646248396797e-05	0.01867858
78994	NM_002514.2	NOV	4.57815361453796e-05	0.01880967
64759	NM_004672.3	MAP3K6	4.57677259130294e-05	0.01880967
2764	NM_000561.2	GSTM1	4.95803374591224e-05	0.01884134
5999	NM_014862.3	ARNT2	4.75746050955722e-05	0.01884134
8717	NM_004457.3	ACSL3	5.05099499300568e-05	0.01886579
9315	NM_005613.3	RGS4	5.25736354256266e-05	0.01938484
55196	NM_021922.2	FANCE	5.71839328783817e-05	0.02055762
2882	NM_178173.2	CCDC36	5.65919122514941e-05	0.02055762
23654	NM_022753.2	S100PBP	5.83550366744613e-05	0.02067423
63901	NM_001357.2	DHX9	5.89460007985228e-05	0.02067423
5329	NM_001008566.1	TPST2	6.24822673614911e-05	0.02099954
1716	NM_020677.2	NMRAL1	6.62684189673022e-05	0.02106347
9761	NM_001042470.1	SUMF2	6.66472865906377e-05	0.02106347
84065	NM_016464.3	TMEM138	6.52029206915914e-05	0.02106347
7022	NM_001098.2	ACO2	6.46911756015795e-05	0.0210634
84309	NM_032928.2	TMEM141	6.83972720948762e-05	0.02106809
22824	NM_014604.2	TAX1BP3	6.87231913095717e-05	0.02106809
54344	NM_001238.1	CCNE1	6.97302129315534e-05	0.02106809
57418	NM_201263.2	WARS2	7.32759028540452e-05	0.02163551
4856	NM_001630.1	ANXA8	7.48097801582648e-05	0.02173261
541578	NM_003068.3	SNAI2	7.66132426993342e-05	0.02178061
7057	NM_003564.1	TAGLN2	7.74967930928184e-05	0.02178061
79447	NM_002622.4	PFDN1	7.76449625104063e-05	0.02178061

898	NM_005949.2	MT1F	8.0881752980737e-05	0.02215389
84056	NM_003486.5	SLC7A5	8.41466580289125e-05	0.02234789
1902	NM_001961.3	EEF2	8.40818399245912e-05	0.02234789
10928	NM_002691.1	POLD1	8.89663907303456e-05	0.02264312
2944	NM_015143.1	METAP1	8.78974126734235e-05	0.02264312
84171	NM_017583.3	TRIM44	9.5518669478487e-05	0.02362486
1200	NM_194272.1	RBPMS2	9.61095121189252e-05	0.02624868
5414	NM_177938.2	P4HTM	9.55167040563837e-05	0.02362486
91373	NM_001002913.1	PTRH1	9.94263729602523e-05	0.02397773
10381	NM_003507.1	FZD7	0.000100371	0.02397773
23054	NM_002996.3	CX3CL1	0.000102798	0.02419092
79077	NM_001467.4	SLC37A4	0.000104586	0.02419092
23636	NM_006066.2	AKR1A1	0.000105141	0.02419092
7317	NM_006793.2	PRDX3	0.000104887	0.02419092
84276	NM_030806.3	C1orf21	0.000107566	0.0245524
5329	NM_002889.2	RARRES2	0.000111236	0.02519007
101	NM_022746.2	MOSC1	0.000115906	0.02544615
10352	NM_001014380.1	KATNAL1	0.000118296	0.02558037
51441	NM_004237.2	TRIP13	0.000122917	0.02580368
8407	NM_000709.2	BCKDHA	0.000132539	0.02666021
2178	NM_198723.1	TCEA2	0.00013804	0.02737947
4814	NM_004772.1	C5orf13	0.000139685	0.02751598
10447	NM_018199.2	EXD2	0.000141228	0.02763069
9064	NM_000391.3	TPP1	0.000145732	0.02798407
593	NM_001010883.1	FAM102B	0.000150389	0.02798407
26579	NM_198597.1	SEC24C	0.000151222	0.02798407
132160	NM_001080432.1	FTO	0.000151791	0.02798407
23016	NM_005853.5	IRX5	0.000150484	0.02798407
6624	NM_018973.3	DPM3	0.000169968	0.02884993
1660	NM_152829.1	TES	0.000179043	0.02884993
23173	NM_005436.2	CCDC6	0.000174379	0.02884993
81563	NM_014286.2	FREQ	0.000178277	0.02884993
7965	NM_007111.3	TFDP1	0.000166887	0.02884993
54872	NM_138809.3	CMBL	0.000175685	0.02884993
9140	NM_023015.3	INTS3	0.000171804	0.02884993
28231	NM_014758.1	SNX19	0.000161444	0.02884993

57007	NM_015509.2	NECAP1	0.00016098	0.02884993
83648	NM_007326.2	CYB5R3	0.000173803	0.02884993
55054	NM_001398.2	ECH1	0.000174269	0.02884993
30834	NM_017727.4	TMEM214	0.000170541	0.02884993
219541	NM_001012633.1	IL32	0.000164238	0.02884993
8546	NM_198836.1	ACACA	0.000179516	0.02889931
54542	NM_006295.2	VARS	0.000184208	0.02910892
10265	NM_139207.1	NAP1L1	0.00018831	0.02914745
7172	NM_001033566.1	RHOT1	0.00018658	0.02914745
284611	NM_016553.3	NUP62	0.000192413	0.02950571
1891	NM_002395.3	ME1	0.000192875	0.02950571
821	NM_003246.2	THBS1	0.000201034	0.03011315
8714	NM_000308.2	CTSA	0.000200184	0.03011315
25842	NM_000600.1	IL6	0.000207829	0.03034092
55081	NM_147157.1	SIGMAR1	0.000206006	0.03034092
5159	NM_002931.3	RING1	0.000205774	0.03034092
25915	NM_006452.3	PAICS	0.000215134	0.03051396
1453	NM_000903.2	NQO1	0.000213398	0.03051396
30851	NM_005180.5	BMI1	0.000212535	0.03051396
79068	NM_005189.1	CBX2	0.00021538	0.03051396
115290	NM_001975.2	ENO2	0.000210595	0.03051396
51110	NM_024545.2	SAP130	0.000213278	0.03051396
2071	NM_001953.2	ECGF1	0.000216948	0.03058540
9915	NM_020311.2	CXCR7	0.000218389	0.03063840
8140	NM_015945.10	SLC35C2	0.000220518	0.03078689
6376	NM_153824.1	PYCR1	0.00022272	0.03082657
55633	NM_024907.5	FBXO17	0.000226146	0.03097120
4939	NM_080597.2	OSBPL1A	0.000229904	0.03120604
2648	NM_000113.2	TOR1A	0.000230031	0.03120604
5480	NM_012280.2	FTSJ1	0.00023574	0.01534365
7546	NM_173659.2	RPUSD3	0.000238813	0.03179745
9887	NM_006745.3	SC4MOL	0.000254466	0.03264302
9419	NM_080918.1	DGUOK	0.000253976	0.03264302
26136	NM_000127.2	EXT1	0.000250206	0.03264302
5476	NM_001382.2	DPAGT1	0.000253379	0.03264302
37	NM_000532.3	PCCB	0.000248994	0.03264302

1915	NM_024031.2	PRR14	0.000252986	0.03264302
29894	NM_001033714.1	NOP2	0.000254033	0.03264302
7035	NM_001098209.1	CTNNB1	0.000254368	0.03264302
8459	NM_018677.2	ACSS2	0.000259204	0.03266266
64757	NM_002885.1	RAP1GAP	0.000260075	0.0326626
9166	NM_004613.2	TGM2	0.000261711	0.03272521
8563	NM_138768.2	MYEOV	0.000263259	0.03277636
25977	NM_005510.3	DOM3Z	0.00026804	0.03296090
56935	NM_001024943.1	ASL	0.00026979	0.03296090
29128	NM_006827.5	TMED10	0.000280801	0.03311049
11120	NM_004104.4	FASN	0.000272866	0.03311049
57407	NM_031266.2	HNRNPAB	0.000281387	0.03311049
1938	NM_007111.3	TFDP1	0.000277765	0.03311049
10309	NM_080927.3	DCBLD2	0.000281675	0.03311049
51026	NM_021976.3	RXRB	0.000276902	0.03311049
80023	NM_001037984.1	SLC38A10	0.000283212	0.03311049
124565	NM_022748.10	TNS3	0.000297471	0.03381531
55450	NM_005914.2	MCM4	0.000297051	0.03381531
6856	NM_005984.1	SLC25A1	0.000298726	0.03382429
9123	NM_182776.1	MCM7	0.000304556	0.03394978
8324	NM_017857.2	SSH3	0.000304225	0.03394978
340526	NM_014313.2	TMEM50A	0.000304416	0.03394978
2026	NM_080415.1	SEPT4	0.000302094	0.03394978
648	NM_002333.1	LRP3	0.000309031	0.03431560
10538	NM_001070.3	TUBG1	0.000310619	0.03435925
3429	NM_001017369.1	SC4MOL	0.000316433	0.03438257
9270	NM_022842.3	CDCP1	0.000316626	0.03438257
10935	NM_002388.3	MCM3	0.000316509	0.03438257
10327	NM_001402.5	EEF1A1	0.000327241	0.03467315
6274	NM_003677.3	DENR	0.000327809	0.03467315
10972	NM_002576.3	PAK1	0.000327158	0.03467315
4173	NM_001033859.1	ACADVL	0.000327924	0.03467315
25907	NM_021078.2	KAT2A	0.000325163	0.03467315
118429	NM_014388.5	C1orf107	0.000336112	0.03471458
91966	NM_005505.3	SCARB1	0.000335411	0.03471458
6015	NM_001078173.1	FAM127C	0.000333045	0.03471458

64689	NM_058219.2	EXOSC6	0.000355071	0.03509220
4302	NM_004140.3	LLGL1	0.000345874	0.03509220
153129	NM_016072.3	GOLT1B	0.000354646	0.03509220
85236	NM_003809.2	TNFSF12	0.00034953	0.03509220
55718	NM_001343.2	DAB2	0.000351302	0.03509220
134147	NM_020750.1	XPO5	0.000350646	0.03509220
54946	NM_173511.2	FAM117B	0.000348505	0.03509220
7027	NM_000485.2	APRT	0.000357117	0.03517359
90550	NM_001012614.1	CTBP1	0.000367351	0.03597785
83637	NM_001070.3	TUBG1	0.000373711	0.03643367
1601	NM_006430.2	CCT4	0.000384073	0.03719170
84619	NM_030782.3	CLPTM1L	0.000387018	0.03735110
154	NM_015252.2	EHBP1	0.000404959	0.03818568
157567	NM_003335.2	UBA7	0.000412487	0.03872297
4893	NM_001048197.1	SNHG3-RCC1	0.000415366	0.03872297
2348	NM_003489.2	NRIP1	0.000416043	0.03872297
9677	NM_001005245.1	OR5M11	0.000421566	0.03911045
4034	NM_016724.1	FOLR1	0.000426705	0.03933859
4199	NM_053275.3	RPLP0	0.000429611	0.03947481
23530	NM_004462.3	FDFT1	0.000441287	0.03964234
1140	NM_138387.2	G6PC3	0.000433172	0.03964234
79109	NM_144641.1	PPM1M	0.000436942	0.03964234
23301	NM_001806.2	CEBPG	0.000443599	0.03964234
64855	NM_152341.2	PAQR4	0.000449277	0.03988027
10575	NM_022168.2	IFIH1	0.000456335	0.04025829
10295	NM_014564.2	LHX3	0.000455799	0.04025829
1123	NM_057159.2	LPAR1	0.000463767	0.04033545
84733	NM_015899.1	PLEKHA9	0.000474145	0.04095017
31	NM_014223.2	NFYC	0.000481775	0.04102250
3569	NM_001025201.1	CHN1	0.000488202	0.04102250
5909	NM_024100.3	WDR18	0.000480052	0.04102250
3996	NM_024407.3	NDUFS7	0.000489246	0.04102250
8970	NM_002609.3	PDGFRB	0.000478792	0.04102250
587	NM_144732.2	HNRNPUL1	0.000487434	0.04102250
3421	NM_018010.2	IFT57	0.000483905	0.04102250

51318	NM_153450.1	MED19	0.000493951	0.04129661
1755	NM_024336.1	IRX3	0.000525015	0.04151911
3054	NM_001190.2	BCAT2	0.000525378	0.04151911
83787	NM_017823.3	DUSP23	0.000514068	0.04151911
29083	NM_032316.3	NICN1	0.000525485	0.04151911
5201	NM_015696.3	GPX7	0.000507163	0.04151911
4750	NM_005881.1	BCKDK	0.000508227	0.04151911
9319	NM_020179.1	C11orf75	0.000512384	0.04151911
7407	NM_024516.2	C16orf53	0.000509929	0.04151911
64853	NM_022074.2	FAM111A	0.000500617	0.04151911
8634	NM_007129.2	ZIC2	0.000501788	0.04151911
353091	NM_016644.1	PRR16	0.00051434	0.04151911
131566	NM_012401.2	PLXNB2	0.000518662	0.04151911
5058	NM_006337.3	MCRS1	0.000521446	0.04151911
27042	NM_004937.2	CTNS	0.000523422	0.04151911
25886	NM_177414.1	PPAP2B	0.000511873	0.04151911
51054	NM_003334.3	UBA1	0.000510792	0.04151911
64866	NM_003664.3	AP3B1	0.000529745	0.04164349
6307	NM_013265.2	C11orf2	0.000529956	0.04164349
55818	NM_003504.3	CDC45L	0.000539514	0.04180227
348093	NM_000234.1	LIG1	0.000536005	0.04180227
1890	NM_024958.1	NRSN2	0.000547103	0.04180227
6576	NM_001024463.2	HISPPD2A	0.000535383	0.04180227
6175	NM_004526.2	MCM2	0.000542826	0.04180227
79595	NM_025230.3	WDR23	0.000552843	0.04195189
65249	NM_024096.1	DCTPP1	0.000564698	0.04202581
22884	NM_153741.1	DPM3	0.000565599	0.04202581
6591	NM_145792.1	MGST1	0.000558806	0.04202581
2542	NM_005915.4	MCM6	0.000561352	0.04202581
5532	NM_001007.3	RPS4X	0.000562572	0.04202581
994	NM_002345.3	LUM	0.000570498	0.04208729
79582	NM_001093771.1	TXNRD1	0.000570725	0.04208729
51524	NM_000389.2	CDKN1A	0.000572351	0.04209925
57472	NM_018988.2	GFOD1	0.000574223	0.04212919
399979	NM_152766.2	C17orf61	0.000587185	0.04221862
4839	NM_001037582.1	SCD5	0.000579978	0.04221862

54935	NM_003348.3	UBE2N	0.000585709	0.04221862
7052	NM_005168.3	RND3	0.000600777	0.04234891
23585	NM_015171.2	XPO6	0.000597791	0.04234891
353	NM_003574.4	VAPA	0.000593731	0.04234891
81603	NM_032530.1	ZNF594	0.000599992	0.04234891
81037	NM_006674.2	HCP5	0.000591838	0.04234891
1054	NM_000992.2	RPL29	0.000599269	0.04234891
8022	NM_173510.1	CCDC117	0.000597381	0.04234891
50	NM_001204.5	BMPR2	0.000619189	0.04242349
997	NM_001436.2	FBL	0.000614541	0.04242349
2194	NM_001040437.1	C6orf48	0.000616914	0.04242349
7318	NM_147148.1	GSTM4	0.00061806	0.04242349
51185	NM_152409.2	C5orf24	0.000620143	0.04242349
54765	NM_017815.1	HAUS4	0.000634662	0.04278651
285367	NM_016223.3	PACSIN3	0.000632239	0.04278651
8728	NM_014899.3	RHOBTB3	0.000630768	0.04278651
2720	NM_148912.2	ABHD11	0.000633438	0.04278651
26061	NM_003469.3	SCG2	0.00064372	0.04283856
79693	NM_032493.2	AP1M1	0.00064943	0.04283856
9587	NM_018054.4	ARHGAP17	0.000639125	0.04283856
689	NM_017771.3	PXK	0.000640673	0.04283856
79191	NM_006502.1	POLH	0.000647179	0.04283856
5096	NM_173462.3	PAPLN	0.000654123	0.04304938
63908	NM_003025.2	SH3GL1	0.00066475	0.04338434
6919	NM_000884.2	IMPDH2	0.000667567	0.04338434
93643	NM_000154.1	GALK1	0.000667511	0.04338434
51334	NM_005675.3	DGCR6	0.000665923	0.04338434
146754	NM_020360.2	PLSCR3	0.000679702	0.04362524
6804	NM_057182.1	CCNE1	0.000681076	0.04362524
55218	NM_015012.1	TMEM41B	0.000678362	0.04362524
821	NM_001070.3	TUBG1	0.000681005	0.04362524
10606	NM_014063.5	DBNL	0.00068331	0.04367107
64766	NM_003164.3	STX5	0.000685873	0.04373769
138428	NM_003068.3	SNAI2	0.000699122	0.04399723
8562	NM_022075.3	LASS2	0.00069906	0.04399723
4802	NM_018353.3	C14orf106	0.000703016	0.04403466

5919	NM_080927.3	DCBLD2	0.000712664	0.04436409
23413	NM_001127218.1	POLD2	0.000716696	0.04439446
94241	NM_017741.3	DCAF16	0.000717783	0.04439446
6257	NM_017481.2	UBQLN3	0.0007218	0.04454715
50861	NM_033290.2	MID1	0.000738139	0.04461884
65123	NM_004463.2	FGD1	0.000728951	0.04461884
4673	NM_032827.4	ATOH8	0.000743706	0.04461884
2131	NM_014972.1	TCF25	0.000742752	0.04461884
134492	NM_003377.3	VEGFB	0.000742445	0.04461884
1797	NM_002388.3	MCM3	0.000744682	0.04461884
5534	NM_170662.3	CBLB	0.000735678	0.04461884
3159	NM_199189.1	MATR3	0.000734773	0.04461884
7283	NM_018330.4	KIAA1598	0.000728324	0.04461884
51247	NM_194313.2	KIF24	0.000748505	0.04463561
10658	NM_031455.2	CCDC3	0.00076176	0.04464056
6307	NM_018101.2	CDCA8	0.000758987	0.04464056
1798	NM_033212.2	CCDC102A	0.000755786	0.04464056
4037	NM_002586.4	PBX2	0.000756601	0.04464056
28988	NM_016147.1	PPME1	0.000774101	0.04485836
54961	NM_032230.1	C12orf26	0.000776755	0.04485836
51333	NM_014599.4	MAGED2	0.000776015	0.04485836
4176	NM_001567.2	INPPL1	0.000784869	0.0449658
7283	NM_005866.2	SIGMAR1	0.000782114	0.0449658
5424	NM_001619.3	ADRBK1	0.000788072	0.04505952
10445	NM_006579.1	EBP	0.000790369	0.04509776
85014	NM_058182.4	FAM165B	0.00079855	0.04527541
2539	NM_002205.2	ITGA5	0.000809365	0.04529449
1839	NM_001128591.1	PSMG4	0.000804531	0.04529449
26018	NM_207514.1	DEF8	0.000813456	0.04529449
7052	NM_213618.1	ST5	0.00080303	0.04529449
150864	NM_080725.1	SRXN1	0.000813534	0.04529449
1497	NM_030573.2	THAP7	0.000811648	0.04529449
8613	NM_031407.3	HUWE1	0.000807429	0.04529449
51090	NM_001017922.1	ERMAP	0.000817153	0.04536933
26100	NM_018241.2	TMEM184C	0.000823412	0.04544155
79669	NM_003861.1	WDR22	0.000830385	0.04544155

92579	NM_001789.2	CDC25A	0.000831094	0.04544155
339834	NM_138927.1	SON	0.000842126	0.04595738
1727	NM_015043.3	TBC1D9B	0.000847783	0.04616984
219487	NM_000294.1	PHKG2	0.00085244	0.04616984
8204	NM_012446.2	SSBP2	0.000860389	0.04651276
1716	NM_021239.1	RBM25	0.000866367	0.04655745
3182	NM_032937.3	C9orf37	0.000872118	0.04655745
8742	NM_018482.2	ASAP1	0.000873973	0.04655745
1487	NM_174940.2	TMEM80	0.000873755	0.04655745
10482	NM_030793.3	FBXO38	0.000863369	0.04655745
116092	NM_001040409.1	MTHFD2	0.00086934	0.04655745
55288	NM_001002027.1	ATP5G1	0.000881402	0.04668348
54867	NM_003494.2	DYSF	0.000885155	0.04679606
1021	NM_025205.3	MED28	0.000896396	0.04680077
4494	NM_019063.2	EML4	0.000902878	0.04681842
56267	NM_031845.2	MAP2	0.000901844	0.04681842
90416	NM_006777.3	ZBTB33	0.000899449	0.04681842
51092	NM_024103.2	SLC25A23	0.000908701	0.04700404
6774	NM_012280.2	FTSJ1	0.000911338	0.04705578
29950	NM_015537.3	NELF	0.000914681	0.04705945
3231	NM_001005753.1	VPS24	0.000920294	0.04726367
25870	NM_032195.1	SON	0.000922745	0.04730507
5327	NM_002868.2	RAB5B	0.000935415	0.04737679
114876	NM_016947.1	C6orf48	0.000935241	0.04737679
6515	NM_004946.1	DOCK2	0.000932631	0.04737679
8365	NM_024053.3	CENPM	0.000927474	0.04737679
11100	NM_007229.1	PACSIN2	0.000933377	0.04737679
738	NM_004775.2	B4GALT6	0.000935675	0.04737679
397	NM_014452.3	TNFRSF21	0.000943967	0.04751728
1499	NM_005412.4	SHMT2	0.000945059	0.04751728
167227	NM_198580.1	SLC27A1	0.000959337	0.0477304
10280	NM_024736.5	GSDMD	0.000960528	0.04773044
54946	NM_005902.3	SMAD3	0.000952393	0.04773044
2222	NM_080645.2	COL12A1	0.000954068	0.04773044
949	NM_004117.2	FKBP5	0.000976899	0.04810893
64135	NM_016016.1	SLC25A39	0.000978788	0.04811956

4172	NM_033161.2	SURF4	0.00098456	0.04824391
57510	NM_080670.2	SLC35A4	0.000986244	0.04824391
124222	NM_133491.2	SAT2	0.000986407	0.04824391
23266	NM_032866.3	CGNL1	0.001003289	0.04852492
54681	NM_144998.2	STRA13	0.001004664	0.04852492
3484	NM_013401.2	RAB3IL1	0.000999402	0.04852492
751867	NM_001709.3	BDNF	0.001005305	0.04852492
374291	NM_001042437.1	ST3GAL5	0.001009551	0.04863432
435	NM_018026.2	PACS1	0.001018274	0.04889073
140576	NM_144654.2	C9orf116	0.001024248	0.04909561
3017	NM_014865.2	NCAPD2	0.001030573	0.04923467
24140	NM_000097.4	CPOX	0.001030065	0.04923467
90701	NM_006097.3	MYL9	0.001033735	0.04930382
56998	NM_001852.3	COL9A2	0.001039877	0.04951469
94234	NM_004712.3	HGS	0.00104849	0.04984224
8649	NM_000075.2	CDK4	0.001052013	0.04992720

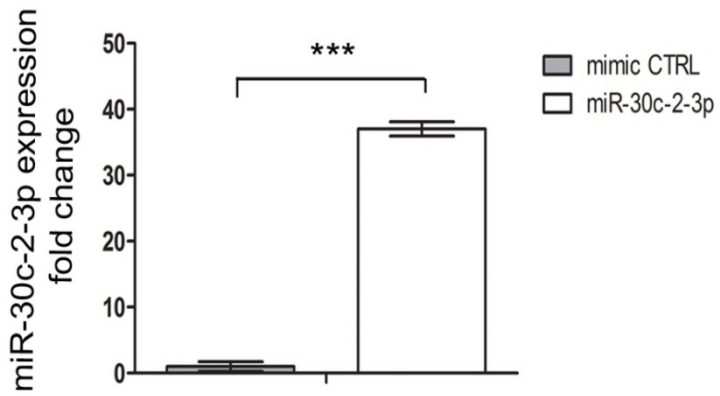

Supplementary figure 1: Overexpression of miR-30c-2-3p in MDA-MB-231 cell line. miR-30c-2-3p was overexpressed about 38 fold higher when MDA-MB-231 cells were transfected with the same concentration of miRNA to perform whole transcriptome analysis (***p≤0.001 compared to control, *t* test). Data are shown as mean±s.d of two biological and three technical replicates.

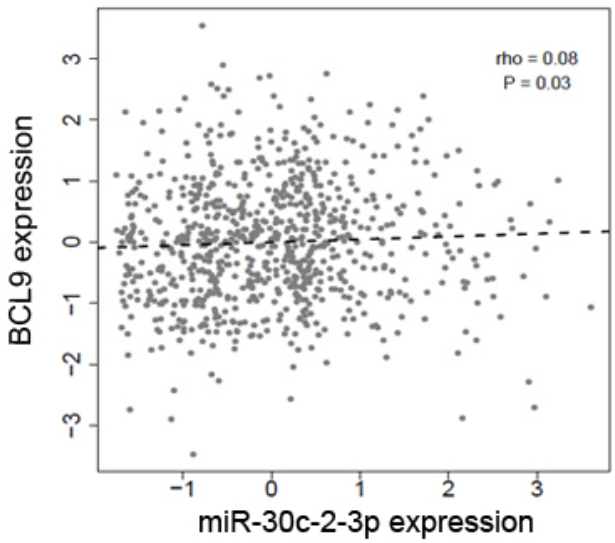

Supplementary figure 2: Linear regression analysis (Spearman rank correlation) between scale normalized miR-30c-2-3p and BCL9 mRNA levels identified anticorrelation in breast cancer patients (N = 781) from the METABRIC study [106, 111].

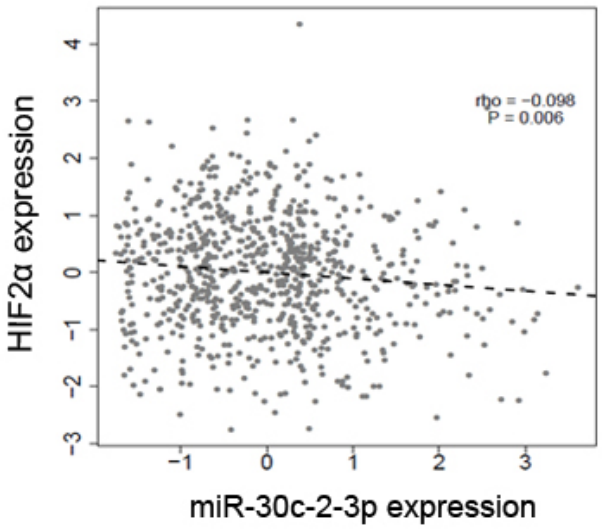

Supplementary figure 3: Linear regression analysis between miR-30c-2-3p and HIF2α mRNA levels identified anticorrelation in breast cancer patients from METABRIC study [106, 111].

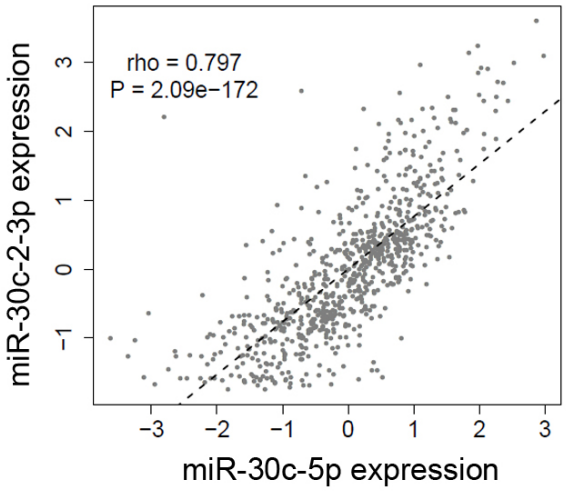

Supplementary figure 4: Linear regression analysis between scale normalized miR-30c-2-3p and miR-30c-5p according to Spearman rank correlation mRNA levels identified positive correlation in breast cancer patients from METABRIC study [106].